Eradication of MRSA Biofilms using Amphiphilic Cationic Coumarin Derivatives

Samuel O. Nitschke,[a] Muhammed Awad,[a, b] Alysha Elliott,[c] Gabrielle Lowe,[c] Chris Leigh,[d] Ken Neubauer,[d] Nicky Thomas,[a] Shane M. Hickey,[a, *] and Sally E. Plush[a, *]

[a] Clinical and Health Sciences, University of South Australia, Adelaide, South Australia, 5000, Australia.

[b] Basil Hetzel Institute for Translational Health Research, Woodville, South Australia, 5011, Australia.

[c] Institute for Molecular Bioscience, The University of Queensland, Brisbane, Queensland, 4072, Australia.

[d] Adelaide Microscopy, The University of Adelaide, Adelaide, South Australia, 5000, Australia.

* Emails: sally.plush@unisa.edu.au or shane.hickey@unisa.edu.au

Supporting Information

This supporting information provides tabulated versions of the data discussed in the main manuscript as well as additional data to complement the findings. Physicochemical characterisation, including Log*P* determination and dynamic light scattering (DLS) experimental methods and normalised intensity-weighted size distributions of the relevant coumarin compounds are first presented, followed by experimental details and supplementary data for antibacterial testing, cytotoxicity, haemolytic activity, and antibiofilm activity. General experimental details and procedures for the syntheses of all compounds are then presented followed by the ^{1}H, ^{13}C, HSQC, and HMBC NMR spectra, ESI-TOF mass spectra, and RP-HPLC chromatograms to further support the structural characterisation of the synthesised compounds described. Finally, the stability of compound **4** in aqueous solution is reported using ^{1}H NMR analysis.

The NMR spectral data for the synthesised compounds are available on figshare at https://doi.org/10.6084/m9.figshare.28340399.v3. FID files are numbered according to the compound numbers in the manuscript and ESI, experiments are numbered according to the following: 1 (^{1}H NMR), 2 (^{13}C NMR), 3 (HSQC), and 4 (HMBC).

Table of Contents

List of Figures

List of Tables

List of Compounds

Physicochemical Characterisation

It has been well reported that a correlation exists between lipophilicity and antibacterial activity.[1] Compounds that are more hydrophobic overall show a greater propensity to interact with lipid membranes, contributing to improved antibacterial activity. For amphiphilic compounds, hydrophobic tail lengths between 6–16 carbons have been shown to give optimal activity, depending on the type of bacteria.[2] Molecules that are too hydrophobic typically lead to a loss in antibacterial activity, increased cytotoxicity against mammalian cell lines, a poor haemolytic profile, and lower bioavailability.[3, 4] As such, cLog*P* values were calculated for the six coumarin derivatives, using the calculator plugins from the ChemAxon Marvin software,[5] in both their neutral and cationic states (Table S1). The accuracy of these computer-simulated calculations has been well demonstrated, with advancements enabling the prediction of MIC values for CAMPs based on computer modelled membrane-interactions.[6] The same software was used to calculate the pK_a values of each of the coumarin amphiphiles (Table S1), as the charge state of the cationic headgroup is predicted to effect selectivity.

Table S1: Calculated and experimentally determined physicochemical properties (pK_a, Log*P*, Z-average diameter, and polydispersity index) of coumarin amphiphiles.

Compound	Hydrophilic Head	Hydrophobic Tail	Calculated pK_a[a]	Neutral cLog*P*[a]	Cationic cLog*P*[a]	Z-Average Diameter (nm)	Polydispersity Index (PDI)
1	Amine	Benzyl	9.22	2.40	–0.63	377	0.32
2	Amine	Octyl	9.22	3.78	0.75	983	0.78
3	Guanidine	Benzyl	11.92	2.07	–0.68	63.7	0.22
4	Guanidine	Octyl	11.92	3.45	0.70	180	0.41
5	Biguanide	Octyl	11.63	3.22	0.48, –2.94[b]	20.7	0.50

[a] Marvin Calculator Plugins were used for structure property prediction and calculation.[5]
[b] cLog*P* values for mono- and di-cationic species.
For DLS measurements, solutions of each compound were prepared at a concentration of 1 mM in 1:99, DMSO:10 mM NaCl. PDI is an indicator of the size dispersity of aggregate particles in the measured solution.

Firstly, the pK_a values of the compounds were calculated to ensure their cationic charge state at physiological pH (Table S1). The pK_a values for the two amine coumarins (**1** and **2**) were calculated to be 9.22, while the two guanidine coumarins (**3** and **4**) were calculated to be 11.92. Interestingly, the biguanide coumarin **5** was calculated to have a slightly lower pK_a (11.63). Overall, the pK_a values for the amines and guanidines are slightly lower than the basic pK_a values of lysine (10.53) and arginine (12.48), respectively,[7] indicating these molecules will retain their cationic charge at physiological pH.

When coumarin amphiphiles were in their neutral charge state, cLog*P* values indicated moderate lipophilicity (Table S1). Both benzyl (**1** and **3**) and octyl (**2** and **4**) coumarins showed a small decrease in cLog*P* when the amine headgroup was substituted for a guanidine moiety. This same trend was observed between octyl guanidine coumarin **4** (cLog*P* = 3.45) and biguanide coumarin **5** (cLog*P* = 3.22). Both amine and guanidine coumarins exhibited a 1.6-fold increase in relative lipophilicity when comparing an octyl tail to a benzyl tail. For all coumarins, a significant decrease in lipophilicity was observed when cLog*P* was calculated for the molecules in their cationic charge state. For the benzyl coumarins (**1** and **3**), the cLog*P* values of the compounds in their cationic state were below 0 (–0.63 and –0.68, respectively). The octyl coumarins (**2**, **4**, and **5**) displayed slightly higher cLog*P* values in their cationic state (0.75, 0.48, and 0.70, respectively). The cLog*P* of biguanide coumarin **5** was determined for both mono- and di-cationic species, with the di-cationic molecule exhibiting low lipophilicity (–2.94). The cLog*P* values enable the determination of the lipophilicity window of activity for antibacterial amphiphiles, which can then be utilised in the design and synthesis of later iterations of compounds.[8]

The mechanism of action of cationic amphiphilic antibacterial agents relies on their ability to form aggregates in aqueous solutions. Dynamic light scattering (DLS) was used to assess the ability of each coumarin to form aggregates in aqueous solutions (Table S1). All coumarin amphiphiles displayed the ability to form aggregate particles in aqueous solutions with Z-average diameters ranging from 21–983 nm. In general, compounds functionalised with an octyl hydrophobic tail displayed larger particle sizes than their benzyl counterparts. For both benzyl and octyl coumarins, amine derivatives (**1**, 377 nm and **2**, 983 nm) exhibited larger particle sizes than their respective guanidine counterparts (**3**, 63.7 nm and **4**, 180 nm). The decrease in particle size between amine and guanidine cationic headgroups can be attributed to a decrease in lipophilicity that may cause tighter packing of the aggregate particles, which is further justified by the small particle size of biguanide coumarin **5** (20.7 nm). Given the high polydispersity index (PDI) of most of the compounds, it can be reasoned that the coumarin amphiphiles do not form uniform aggregate structures in aqueous solutions. Instead, the aggregates may be reaching a critical mass, followed by fragmentation, thus reaching a dynamic equilibrium in aqueous solutions.[9] Indeed, multiple populations of particle sizes were observed in the intensity-weighted size distribution graph of the biguanide derivative **5** (Figure S3). The experimentally determined Log*P* of 7-benzyloxy guanidine coumarin **3** was in good agreement with the calculated cationic value (0.5-unit difference).

LogP Determination (Shake-Flask Method)

Log*P* was determined for 7-benzyloxy guanidine coumarin **3** according to OECD guidelines[10] following previously reported Shake-Flask methods with RP-HPLC analysis (Table S2).[11, 12] Calibration curve samples were prepared in duplicate in H_2O and *n*-octanol at 10, 50, 100, 200, and 300 µM (Figure S1 and Figure S2). Log*P* samples were prepared in triplicate using the Shake-Flask method at 50, 100, and 150 µM. All samples were analysed using RP-HPLC, C18, 5–95% MeOH in H_2O gradient over 10 minutes (t_R = 6.6 minutes). Compound concentration was calculated using the linear regression equation from the calibration curves of the compound in each respective solvent (y = mx + c), where y = peak area, m = slope, x = concentration (µM), and c = y-intercept. Partition coefficient (*P*) is the molar concentration ratio of the compound in *n*-octanol/H_2O. The log of *P* (Log*P*) is the $\log_{10}$ of this ratio and used to describe the relative hydrophobicity of organic compounds. Chromatograms were acquired and processed using Shimadzu LabSolutions 5.54 SP5. All data was processed using processed using Microsoft Excel version 2402.

Table S2: Log*P* determination for 7-benzyloxy guanidine coumarin **3**.

Starting Concentration (µM)	[Compound] in H_2O (µM)	[Compound] in *n*-octanol (µM)	Partition Coefficient (*P*)	LogP
50	51.2	43.9	0.858	-0.0666
100	114	81.8	0.719	-0.143
150	174	125	0.719	-0.143
		Mean	0.765	-0.118
		SD	0.0800	NA
		%CV	10.5	NA
		n	3	3

All samples were prepared in triplicate (n = 3).

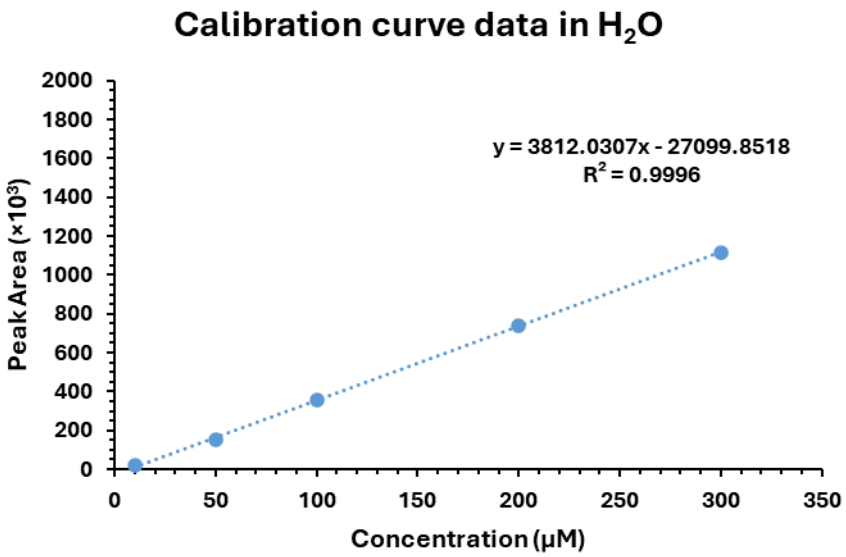

Figure S1: Calibration curve data for compound **3** in H_2O using RP-HPLC analysis.

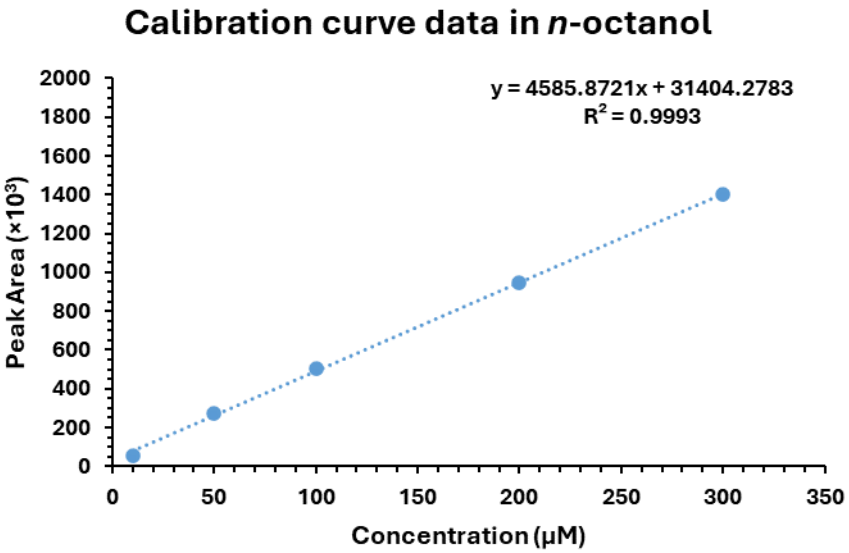

Figure S2: Calibration curve data for compound **3** in *n*-octanol using RP-HPLC analysis.

Dynamic Light Scattering (DLS) Measurements

The size distributions (Z-average diameter) and polydispersity indexes (PDIs) of the amphiphilic aggregates were determined using a Zetasizer Nano ZS (Malvern Instruments, UK) equipped with a 633 nm laser. Samples were prepared by dissolving the coumarin compounds in DMSO at a concentration of 100 mM, followed by dilution to working concentration (1 mM) with aqueous 10 mM NaCl. The final solution of each compound (1 mM in 1:99, DMSO:10 mM NaCl) were then filtered through a Sartorius 0.20 µm syringe filter to remove any large particulates. The measurements were performed at 25 °C with a scattering angle of 173°. Each sample was equilibrated for 2 min prior to data collection, and 3 independent measurements were taken for each sample to ensure reproducibility. The hydrodynamic diameter (Dh) was calculated using the Stokes-Einstein equation, and the PDI was obtained from the cumulant analysis of the correlation function. Data analysis was conducted using the Zetasizer software version 7.12, and results were reported as the average ± standard deviation of the triplicate measurements. DLS size measurements were processed using Microsoft Excel version 2402. The intensity-weighted size distributions of all six coumarin amphiphiles are shown below (Figure S3).

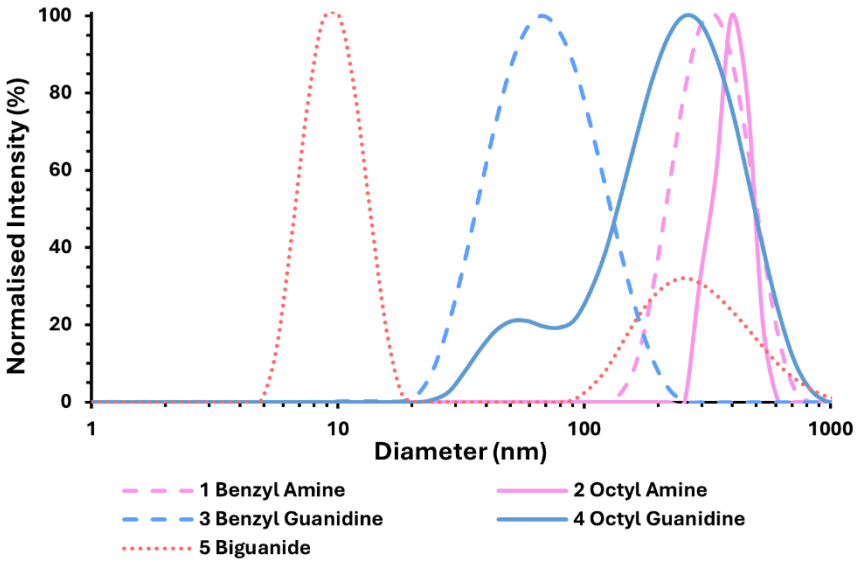

Figure S3: Normalised intensity-weighted size distribution of coumarin amphiphiles (1 mM in 1:99, DMSO:10 mM NaCl at 25 °C).

Antibacterial and Toxicity Screening

All antibacterial susceptibility screening, cytotoxicity, and haemolysis evaluations were performed by CO-ADD.[13, 14] Samples were prepared in DMSO and water to a final testing concentration of 32 μg/mL and serially diluted 1:2 fold for 8 times. Each sample concentration was prepared in 384-well plates, non-binding surface plate (NBS; Corning 3640) for each bacterial strain, tissue-culture treated (TC-treated; Corning 3712/3764) black for mammalian cell types and polypropylene 384-well (PP; Corning 3657) for haemolysis assays, all in duplicate (n = 2), and keeping the final DMSO concentration to a maximum of 0.5%. All sample preparation was done using liquid handling robots.

Raw data supplied by the CO-ADD was processed using Microsoft Excel version 2402.

Antibacterial Assay

All bacteria were cultured in cation-adjusted Mueller Hinton broth (CaMHB) at 37 °C overnight. A sample of each culture was then diluted 40-fold in fresh broth and incubated at 37 °C for 1.5–3 h. The resultant mid-log phase cultures were diluted (CFU/mL measured by OD_{600}), then added to each well of the compound-containing plates, giving a cell density of 5×10^5 CFU/mL and a total volume of 50 µL. All the plates were covered and incubated at 37 °C for 18 h without shaking. Inhibition of bacterial growth was determined measuring absorbance at 600 nm (OD_{600}), using a Tecan M1000 Pro monochromator plate reader. The percentage of growth inhibition was calculated for each well, using the negative control (media only) and positive control (bacteria without inhibitors) on the same plate as references. The percentage of growth inhibition was calculated for each well, using the negative control (media only) and positive control (bacteria without inhibitors) on the same plate. The MIC was determined as the lowest concentration at which the growth was fully inhibited, defined by an inhibition ≥ 80%. Hits were classified by MIC ≤ 16 µg/mL in either replicate (n = 2 on different plates). Colistin and vancomycin were used as positive bacterial inhibitor standards for Gram-negative and Gram-positive bacteria, respectively.

Table S3: Antibacterial activity for coumarin derivatives.

Microorganism	***S. aureus*** **ATCC 43300 MRSA**	***E. coli*** **ATCC 25922 FDA control**	***K. pneumoniae*** **ATCC 700603 K6, ESBL**	***A. baumannii*** **ATCC 19606 Type strain**	***P. aeruginosa*** **ATCC 27853 QC strain**
Compound			**MIC (µg/mL)**		
1	32	32	>32	32	>32
2	2	8	>32	>32	>32
3	16	>32	>32	>32	>32
4	8	16	32	32	32
5	4	32	32	32	32
vancomycin	1	NT	NT	NT	NT
colistin	NT	0.125	0.25	0.25	0.25

NT = not tested. All assays performed using two biological replicates and two technical replicates (n = 4).

Mammalian Cytotoxicity Assay

HEK-293 (CRL-1573, human embryonic kidney) cells were counted manually in a Neubauer haemocytometer and then plated in 384-well plates containing the compounds to give a density of 5000 cells/well in a final volume of 50 µL. Dulbecco's modified eagle medium (DMEM) supplemented with 10% fetal bovine serum (FBS) was used as growth media and the cells were incubated together with the compounds for 20 h at 37 °C in 5% CO_2. Cytotoxicity (or cell viability) was measured by fluorescence, ex: 560/10 nm, em: 590/10 nm (F560/590), after addition of 5 µL of 25 µg/mL resazurin (2.3 µg/mL final concentration) and after incubation for further 3 h at 37 °C in 5% CO_2. The fluorescence intensity was measured using a Tecan M1000 Pro monochromator plate reader, using automatic gain calculation. CC_{50} (concentration at 50% cytotoxicity) values were calculated by curve fitting the inhibition values *versus* log(concentration) using a sigmoidal dose-response function, with variable fitting values for bottom, top and slope. Curve fitting was implemented using Pipeline Pilot's dose-response component, resulting in similar values to curve fitting tools such as GraphPad's Prism and IDBS's XlFit. Cytotoxic samples were classified by $CC_{50} \leq 32$ µg/mL in either replicate (n = 2 on different plates). Tamoxifen was used as a positive cytotoxicity standard.

Table S4: Mammalian cytotoxicity for coumarin derivatives.

Compound	Mammalian Cytotoxicity (µg/mL)	
	CC_{50} (HEK-293)	**HC_{10} (RBC)**
1	7.101	>32
2	4.693	1.67
3	>32	>32
4	16	<0.25
5	17	0.5
vancomycin	>100 µM (Ref [15])	>2000 (Ref [16])
colistin	>300 µM (Ref [17])	Approx. 500 (Ref [18])
tamoxifen	9 ± 2.2	NT
melittin	NT	2.7 ± 0.9

NT = Not tested. All assays performed using two biological replicates and two technical replicates (n = 4). CC_{50} is the concentration of the compound which caused 50% growth inhibition of HEK-293 ATCC CRL-1573 cells. HC_{10} is the concentration of the compound which caused 10% haemolysis of red blood cells (RBCs).

Haemolysis Assay

Human whole blood was washed 3 times with 3 volumes of 0.9% NaCl (saline) and then resuspended in saline to a concentration of 0.5×10^8 cells/mL, as determined by manual cell count in a Neubauer haemocytometer. The washed cells were then added to the 384-well compound-containing plates for a final volume of 50 µL. After a 10 min shake on a plate shaker the plates were then incubated for 1 h at 37 °C. After incubation, the plates were centrifuged at 1000 *g* for 10 min to pellet cells and debris, 25 µL of the supernatant was then transferred to a polystyrene 384-well assay plate. The use of human blood (sourced from LifeBlood) for haemolysis assays was approved by the University of Queensland Institutional Human Research Ethics Committee, Approval Number 2020001239. Haemolysis was determined by measuring the supernatant absorbance at 405 nm (OD_{405}). The absorbance was measured using a Tecan M1000 Pro monochromator plate reader. HC_{10} (concentration at 10% haemolysis) values were calculated by curve fitting the inhibition values *versus* log(concentration) using a sigmoidal dose-response function with variable fitting values for top, bottom and slope. Curve fitting was implemented using Pipeline Pilot's dose-response component, resulting in similar values to curve fitting tools such as GraphPad's Prism and IDBS's XlFit. Haemolysis samples were classified by $HC_{10} \leq 32$ µg/mL in either replicate ($n = 2$ on different plates). Melittin was used as a positive haemolytic standard.

Antibiofilm Activity

Biofilm Mass Reduction Assay

Crystal violet assays were performed by Muhammed Awad, Basil Hetzel Institute for Translational Health Research, Woodville, South Australia, 5011, Australia.

The effect of compounds on the biofilm biomass was tested according to literature procedures.[19] A single colony of MRSA ATCC 43300 from a freshly streaked plate was incubated in tryptic soy broth (TSB) at 37 °C for 18 h. The optical density at 600 nm (OD_{600}) of bacterial culture was adjusted to 0.25 ± 0.02, equivalent to 3×10^8 CFU/mL, followed by 1:15 dilutions in TSB. Aliquots (100 µL) of the diluted culture were transferred to flat-bottom 96-well plates and incubated for 24 h in static condition. To test the antibiofilm activity of the compounds, non-adherent cells were removed *via* washing the biofilms twice with PBS, then the biofilms were incubated with 100 µL of the tested compounds diluted in TSB at 37 °C. DMSO concentrations were kept below 5% in all replicates.

To screen the dose-dependent antibiofilm activity of the compounds, a series of concentrations ranging from 32–256 µg/mL were tested. After 24 h, the treatment was removed, and biofilms washed twice with PBS and dried for 1 h at 60 °C. The dry biofilms were stained with 150 µL of crystal violet (0.1%) for 20 min at room temperature, then plates were washed and left to dry overnight. To solubilise the dye, 150 µL of 33% v/v acetic acid was added to the microtiter plate for 20 min and absorbance at 595 nm was recorded using microtiter-plate reader (Bio-Rad, Hercules, CA, USA). The experiment was performed using 6 technical replicates and 3 biological replicates.

In all crystal violet assays, untreated MRSA biofilms were used as growth controls and relative biomass was set to 100% accordingly (data not shown). Raw data was processed using GraphPad Prism 10.1.2 (324) and Microsoft Excel version 2402. Statistical analysis of all biofilm data was completed using GraphPad Prism with ANOVA one-way testing, significance is represented as $p \leq 0.05$.

Table S5: Initial compound screening for antibiofilm activity.

Compound	Biofilm Treatment Concentration (μg/mL)	Biofilm Mass (%) (Mean ± SD, n)
1	300	28.1 ± 8.55, 6
2	20	91.3 ± 11.7, 6
3	128	29.8 ± 15.6, 6
4	80	55.7 ± 16.2, 6
5	40	75.4 ± 7.82, 6

SD = Standard deviation, n = number of total replicates.

Table S6: Secondary compound screening for antibiofilm activity.

Compound	Biofilm Treatment Concentration (μg/mL)	Biofilm Mass (%) (Mean ± SD, n)
1	128	41.0 ± 13.5, 6
2	128	76.3 ± 3.39, 6
3	128	29.8 ± 15.6, 6
4	128	76.6 ± 8.51, 6
5	128	115 ± 6.32, 6

SD = Standard deviation, n = number of total replicates.

Table S7: Dose-dependent antibiofilm activity of compound **1**.

Compound	Biofilm Treatment Concentration (μg/mL)	Biofilm Mass (%) (Mean ± SD, n)
1	16	78.5 ± 9.48, 6
	32	75.4 ± 10.6, 6
	64	82.5 ± 3.54, 6
	128	41.5 ± 11.0, 6
	256	24.2 ± 0.495, 6

SD = Standard deviation, n = number of total replicates.

Table S8: Dose-dependent antibiofilm activity of compound **3**.

Compound	Biofilm Treatment Concentration (μg/mL)	Biofilm Mass (%) (Mean ± SD, n)
3	32	97.5 ± 10.2, 6
	64	77.1 ± 17.5, 6
	128	29.8 ± 15.6, 6
	256	23.1 ± 10.1, 6

SD = Standard deviation, n = number of total replicates.

Minimum Biofilm Eradication Concentration (MBEC) Assay

MBEC assay was performed by Gabrielle J. Lowe at CO-ADD, Institute for Molecular Bioscience, The University of Queensland, Brisbane, Queensland, 4072, Australia.

Methicillin-resistant *S. aureus* ATCC 43300 was cultured in TSB + 3% glucose at 37 °C overnight, then diluted 40-fold and incubated at 37 °C for a further 2–3 h. The resultant mid-log phase cultures were diluted in TSB + 3% glucose and 150 µL was added to each well of a 96-well Calgary Biofilm Device (CBD) to give a final cell density of 1×10^5 CFU/mL. The plates were placed on a shaker at 150 rpm and incubated at 37 °C for 24 h. The CBD was removed from the incubator after 24 h. The MBEC™ lid containing the pegs was removed and was washed in 200 µL of sterile 0.9% NaCl for 5 sec. Three growth control pegs were then broken off the plate using flame sterilised pliers, the pegs were dropped into 200 µL of D/E neutralising broth (in a new 96-well plate). This was then placed in a container within the sonicator and the pegs were sonicated in the neutralising broth for 30 min to dislodge the biofilm from the pegs. After sonication, 180 µL of sterile 0.9% NaCl was added to the remaining wells of the 96-well plate and 20 µL of the sonicated broth was serially diluted down the plate 8 rows to create a 10^0–10^7 serial dilution. A 10 µL aliquot of each dilution was then spotted onto a freshly prepared nutrient agar (NA) plate, and incubated at 37 °C, overnight. After incubation the colonies were counted to determine the biofilm density on the pegs.

A stock solution of compound **1** was prepared in 100% DMSO at a concentration of 20.48 mg/mL. The stock solution was serially diluted in TSB + 3% glucose in a polystyrene (PS) 96-well plates (Corning; Cat. No. 3370) with a final volume of 200 µL to ensure the entirety of the biofilm on the peg would be submerged in compound containing media. After the breaking of the 3 growth control pegs mentioned prior, the MBEC™ lid was transferred to the freshly prepared compound-containing 96-well plate. The entire plate was then placed in the incubator overnight at 37 °C without shaking. To determine the $\log_{10}$ reduction in CFU of the biofilms, the MBEC™ lid was transferred to a recovery plate. The recovery plate consisted of a fresh 96-well PS plate that contained 200 µL of sterile recovery media in every well. The MBEC™ lid was left in the recovery plate for 30 min to equilibrate before it was placed in the sonicator for 30 min to dislodge the biofilm off the pegs. After sonication, 100 µL of each well of a single row of the recovery plate was aspirated and dispensed into a single row of a fresh 96-well PS plate. In the remaining wells of the fresh plate, 180 µL of sterile saline was added, and the recovered biofilm was serially diluted down the plate to create a 10^0–10^7 serial dilution. This process was repeated for all rows of the recovery plate. Following the serial dilution, 10 µL of each dilution was spotted onto a freshly prepared NA plate, and incubated at 37 °C, overnight.

After incubation the colonies were counted, and $\log_{10}$ CFU/peg was calculated using the following equation, where X = CFU counted on spot plate, B = volume plated (e.g., 10 µL), and D = dilution (e.g.,

10^4). Statistical analysis of all biofilm data was completed using GraphPad Prism with ANOVA one-way testing, significance is represented as $p \leq 0.05$.

$$log_{10}\left(\frac{CFU}{peg}\right) = log_{10}\left[\left(\frac{X}{B}\right)(D) + 1\right]$$

Raw data was processed using GraphPad Prism 10.1.2 (324). The minimum biofilm eradication concentration (MBEC) was determined using the Calgary Biofilm Device plate method.

Table S9: MBEC determination of compound **1** against MRSA biofilms.

Compound	Biofilm Treatment Concentration (µg/mL)	Log_{10} CFU/peg (Mean ± SD, n)
Control	0	6.05 ± 0.82, 16
1	64	8.58 ± 0.84, 7
	128	0.95 ± 1.76, 8
	256	0.00 ± 0.00, 6

SD = Standard deviation, n = number of total replicates.

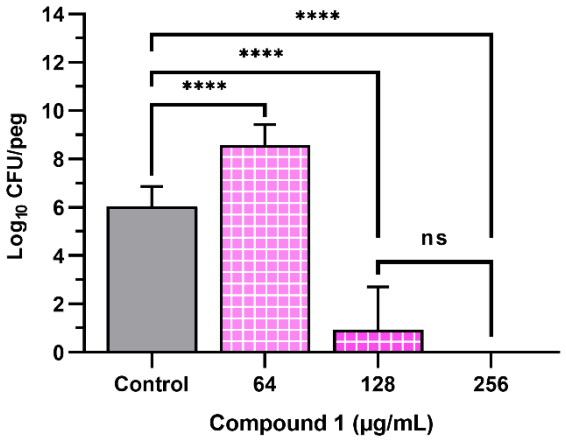

Figure S4: MBEC determination of coumarin **1** against MRSA biofilms. * = $p \leq 0.05$, ** = $p \leq 0.01$, *** = $p \leq 0.001$, **** = $p \leq 0.0001$. Control = no treatment.

Scanning Electron Microscope (SEM) Imaging of Biofilm Morphology

Biofilms were prepared by Muhammed Awad and SEM imaging was performed by Chris Leigh and Ken Neubauer at Adelaide Microscopy, The University of Adelaide, Adelaide, South Australia, 5000, Australia.

An overnight culture of MRSA ATCC 43300 was adjusted to 0.25 ± 0.02 OD_{600}, followed by 1:100 dilution in TSB. Aliquots (4 mL) of this bacterial suspension were transferred to individual wells in a 6-well plate containing sterile coverslips (10 mm × 10 mm) and incubated at 37 °C for 24 h to allow biofilm growth. The wells were then washed twice with sterile PBS to remove non-adherent cells, fresh media containing 128 µg/mL of compound **1** was added to the wells and then the plate was incubated at 37 °C. After removing the media, cells were fixed with a mixture of 4% paraformaldehyde and 2.5% glutaraldehyde in 0.05 M phosphate buffer (pH 7.2) and placed at 4 °C for 12 h. After washing twice in phosphate buffer the samples were treated with 2% osmium tetroxide for 1 h, dehydrated through a graded series of ethanol solutions and then placed in 50% hexamethyldisilazane (HMDS) in absolute ethanol for 30 min. This was followed by 2 changes of pure HMDS for 30 min each and finally the HMDS was removed, and the samples allowed to air dry. Coverslips were mounted on aluminum stubs and coated with platinum 5 nm using a 208 High Resolution Cressington sputter coater. Imaging was performed using the Quanta 450 FEG Environmental SEM.

Compound Synthesis

Chemicals were purchased from commercial sources and used without further purification. Anhydrous CH_2Cl_2, THF, and MeCN were obtained by drying over freshly activated 3 Å molecular sieves, anhydrous acetone was obtained by drying with Na_2SO_4, and anhydrous 1,4-dioxane was purchased from Sigma Aldrich (Australia). Thin layer chromatography (TLC) was performed on silica gel 60 F_{254} plates purchased from Merck (Australia). Silica gel 60 (0.063–0.203 nm) was purchased from Merck (Australia) and used for all chromatographic purification steps. All melting points were obtained using a digital ISG® melting point apparatus and are uncorrected. All ^{1}H and ^{13}C NMR spectra were collected on a BRUKER AVANCE III 500 MHz FT-NMR spectrometer. All NMR experiments were performed at 25 °C. Complete structural characterisation was achieved by performing 2D NMR experiments on most compounds. Samples were dissolved in $CDCl_3$, DMSO-d_6 or MeOD where specified, with the residual solvent peak used as the internal reference—$CDCl_3$: 7.26 (^{1}H) and 77.16 (^{13}C), DMSO-d_6: 2.50 (^{1}H) and 39.52 (^{13}C), and MeOD: 3.31 (^{1}H) and 49.0 (^{13}C).[20] Proton spectra are reported as chemical shift (ppm) δ (multiplicity (s = singlet, br s = broad singlet, d = doublet, dd = doublet of doublets, t = triplet, q = quartet, and m = multiplet), integral, coupling constant (Hz), and assignment). Carbon spectra are reported as chemical shift δ (ppm) and (assignment) where relevant. FID files for all NMR spectra can be found on figshare using the following link: https://doi.org/10.6084/m9.figshare.28340399.v3. FID files are numbered according to the compound numbers in the manuscript and SI, experiments are numbered according to the following: 1 (^{1}H NMR), 2 (^{13}C NMR), 3 (HSQC), and 4 (HMBC). High resolution mass spectrometry (HRMS) data was collected using an AB SCIEX TripleTOF 5600 mass spectrometer using a 95% MeOH in H_2O solvent system containing 0.1% formic acid. All analyte solutions were prepared in HPLC grade MeOH at a concentration of ~100 µg/mL. Reverse phase high-performance liquid chromatography (RP-HPLC) experiments were conducted on a Shimadzu Prominence UltraFast Liquid Chromatography (UFLC) system equipped with a CBM-20A communications bus module, a DGU-20ASR degassing unit, a LC-20AD liquid chromatograph pump, a SIL-20AHT autosampler, and SPD-M20A photo diode array detector, a CTO-20A column oven, and a Phenomenex Kinetex 5 mM C18 100 Å 250 mm × 4.60 mm column. The solvent system used was a gradient beginning at 5% MeOH in H_2O containing 0.1% formic acid and ending with 95% MeOH in H_2O containing 0.1% formic acid, over 30 min. All analyte solutions were prepared in HPLC grade MeOH at a concentration of ~100 µg/mL. Injection volume was 20 µL with a flow rate of 1 mL/min maintained throughout. All compounds used in biological assays are > 95% pure by HPLC analysis.

Overview of Synthetic Procedures

Functionalisation of the coumarin scaffold began with alkylation at the 7-position of 4-methylumbelliferone **S1** (Scheme S1). Alkylation was performed using either 1-bromooctane or

benzyl bromide under basic conditions which supplied the desired products **S2a** and **S2b**. Subsequent regioselective monobromination was achieved using *N*-bromosuccinimide (NBS) and $CuBr_2$ to provide 3-bromo derivatives **S3a** and **S3b** that were then substituted with *N*-Boc-ethylenediamine (Boc-EDA **S4**) under basic conditions. Finally, Boc-deprotection of **S5a** and **S5b** was achieved by treatment with acetyl chloride (AcCl) and MeOH to give primary amine coumarins **1** and **2** as hydrochloride salts. For guanidinylation, amine salts (**1** and **2**) were first converted to amines (**S6a** and **S6b**) by neutralising with $NaHCO_3$. Amine coumarins **S6a** and **S6b** were then reacted with guanidinylating agent **S7** and a final Boc-deprotection afforded the desired guanidinium derivatives **S8a** and **S8b** as hydrochloride salts. For the synthesis of the biguanide derivative, only the *n*-octyl hydrophobic tail was explored to provide comparisons of the guanidine cationic headgroups. Amine coumarin **S6b** was treated with dicyandiamide and $FeCl_3$ in 1,4-dioxane, followed by an acidic (3 M HCl) and extractive workup that provided biguanide coumarin **5** as a dihydrochloride salt. As an indicator of compound stability, the ^{1}H NMR spectrum of a 7-octyloxy derivative (guanidine coumarin **4**) was monitored at room temperature in an aqueous solution, where no significant degradation was observed (Figure S90).

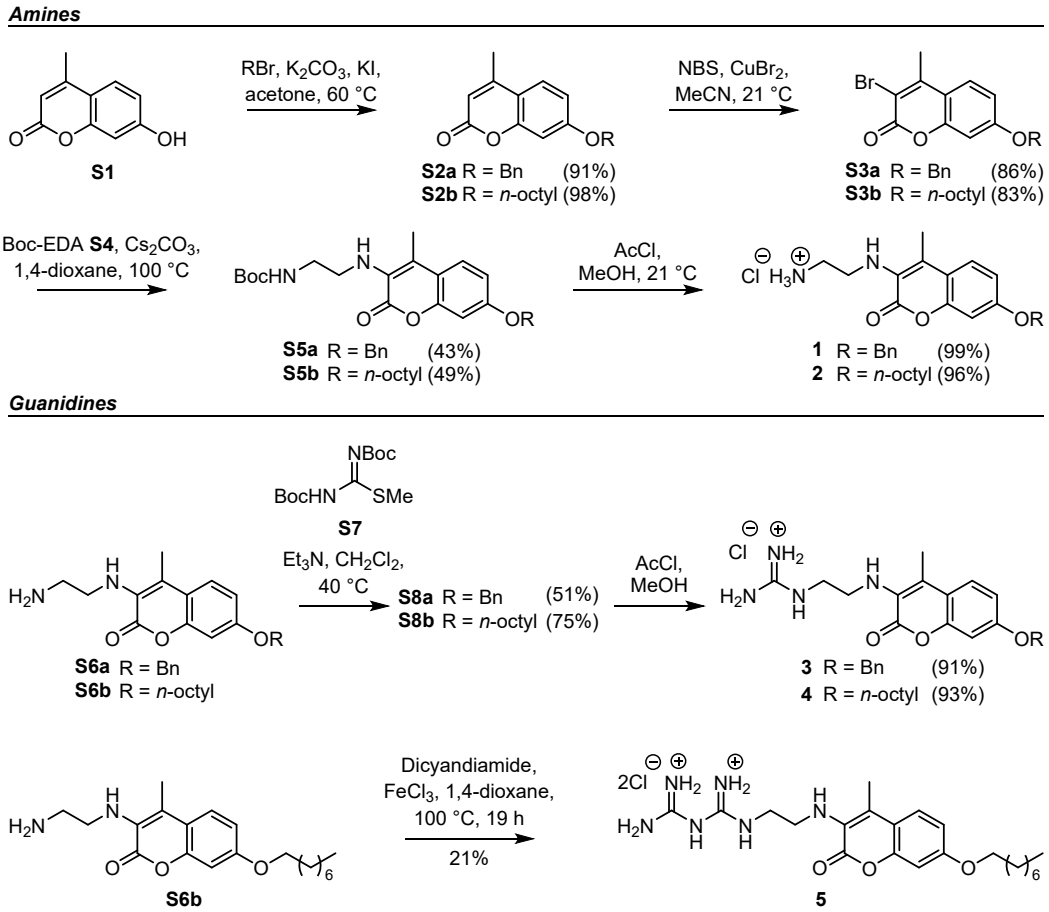

Scheme S1: Synthesis of coumarin amines (**1** and **2**) and coumarin guanidines (**3**, **4**, and **5**).

Synthetic Procedures

1: 2-((7-(Benzyloxy)-4-methyl-2-oxo-2*H*-chromen-3-yl)amino)ethan-1-aminium chloride.

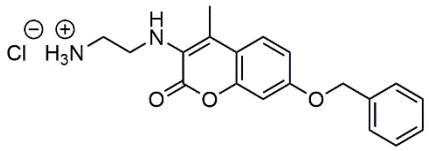

A heterogeneous mixture of **S5a** (127 mg, 0.299 mmol) in MeOH (3.0 mL) was stirred at ambient temperature for 5 min, followed by the dropwise addition of acetyl chloride (220 µL, 3.09 mmol). Stirring was maintained 22 h before the homogeneous reaction mixture was co-evaporated under reduced pressure with MeOH (3 × 5 mL) to give the title compound as a powdery white solid (106 mg, 99%).

m.p. 180–181 °C.

^{1}H NMR (DMSO-d_6, 500 MHz): δ 8.55 (t, 1H, J = 5.7 Hz, NH), 8.02 (br s, 3H, NH_3), 7.63 (d, 1H, J = 8.6 Hz, H5), 7.47 (d, 2H, J = 7.2 Hz, H2′, H6′), 7.40 (app. t, 2H, J = 7.5 Hz, H3′, H5′), 7.33 (app. t, 1H, J = 7.3 Hz, H4′), 7.12 (d, 1H, J = 2.0 Hz, H8), 7.06 (dd, 1H, J = 8.6, 2.0 Hz, H6), 5.21 (s, 2H, OCH_2), 3.53–3.49 (m, 2H, $H_3NCH_2CH_2$), 2.97 (app. t, 2H, J = 6.2 Hz, $H_3NCH_2CH_2$), 2.50 (s, 3H, CH_3).

^{13}C NMR (DMSO-d_6, 125 MHz): δ 160.0 (C3), 158.7 (C7), 153.7 (C4), 142.3 (C2), 136.8 (C1′), 128.5 (C3′, C5′), 128.0 (C4′), 127.7 (C2′, C6′), 122.7 (C4a), 121.6 (C5), 121.5 (C8a), 113.2 (C6), 96.8 (C8), 69.8 (OCH_2), 38.6 ($H_3NCH_2CH_2$), 36.3 ($H_3NCH_2CH_2$), 8.8 (CH_3).

HRMS (ESI-TOF) *m/z*: $[M + H]^+$ Calcd for $C_{19}H_{21}N_2O_3$ 325.1547; Found 325.1550.

Anal. RP-HPLC: t_R = 11.75 min, purity > 99%.

2: 2-((4-Methyl-7-(octyloxy)-2-oxo-2*H*-chromen-3-yl)amino)ethan-1-aminium chloride.

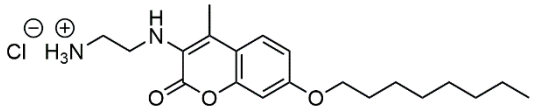

A heterogeneous mixture of **S5b** (56 mg, 0.13 mmol) in MeOH (1.25 mL) was stirred at ambient temperature for 5 min, followed by the dropwise addition of acetyl chloride (90 µL, 1.3 mmol). Stirring was maintained 19 h before the heterogeneous reaction mixture was co-evaporated under reduced pressure with MeOH (3 × 5 mL) to give the title compound as a powdery white solid (46 mg, 96%).

m.p. 233–235 °C.

^{1}H NMR (DMSO-d_6, 500 MHz): δ 8.55 (t, 1H, J = 5.1 Hz, NH), 8.10 (br s, 3H, NH_3), 7.60 (d, 1H, J = 8.6 Hz, H5), 7.05 (s, 1H, H8), 6.96 (d, 1H, J = 8.6 Hz, H6), 4.02 (t, 2H, J = 6.2 Hz, OCH_2), 3.53–3.52 (m, 2H, $H_3NCH_2CH_2$), 2.97 (app. t, 2H, J = 5.7 Hz, $H_3NCH_2CH_2$), 2.50 (s, 3H, CH_3), 1.74–1.71 (m, 2H, OCH_2CH_2), 1.42–1.41 (m, 2H, $OCH_2CH_2CH_2$), 1.29–1.26 (m, 8H, 4 × CH_2), 0.85 (t, 3H, J = 6.0 Hz, CH_2CH_3).

^{13}C NMR (DMSO-d_6, 125 MHz): δ 160.0 (C3), 159.2 (C7), 153.9 (C4), 142.2 (C2), 122.4 (C4a), 121.5 (C5), 121.5 (C8a), 112.8 (C6), 96.2 (C8), 68.1 (OCH_2), 38.6 ($H_3NCH_2CH_2$), 36.3 ($H_3NCH_2CH_2$), 31.3 (CH_2), 28.8 (CH_2), 28.7 (OCH_2CH_2), 28.6 (CH_2), 25.6 ($OCH_2CH_2CH_2$), 22.1 (CH_2), 14.0 (CH_2CH_3), 8.8 (CH_3).

HRMS (ESI-TOF) *m/z*: $[M + H]^+$ Calcd for $C_{20}H_{31}N_2O_3$ 347.2329; Found 347.2332.

Anal. RP-HPLC: t_R = 13.13 min, purity > 95%.

3: Amino((2-((7-(benzyloxy)-4-methyl-2-oxo-2*H*-chromen-3-yl)amino)ethyl)amino)methaniminium chloride.

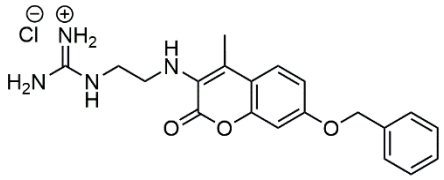

A heterogeneous mixture of **S8a** (452 mg, 0.798 mmol) in MeOH (8.0 mL) was stirred at ambient temperature for 5 min, followed by the dropwise addition of a premixed solution of acetyl chloride (1.14 mL, 16.0 mmol) in MeOH (4.0 mL). The reaction mixture was heated to 40 °C and stirred for 4 days before the addition of a second aliquot of acetyl chloride (570 µL, 8.02 mmol). The reaction mixture was then stirred at 40 °C for an additional 24 h before being co-evaporated under reduced pressure with MeOH (3 × 5 mL) to give the title compound as a powdery off-white solid (292 mg, 91%).

m.p. 215–225 °C.

^{1}H NMR (DMSO-d_6, 500 MHz): δ 8.47 (t, 1H, J = 5.7 Hz, NH), 7.69 (t, 1H, J = 5.6 Hz, NH), 7.62 (d, 1H, J = 8.7 Hz, H5), 7.47 (d, 2H, J = 7.1 Hz, H2′, H6′), 7.40 (t, 2H, J = 7.4 Hz, H3′, H5′), 7.33 (t, 1H, J = 7.3 Hz, H4′), 7.13 (d, 1H, J = 2.2 Hz, H8), 7.05 (dd, 1H, J = 8.7, 2.2 Hz, H6), 5.21 (s, 2H, OCH_2), 3.39–3.31 (m, 4H, 2 × NCH_2), 2.49 (s, 3H, CH_3).

^{13}C NMR (DMSO-d_6, 125 MHz): δ 159.9 (C3), 158.7 (C7), 157.1 (C4), 153.7 (C=N), 142.3 (C2), 136.8 (C1′), 128.5 (C3′, C5′), 128.0 (C4′), 127.7 (C2′, C6′), 122.7 (C4a), 121.6 (C8a), 121.4 (C5), 113.2 (C6), 96.8 (C8), 69.8 (OCH_2), 40.3 ($HNCH_2$), 37.7 ($HNCH_2$), 8.8 (CH_3).

HRMS (ESI-TOF) *m/z*: $[M + H]^+$ Calcd for $C_{20}H_{23}N_4O_3$ 367.1765; Found 367.1779.

Anal. RP-HPLC: t_R = 11.78 min, purity > 96%.

4: 2-((4-Methyl-7-(octyloxy)-2-oxo-2*H*-chromen-3-yl)amino)ethan-1-guanidinium chloride.

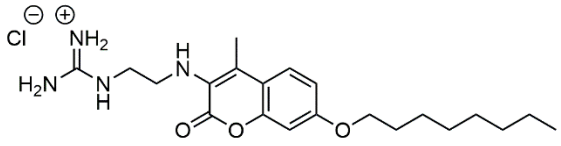

A heterogeneous mixture of **S8b** (292 mg, 0.496 mmol) in MeOH (5.0 mL) was stirred at ambient temperature for 5 min, followed by the dropwise addition of AcCl (360 µL, 5.06 mmol). Stirring was maintained 46 h before an additional aliquot of AcCl (350 µL, 4.92 mmol) was added and the reaction was stirred at ambient temperature for a further 5 d. An additional aliquot of AcCl (350 µL, 4.92 mmol) was added and the reaction was stirred for 24 h before being heated to 60 °C and stirred for 2 h. The reaction mixture was then concentrated under reduced pressure and co-evaporated with MeOH (3 × 5 mL) to give the title compound as a fluffy white solid (196 mg, 93%).

m.p. 223–225 °C.

^{1}H NMR (MeOD, 500 MHz): δ 7.53 (d, 1H, J = 8.7 Hz, H5), 7.04 (d, 1H, J = 2.1 Hz, H8), 6.94 (dd, 1H, J = 8.7, 2.1 Hz, H6), 4.02 (t, 2H, J = 6.5 Hz, OCH_2), 3.57 (app. t, 2H, J = 6.3 Hz, $HNCH_2CH_2$), 3.42 (app. t, 2H, J = 6.3 Hz, $HNCH_2CH_2$), 2.55 (s, 3H, CH_3), 1.83–1.78 (m, 2H, OCH_2CH_2), 1.53–1.47 (m, 2H, $OCH_2CH_2CH_2$), 1.42–1.28 (m, 8H, 4 × CH_2), 0.91 (t, 3H, J = 7.0 Hz, CH_3).

^{13}C NMR (MeOD, 125 MHz): δ 163.2 (C3), 161.5 (C7), 158.9 (C=N), 156.3 (C4), 143.0 (C2), 124.4 (C8a), 123.9 (C4a), 122.3 (C5), 114.4 (C6), 97.1 (C8), 69.6 (OCH_2), 42.2 ($HNCH_2CH_2$), 39.1 ($HNCH_2CH_2$), 33.0 (CH_2), 30.5 (CH_2), 30.4 (CH_2), 30.3 (OCH_2CH_2), 27.2 ($OCH_2CH_2CH_2$), 23.7 (CH_2), 14.4 (CH_3), 9.1 (CH_3).

HRMS (ESI-TOF) *m/z*: $[M + H]^+$ Calcd for $C_{21}H_{33}N_4O_3$ 389.2547; Found 389.2558.

Anal. RP-HPLC: t_R = 15.55 min, purity > 95%.

5: Amino((iminio((2-((4-methyl-7-(octyloxy)-2-oxo-2*H*-chromen-3-yl)amino)ethyl)amino)methyl)amino)methaniminium chloride.

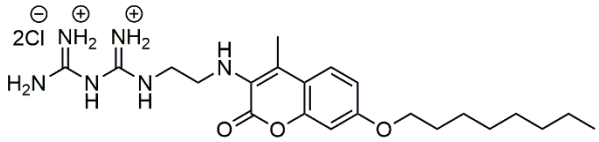

The free amine derivative of amino coumarin **2** was generated using liquid-liquid extraction with sat. $NaHCO_3$ and CH_2Cl_2 to provide amino coumarin **S6b** prior to the following reaction.

The synthesis was adapted from the literature.[21]

A heterogeneous mixture of **S6b** (187 mg, 0.540 mmol), dicyandiamide (48 mg, 0.57 mmol) and $FeCl_3$ (90 mg, 0.55 mmol) in anhydrous 1,4-dioxane (2.2 mL) was stirred at 100 °C under N_2 atmosphere and protected from light for 19 h. The reaction mixture was then cooled to ambient temperature, quenched with 3 M HCl (550 µL) and stirred at ambient temperature for 5 min before the addition of EtOAc (1 mL) and stirred for an additional 5 min. The heterogeneous mixture was diluted with EtOAc (40 mL) and washed with 1 M HCl (20 mL) and brine (2 × 20 mL). The aqueous portions were combined and concentrated under a stream of N_2 until a brown precipitate formed which was isolated using vacuum filtration. The crude material was then diluted in MeOH (20 mL), filtered, and concentrated under reduced pressure to give a brown solid. The crude material was stirred in Et_2O (10 mL) for 5 min and the solid was isolated using vacuum filtration. After rinsing with Et_2O (15 mL) the title compound was afforded as an amorphous brown solid (57 mg, 21%).

m.p. 238–240 °C.

^{1}H NMR (DMSO-d_6, 500 MHz): δ 9.50–8.38 (m, 6H, NH), 7.60 (d, 1H, J = 8.4 Hz, H5), 7.07 (s, 1H, H8), 6.95 (d, 1H, J = 8.4 Hz, H6), 4.04 (t, 2H, J = 5.7 Hz, OCH_2), 3.50 (br s, 2H, $HNCH_2CH_2$), 3.46 (br s, 2H, $HNCH_2CH_2$), 2.50 (s, 3H, CH_3), 1.74–1.72 (m, 2H, OCH_2CH_2), 1.42 (br s, 2H, $OCH_2CH_2CH_2$), 1.30–1.26 (m, 8H, 4 × CH_2), 0.86 (t, 3H, J = 6.0 Hz, CH_2CH_3).

^{13}C NMR (DMSO-d_6, 125 MHz): δ 159.8 (C3), 159.1 (C7), 155.3 (C=N), 153.8 (C4), 152.8 (C=N), 142.1 (C2), 122.3 (C4a), 121.4 (C8a), 121.4 (C5), 112.9 (C6), 96.1 (C8), 68.0 (OCH_2), 41.9 ($HNCH_2CH_2$), 36.7 ($HNCH_2CH_2$), 31.2 (CH_2), 28.7 (CH_2), 28.6 (CH_2), 28.6 (OCH_2CH_2), 25.5 ($OCH_2CH_2CH_2$), 22.0 (CH_2), 13.9 (CH_3), 8.7 (CH_3).

HRMS (ESI-TOF) *m/z*: $[M + H]^+$ Calcd for $C_{22}H_{35}N_6O_3$ 431.2765; Found 431.2768.

Anal. RP-HPLC: t_R = 13.15 min, purity > 97%.

S2a: 7-(Benzyloxy)-4-methyl-2*H*-chromen-2-one.

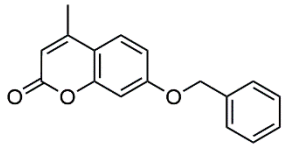

The synthesis was adapted from the literature.[22]

A mixture of 4-methylumbelliferone **S1** (362 mg, 2.05 mmol), K_2CO_3 (570 mg, 4.12 mmol) and anhydrous acetone (10 mL) was stirred at ambient temperature for 20 min. To this mixture was then added BnBr (490 µL, 4.13 mmol) and KI (46 mg, 0.28 mmol), after which the mixture was heated to 60 °C, protected from light and stirred for 5 h. The reaction was quenched with H_2O (20 mL) and stirred at ambient temperature for 10 min to give a crystalline white precipitate. The crystalline solid was isolated using vacuum filtration and washed with H_2O (2 × 30 mL) to give the title compound as a crystalline white solid (499 mg, 91%).

R_F = 0.23 (20% EtOAc in pet. spirits).

mp 120–125 °C (lit.[23] 115 °C).

^{1}H NMR ($CDCl_3$, 500 MHz): δ 7.50 (d, 1H, *J* = 8.8 Hz, H5), 7.51–7.39 (m, 4H, H2′, H3′, H5′, H6′), 7.37–7.34 (m, 1H, H4′), 6.94 (dd, 1H, *J* = 8.8, 2.5 Hz, H6), 6.89 (d, 1H, *J* = 2.5 Hz, H8), 6.12 (d, 1H, *J* = 1.0 Hz, H3), 5.13 (s, 2H, OCH_2), 2.40 (d, 3H, *J* = 1.0 Hz, CH_3).

^{13}C NMR ($CDCl_3$, 125 MHz): δ 161.8 (C7), 161.4 (C2), 155.3 (C8a), 152.7 (C4), 136.0 (C1′), 128.9 (C3′, C5′), 128.5 (C4′), 127.7 (C2′, C6′), 125.7 (C5), 113.9 (C4a), 113.1 (C6), 112.2 (C3), 102.1 (C8), 70.6 (OCH_2), 18.8 (CH_3).

HRMS (ESI-TOF) *m/z*: $[M + H]^+$ Calcd for $C_{17}H_{15}O_3$ 267.1016; Found 267.1018.

Anal. RP-HPLC: t_R = 13.29 min, purity > 98%. Data is in accordance with the literature.[22]

S2b: 4-Methyl-7-(octyloxy)-2*H*-chromen-2-one.

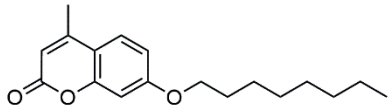

The synthesis was adapted from the literature.[24]

A mixture of 4-methylumbelliferone **S1** (1.41 g, 8.00 mmol), K_2CO_3 (2.21 g, 16.0 mmol) and anhydrous acetone (80 mL) was stirred at ambient temperature for 10 min. To this mixture was added 1-bromooctane (2.8 mL, 16.2 mmol) and KI (139 mg, 0.837 mmol), after which the mixture was heated to 60 °C, protected from light and stirred for 22 h. The mixture was then cooled to ambient temperature, quenched with H_2O (40 mL), and concentrated under reduced pressure to remove acetone before being diluted further with H_2O (20 mL) and extracted with CH_2Cl_2 (3 × 40 mL). The organic phase was washed with brine (40 mL), dried (Na_2SO_4), filtered and concentrated under reduced pressure to give a colourless oil.* The crude material was purified using column chromatography (20% EtOAc in pet. spirits) to give the title compound as a colourless oil (2.26 g, 98%).

*Alternatively, this material could be purified from recrystallisation (pet. spirits) at a decreased temperature (-10 °C) to give the title compound as an amorphous white solid (77%).

R_F = 0.26 (20% EtOAc in pet. spirits). mp 38–40 °C (lit.[25] 48–50 °C).

^{1}H NMR ($CDCl_3$, 500 MHz): δ 7.48 (d, 1H, *J* = 8.7 Hz, H5), 6.85 (d, 1H, *J* = 8.7 Hz, H6), 6.80 (s, 1H, H8), 6.12 (s, 1H, H3), 4.01 (t, 2H, *J* = 6.5 Hz, OCH_2), 2.39 (s, 3H, CH_3), 1.84–1.78 (m, 2H, OCH_2CH_2), 1.48–1.43 (m, 2H, $OCH_2CH_2CH_2$), 1.34–1.29 (m, 8H, 4 × CH_2), 0.89 (t, 3H, *J* = 6.3 Hz, CH_2CH_3).

^{13}C NMR ($CDCl_3$, 125 MHz): δ 162.4 (C7), 161.5 (C2), 155.4 (C8a), 152.7 (C4), 125.6 (C5), 113.5 (C4a), 112.8 (C6), 111.9 (C3), 101.5 (C8), 68.8 (OCH_2), 31.9 (CH_2), 29.4 (CH_2), 29.3 (CH_2), 29.1 (OCH_2CH_2), 26.1 ($OCH_2CH_2CH_2$), 22.8 (CH_2), 18.8 (CH_3), 14.2 (CH_2CH_3).

HRMS (ESI-TOF) *m/z*: $[M + H]^+$ Calcd for $C_{18}H_{25}O_3$ 289.1798; Found 289.1799.

Anal. RP-HPLC: t_R = 15.09 min, purity > 99%.

Data is in accordance with the literature.[24, 25]

S3a: 7-(Benzyloxy)-3-bromo-4-methyl-2*H*-chromen-2-one.

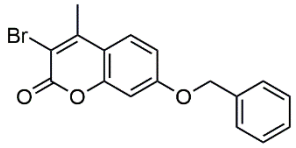

The synthesis was adapted from the literature.[26]

A mixture of **S2a** (267 mg, 1.00 mmol), NBS (181 mg, 1.02 mmol), $CuBr_2$ (33 mg, 0.15 mmol) and anhydrous MeCN (20 mL) was stirred at room temperature for 2.5 h. The reaction was then quenched with 5% $NaHSO_3$ (5 mL) and stirred for 5 min before being diluted with H_2O (25 mL). The white precipitate was isolated using vacuum filtration and washed with H_2O (2 × 30 mL) to give the title compound as a fluffy white solid (294 mg, 86%).

m.p. 137–138 °C (lit.[27] 145–147 °C).

^{1}H NMR ($CDCl_3$, 500 MHz): δ 7.56 (d, 1H, J = 8.9 Hz, H5), 7.44–7.34 (m, 5H, H2′, H3′, H4′, H5′, H6′), 6.96 (d, 1H, J = 8.9 Hz, H6), 6.89 (s, 1H, H8), 5.13 (s, 2H, OCH_2), 2.59 (s, 3H, CH_3).

^{13}C NMR ($CDCl_3$, 125 MHz): δ 161.9 (C7), 157.5 (C2), 153.6 (C8a), 151.2 (C4), 135.7 (C1′), 128.9 (C3′, C5′), 128.6 (C4′), 127.7 (C2′, C6′), 126.2 (C5), 113.8 (C6), 113.7 (C4a), 109.9 (C3), 101.9 (C8), 70.7 (OCH_2), 19.6 (CH_3).

HRMS (ESI-TOF) *m/z*: $[M + H]^+$ Calcd for $C_{17}H_{14}{}^{79}BrO_3$ 345.0121; Found 345.0123.

Anal. RP-HPLC: t_R = 13.84 min, purity > 97%. Data is in accordance with the literature.[27]

S3b: 3-Bromo-4-methyl-7-(octyloxy)-2*H*-chromen-2-one.

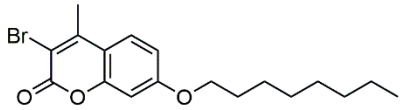

The synthesis was adapted from the literature.[26]

A mixture of **S2b** (2.26 g, 7.84 mmol), NBS (1.41 g, 7.90 mmol), $CuBr_2$ (181 mg, 0.810 mmol) and anhydrous MeCN (150 mL) was stirred at room temperature for 1.5 h. The reaction was then quenched with 5% $NaHSO_3$ (100 mL) and stirred for 10 min before being diluted with H_2O (150 mL). The white precipitate was isolated using vacuum filtration and washed with H_2O (4 × 50 mL) to give the title compound as a fluffy white solid (2.38 g, 83%).

R_F = 0.38 (20% EtOAc in pet. spirits).

m.p. 60–61 °C (lit.[25] reported as oil).

^{1}H NMR ($CDCl_3$, 500 MHz): δ 7.54 (d, 1H, *J* = 9.0 Hz, H5), 6.88 (d, 1H, *J* = 9.0 Hz, H6), 6.81 (s, 1H, H8), 4.01 (t, 2H, *J* = 6.5 Hz, OCH_2), 2.59 (s, 3H, CH_3), 1.84–1.78 (m, 2H, OCH_2CH_2), 1.49–1.43 (m, 2H, $OCH_2CH_2CH_2$), 1.34–1.29 (m, 8H, 4 × CH_2), 0.89 (t, 3H, *J* = 6.5 Hz, CH_2CH_3).

^{13}C NMR ($CDCl_3$, 125 MHz): δ 162.5 (C7), 157.6 (C2), 153.8 (C8a), 151.3 (C4), 126.1 (C5), 113.5 (C6), 113.3 (C4a), 109.6 (C3), 101.3 (C8), 68.9 (OCH_2), 31.9 (CH_2), 29.4 (CH_2), 29.3 (CH_2), 29.1 (OCH_2CH_2), 26.1 ($OCH_2CH_2CH_2$), 22.8 (CH_2), 19.6 (CH_3), 14.2 (CH_2CH_3).

HRMS (ESI-TOF) *m/z*: $[M + H]^+$ Calcd for $C_{18}H_{24}{}^{79}BrO_3$ 367.0903; Found 367.0914.

Anal. RP-HPLC: t_R = 15.74 min, purity > 98%.

Data is in accordance with the literature.[25]

S4: *tert*-Butyl (2-aminoethyl)carbamate

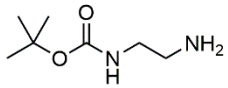

A solution of Boc_2O (4.37 g, 20.0 mmol) in THF (13 mL) was added dropwise over 1 h to a stirred solution of ethylenediamine (4.30 mL, 64.3 mmol) in THF (40 mL). The reaction was stirred for a further 5 h before the reaction mixture was filtered and the filtrate was collected and concentrated under reduced pressure to give the title compound as a colourless oil (3.13 g, 98%).

^{1}H NMR ($CDCl_3$, 500 MHz): δ 4.92 (br s, 1H, NH), 3.15 (app. d, 2H, J = 5.8 Hz, CH_2NH_2), 2.78 (app. t, 2H, J = 5.8 Hz, HNCH_2), 1.43 (s, 9H, *t*-Bu), 1.31 (br s, 2H, NH_2).

^{13}C NMR ($CDCl_3$, 125 MHz): δ 156.3 (C=O), 79.2 ($C(CH_3)_3$), 43.5 (CH_2NH_2), 41.9 ($HNCH_2$), 28.5 (*t*-Bu).

HRMS (ESI-TOF) *m/z*: $[M + H]^+$ Calcd for $C_7H_{17}N_2O_2$ 161.1285; Found 161.1290.

Data is in accordance with the literature.[28]

S5a: *tert*-Butyl (2-((7-(benzyloxy)-4-methyl-2-oxo-2*H*-chromen-3-yl)amino)ethyl)carbamate.

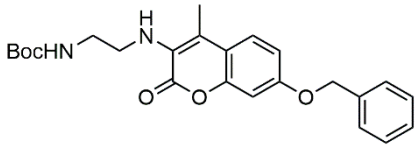

The amination procedure was adapted from a literature report.[29, 30]

A mixture of Boc-EDA **S4** (190 mg, 1.19 mmol), **S3a** (257 mg, 0.745 mmol), Cs_2CO_3 (486 mg, 1.49 mmol) and anhydrous 1,4-dioxane (3.8 mL) was degassed with N_2 for 3 min. The mixture was then heated to 100 °C, stirred under N_2 and protected from light for 24 h before being cooled to ambient temperature and concentrated under a stream of N_2 to give an off-white solid. The crude material was purified using column chromatography (20–40% EtOAc in pet. spirits) to give the title compound as a white solid (137 mg, 43%).

R_F = 0.32 (40% EtOAc in pet. spirits).

m.p. 185–186 °C.

^{1}H NMR ($CDCl_3$, 500 MHz): δ 7.47–7.45 (m, 3H, H5, H2′, H6′), 7.40 (app. t, 2H, *J* = 7.5 Hz, H3′, H5′), 7.34 (app. t, 1H, *J* = 7.2 Hz, H4′), 7.00–6.98 (m, 3H, NH, H6, H8), 5.12 (s, 2H, OCH_2), 4.94 (br s, 1H, NH), 3.57–3.54 (m, 2H, BocHNCH_2CH_2), 3.40 (br s, 2H, BocHNCH_2CH_2), 2.58 (s, 3H, CH_3), 1.42 (s, 9H, *t*-Bu).

^{13}C NMR ($CDCl_3$, 125 MHz): δ 161.1 (C3), 159.3 (C7), 156.8 (C=O), 154.5 (C4), 142.3 (C2), 136.7 (C1′), 128.8 (C3′, C5′), 128.3 (C4′), 127.6 (C2′, C6′), 123.5 (C8a), 122.9 (C4a), 121.4 (C5), 113.4 (C6), 96.9 (C8), 79.8 (*C*$(CH_3)_3$), 70.7 (OCH_2), 40.5 (BocHN*C*H_2CH_2), 40.0 (BocHNCH_2*C*H_2), 28.5 (*t*-Bu), 9.1 (CH_3).

HRMS (ESI-TOF) *m/z*: $[M + Na]^+$ Calcd for $C_{24}H_{28}N_2O_5Na$ 447.1890; Found 447.1892.

Anal. RP-HPLC: t_R = 14.00 min, purity > 99%.

S5b: *tert*-Butyl (2-((4-methyl-7-(octyloxy)-2-oxo-2*H*-chromen-3-yl)amino)ethyl)carbamate.

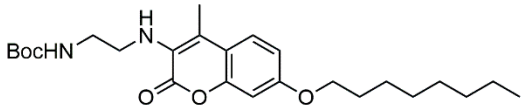

The amination procedure was adapted from a literature report.[29, 30]

A mixture of Boc-EDA **S4** (1.31 g, 8.19 mmol), **S3b** (1.97 g, 5.37 mmol), Cs_2CO_3 (3.51 g, 10.8 mmol) and anhydrous 1,4-dioxane (27 mL) was degassed with N_2 for 5 min. The mixture was then heated to 100 °C, stirred under N_2 and protected from light for 24 h before being cooled to ambient temperature and concentrated under a stream of N_2 to give an off-white solid. The crude material was purified using column chromatography (20% EtOAc in pet. spirits) to give the title compound as a white solid (1.18 g, 49%).

R_F = 0.27 (20% EtOAc in pet. spirits).

m.p. 158–160 °C.

^{1}H NMR ($CDCl_3$, 500 MHz): δ 7.44 (d, 1H, *J* = 8.8 Hz, H5), 6.96 (br s, 1H, NH), 6.91–6.90 (m, 2H, H6, H8), 4.94 (br s, 1H, NH), 3.99 (t, 2H, *J* = 6.4 Hz, OCH_2), 3.57–3.56 (m, 2H, BocHNCH$_2$CH_2), 3.40 (br s, 2H, BocHNCH_2CH$_2$), 2.58 (s, 3H, CH_3), 1.84–1.79 (m, 2H, OCH$_2$CH_2), 1.49–1.46 (m, 2H, OCH$_2$CH$_2$CH_2), 1.43 (s, 9H, *t*-Bu), 1.35–1.29 (m, 8H, 4 × CH_2), 0.89 (t, 3H, *J* = 6.4 Hz, CH$_2$CH_3).

^{13}C NMR ($CDCl_3$, 125 MHz): δ 161.2 (C3), 159.8 (C7), 156.7 (C=O), 154.7 (C4), 142.1 (C2), 123.1 (C4a), 123.0 (C8a), 121.2 (C5), 113.2 (C6), 96.3 (C8), 79.8 (*C*(CH$_3$)$_3$), 68.7 (OCH_2), 40.5 (BocHN*C*H$_2$CH$_2$), 39.9 (BocHNCH$_2$*C*H$_2$), 32.0 (CH_2), 29.5 (CH_2), 29.4 (OCH$_2$*C*H$_2$), 29.3 (CH_2), 28.5 (*t*-Bu), 26.2 (OCH$_2$CH$_2$*C*H$_2$), 22.8 (CH_2), 14.2 (CH$_2$*C*H$_3$), 9.1 (CH_3).

HRMS (ESI-TOF) *m/z*: $[M + Na]^+$ Calcd for $C_{25}H_{38}N_2O_5Na$ 469.2673; Found 469.2674.

Anal. RP-HPLC: t_R = 15.65 min, purity > 95%.

S7: *N*,*N*'-Bis(*tert*-butoxycarbonyl)-*S*-methylisothiourea

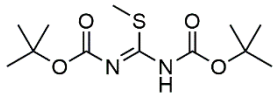

A biphasic mixture of 2-methylisothiouronium iodide **S9** (4.24 g, 19.4 mmol), sat. $NaHCO_3$ (22 mL) and CH_2Cl_2 (44 mL) was vigorously stirred at ambient temperature for 5 min before a solution of Boc_2O (8.57 g, 39.3 mmol) in CH_2Cl_2 (33 mL) was added. The biphasic mixture was stirred vigorously at ambient temperature for 3 d before the organic phase was separated and the aqueous phase extracted with CH_2Cl_2 (2 × 20 mL). The organic portions were combined, dried (Na_2SO_4), filtered and concentrated under reduced pressure to give a white solid. The crude material was stirred in 10% EtOH in H_2O (50 mL) at ambient temperature for 90 min and the insoluble material was collected using vacuum filtration. After rinsing with H_2O (100 mL), the title compound was isolated as an amorphous white solid (4.42 g, 78%).

m.p. 123–125 °C (lit.[31] 122–124 °C).

^{1}H NMR ($CDCl_3$, 500 MHz): δ 11.61 (br s, 1H, NH), 2.40 (s, 3H, Me), 1.51 (s, 18H, 2 × *t*-Bu).

^{13}C NMR ($CDCl_3$, 125 MHz): δ 171.6 (C=N), 160.9 (C=O), 150.9 (C=O), 83.4 ($C(CH_3)_3$), 81.1 ($C(CH_3)_3$), 28.1 (2 × *t*-Bu), 14.5 (Me).

HRMS (ESI-TOF) *m/z*: $[M + H]^+$ Calcd for $C_{12}H_{23}N_2O_4S$ 291.1373; Found 291.1382.

Data is in accordance with the literature.[31]

S8a: (*E*)-1-(2-((7-(Benzyloxy)-4-methyl-2-oxo-2*H*-chromen-3-yl)amino)ethyl)-2,3-di-*tert*-butoxycarbonyl-butylguanidine.

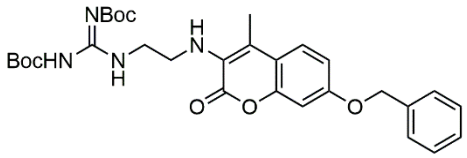

The free amine derivative of amino coumarin **1** was generated using liquid-liquid extraction with sat. $NaHCO_3$ and CH_2Cl_2 to provide amino coumarin **S6a** prior to the following reaction.

To a stirred mixture of **S6a** (39 mg, 0.120 mmol), **S7** (71 mg, 0.245 mmol) and anhydrous CH_2Cl_2 (1.2 mL) under a N_2 atmosphere was added Et_3N (30 µL, 0.215 mmol). The reaction mixture was then heated to 40 °C and stirred under a N_2 atmosphere, protected from light for 19 h before being diluted in CH_2Cl_2 (20 mL) and washed with brine (20 mL). The aqueous phase was extracted with CH_2Cl_2 (10 mL), and the organic phases were combined, dried (Na_2SO_4), filtered and concentrated under reduced pressure to give a brown solid. The crude material was purified using column chromatography (10% EtOAc in CH_2Cl_2) to give the title compound as a colourless glassy solid (35 mg, 51%).

m.p. 85–90 °C.

^{1}H NMR ($CDCl_3$, 500 MHz): δ 11.48 (s, 1H, NH), 8.58 (t, 1H, *J* = 5.0 Hz, NH), 7.47–7.44 (m, 3H, H5, H2′, H6′) 7.40 (app. t, 2H, *J* = 7.5 Hz, H3′, H5′),7.34 (app. t, 1H, *J* = 7.2 Hz, H4′), 7.00–6.98 (m, 2H, H6, H8), 6.91 (t, 1H, *J* = 5.4 Hz, NH), 5.11 (s, 2H, OCH_2), 3.69–3.65 (m, 4H, 2 × HNCH_2), 2.58 (s, 3H, CH_3), 1.50 (s, 9H, *t*-Bu), 1.48 (s, 9H, *t*-Bu).

^{13}C NMR ($CDCl_3$, 125 MHz): δ 163.6 (C=O (NBoc)), 160.9 (C3), 159.3 (C7), 156.9 (C4), 154.5 (C=N), 153.2 (C=O (NHBoc)), 142.3 (C2), 136.7 (C1′), 128.8 (C3′, C5′), 128.3 (C4′), 127.6 (C2′, C6′), 123.6 (C4a), 122.9 (C8a), 121.4 (C5), 113.4 (C6), 96.9 (C8), 83.4 ($C(CH_3)_3$), 79.5 ($C(CH_3)_3$), 70.7 (OCH_2), 40.4 ($HNCH_2$), 38.9 ($HNCH_2$), 28.5 (*t*-Bu), 28.2 (*t*-Bu), 9.1 (CH_3).

HRMS (ESI-TOF) *m/z*: $[M + H]^+$ Calcd for $C_{30}H_{39}N_4O_7$ 567.2813; Found 567.2694.

Anal. RP-HPLC: t_R = 22.36 min, purity > 84%.

S8b: (*Z*)-1,2-Di-*tert*-butoxy-3-(2-((4-methyl-7-(octyloxy)-2-oxo-2*H*-chromen-3-yl)amino)ethyl)guanidine.

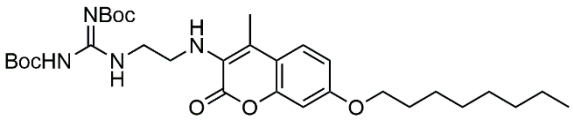

The free amine derivative of amino coumarin **2** was generated using liquid-liquid extraction with sat. $NaHCO_3$ and CH_2Cl_2 to provide amino coumarin **S6b** prior to the following reaction.

To a stirred mixture of **S6b** (251 mg, 0.724 mmol), anhydrous CH_2Cl_2 (1.3 mL) and Et_3N (160 µL, 1.15 mmol) under a N_2 atmosphere was added a solution of **S7** (421 mg, 1.45 mmol) in anhydrous CH_2Cl_2 (3.8 mL). The reaction mixture was then heated to 40 °C and stirred under a N_2 atmosphere, protected from light for 23 h before being diluted in CH_2Cl_2 (50 mL), washed with H_2O (30 mL), brine (30 mL), dried (Na_2SO_4), filtered and concentrated under reduced pressure to give a brown solid. The crude material was purified using column chromatography (10% EtOAc in CH_2Cl_2) to give the title compound as an amorphous white solid (319 mg, 75%).

*Methanethiol is a malodourous gas generated as a by-product of this reaction. All workups were conducted in the confines of a fume cupboard and all equipment was soaked in warm bleach solution overnight.

R_F = 0.22 (10% EtOAc in CH_2Cl_2).

m.p. 117–119 °C.

^{1}H NMR ($CDCl_3$, 500 MHz): δ 11.47 (s, 1H, NH), 8.71 (br s, 1H, NH), 7.44 (d, 1H, *J* = 8.5 Hz, H5), 7.00 (br s, 1H, NH), 6.92 (d, 1H, *J* = 2.0 Hz, H8), 6.90 (dd, 1H, *J* = 8.5, 2.0 Hz, H6), 3.98 (t, 2H, *J* = 6.6 Hz, OCH_2), 3.75–3.74 (m, 2H, $HNCH_2CH_2$), 3.69–3.65 (m, 2H, $HNCH_2CH_2$), 2.57 (s, 3H, CH_3), 1.84–1.78 (m, 2H, OCH_2CH_2), 1.50 (s, 9H, *t*-Bu), 1.49 (s, 9H, *t*-Bu), 1.47–1.44 (m, 2H, $OCH_2CH_2CH_2$), 1.37–1.29 (m, 8H, 4 × CH_2), 0.89 (t, 3H, *J* = 6.9 Hz, CH_2CH_3).

^{13}C NMR ($CDCl_3$, 125 MHz): δ 161.1 (C3), 159.8 (C7), 156.6 (2 × C=O), 154.7 (C4), 152.3 (C=N), 142.1 (C2), 123.1 (C8a), 123.0 (C4a), 121.2 (C5), 113.3 (C6), 96.3 (C8), 84.0 (2 × $C(CH_3)_3$), 68.7 (OCH_2), 40.9 ($HNCH_2CH_2$), 38.9 ($HNCH_2CH_2$), 32.0 (CH_2), 29.5 (CH_2), 29.4 (CH_2), 29.3 (OCH_2CH_2), 28.4 (*t*-Bu), 28.2 (*t*-Bu), 26.2 ($OCH_2CH_2CH_2$), 22.8 (CH_2), 14.2 (CH_2CH_3), 9.1 (CH_3).

HRMS (ESI-TOF) *m/z*: $[M + H]^+$ Calcd for $C_{31}H_{49}N_4O_7$ 589.3596; Found 589.3597.

Anal. RP-HPLC: t_R = 24.15 min, purity > 99%.

S9: 2-Methylisothiouronium iodide

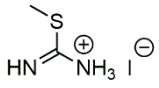

A mixture of thiourea (1.54 g, 20.2 mmol) and MeOH (15 mL) was stirred at ambient temperature under a N_2 atmosphere for 5 min before the careful addition of MeI (1.30 mL, 20.9 mmol). The reaction mixture was heated to 65 °C and stirred under a N_2 atmosphere, protected from light, for 90 min before being co-evaporated under reduced pressure with Et_2O (2 × 10 mL). The resulting yellow solid was transferred a fritted funnel and rinsed with Et_2O (300 mL). After drying the title compound was isolated as an amorphous white solid (4.26 g, 97%).

m.p. 114–116 °C (lit.[31] 115–117 °C).

^{1}H NMR (DMSO-d_6, 500 MHz): δ 8.89 (s, 4H, 2 × NH_2), 2.56 (s, 3H, CH_3).

^{13}C NMR (DMSO-d_6, 125 MHz): δ 171.1, 13.4 (CH_3).

HRMS (ESI-TOF) *m/z*: $[M + H]^+$ Calcd for $C_2H_6N_2S$ 91.0324; Found 91.0324.

Data is in accordance with the literature.[31]

^{1}H, ^{13}C, HSQC, and HMBC NMR Spectra

NMR spectra were processed using Bruker TopSpin 3.6.1.

The NMR spectral data for the synthesised compounds are available on figshare at https://doi.org/10.6084/m9.figshare.28340399.v2. FID files for all NMR spectra are numbered according to their appearance in the manuscript and ESI, experiments are numbered according to the following: 1 (^{1}H NMR), 2 (^{13}C NMR), 3 (HSQC), and 4 (HMBC).

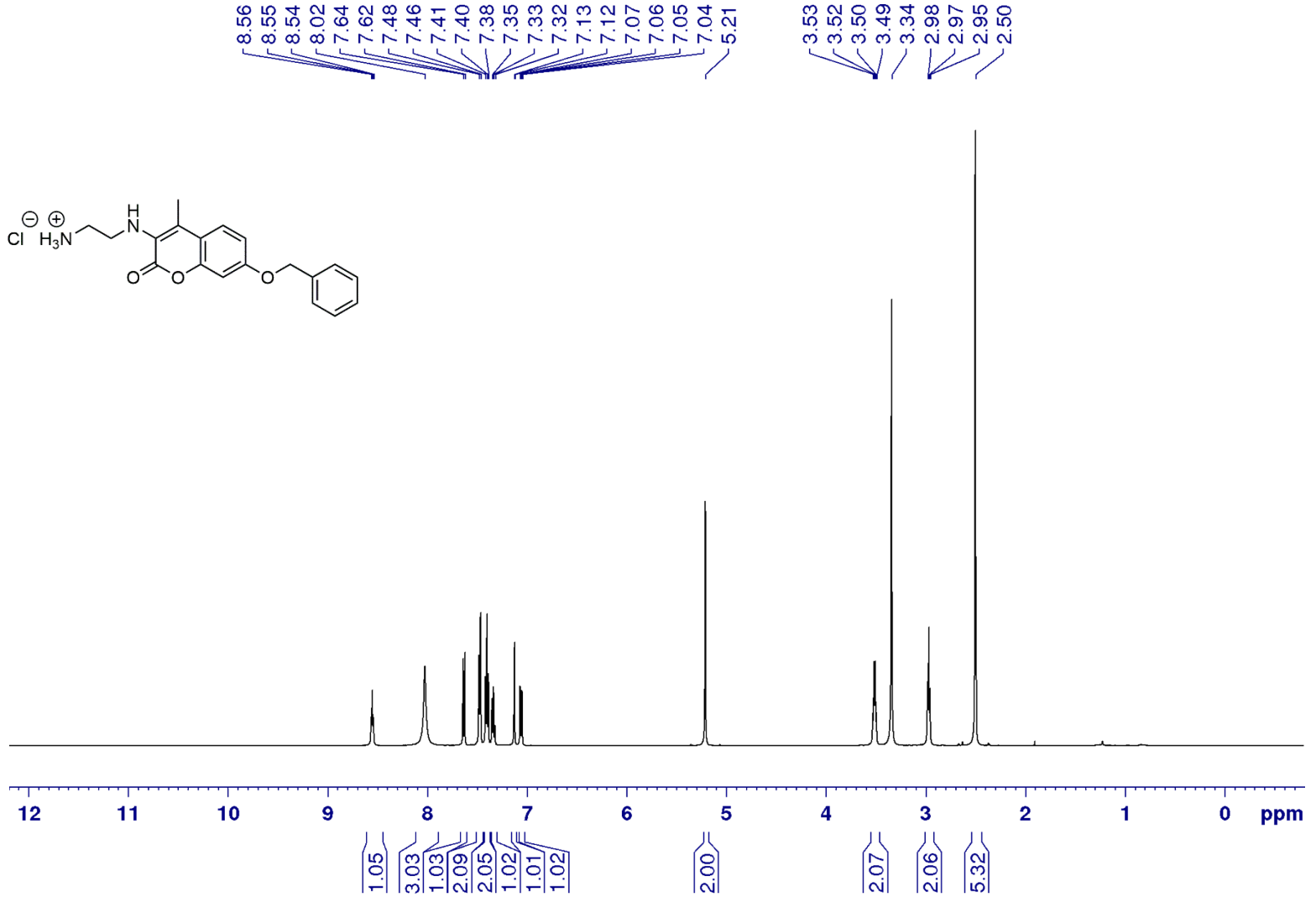

Figure S5: ^{1}H NMR (500 MHz) spectrum of coumarin **1** in DMSO-d_6.

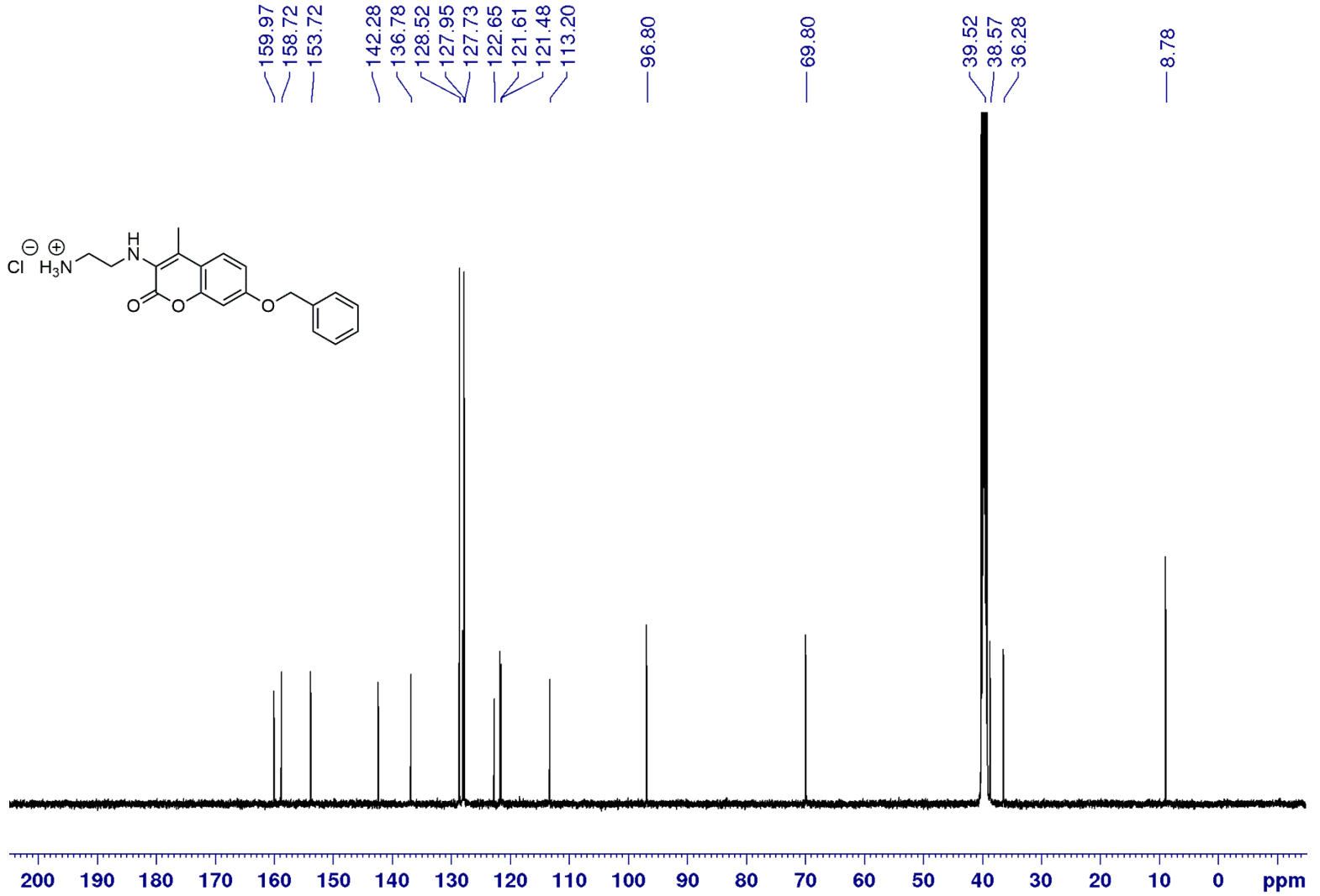

Figure S6: ^{13}C NMR (125 MHz) spectrum of coumarin **1** in DMSO-d_6.

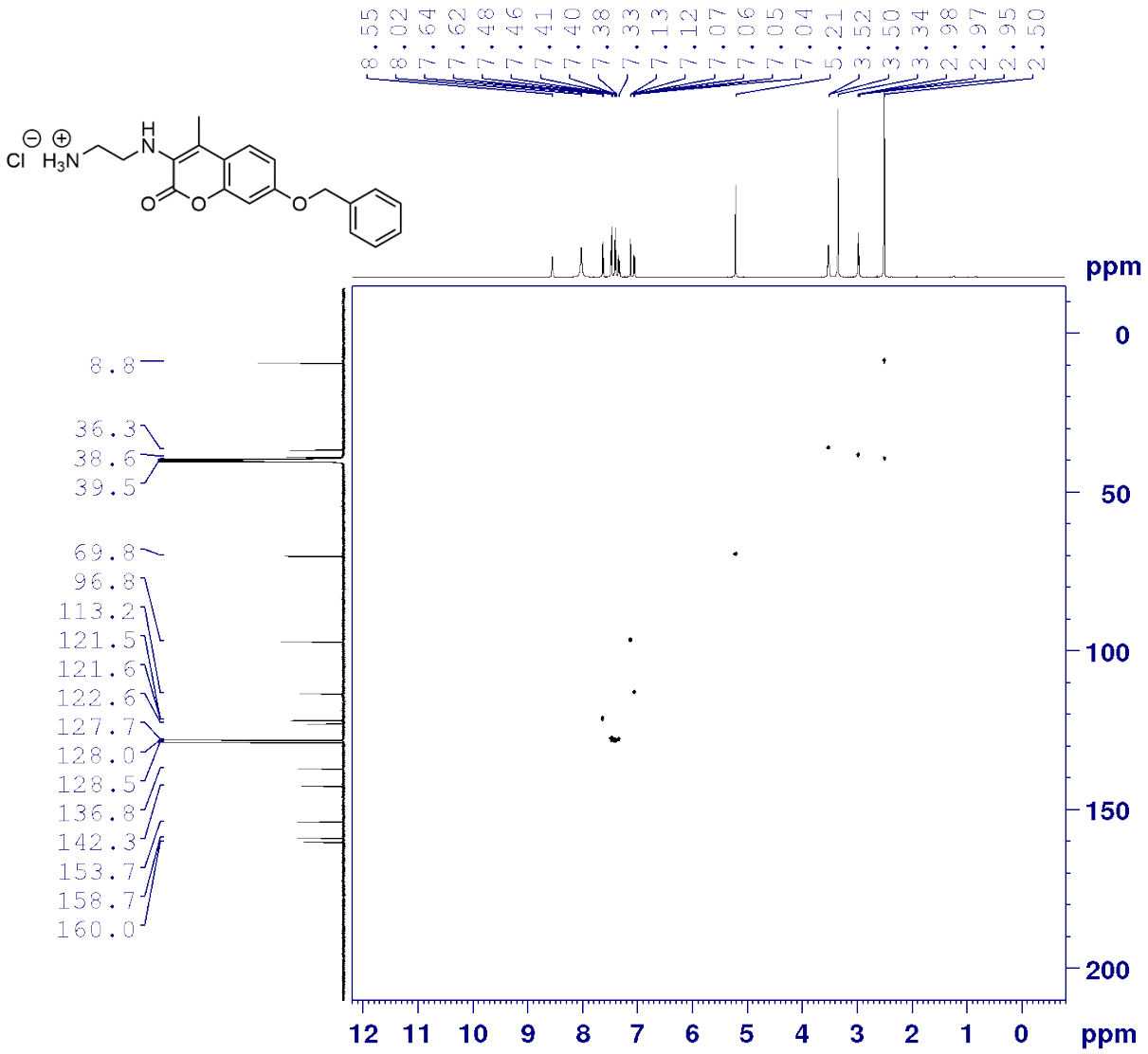

Figure S7: HSQC NMR (500 MHz) spectrum of coumarin **1** in DMSO-d_6.

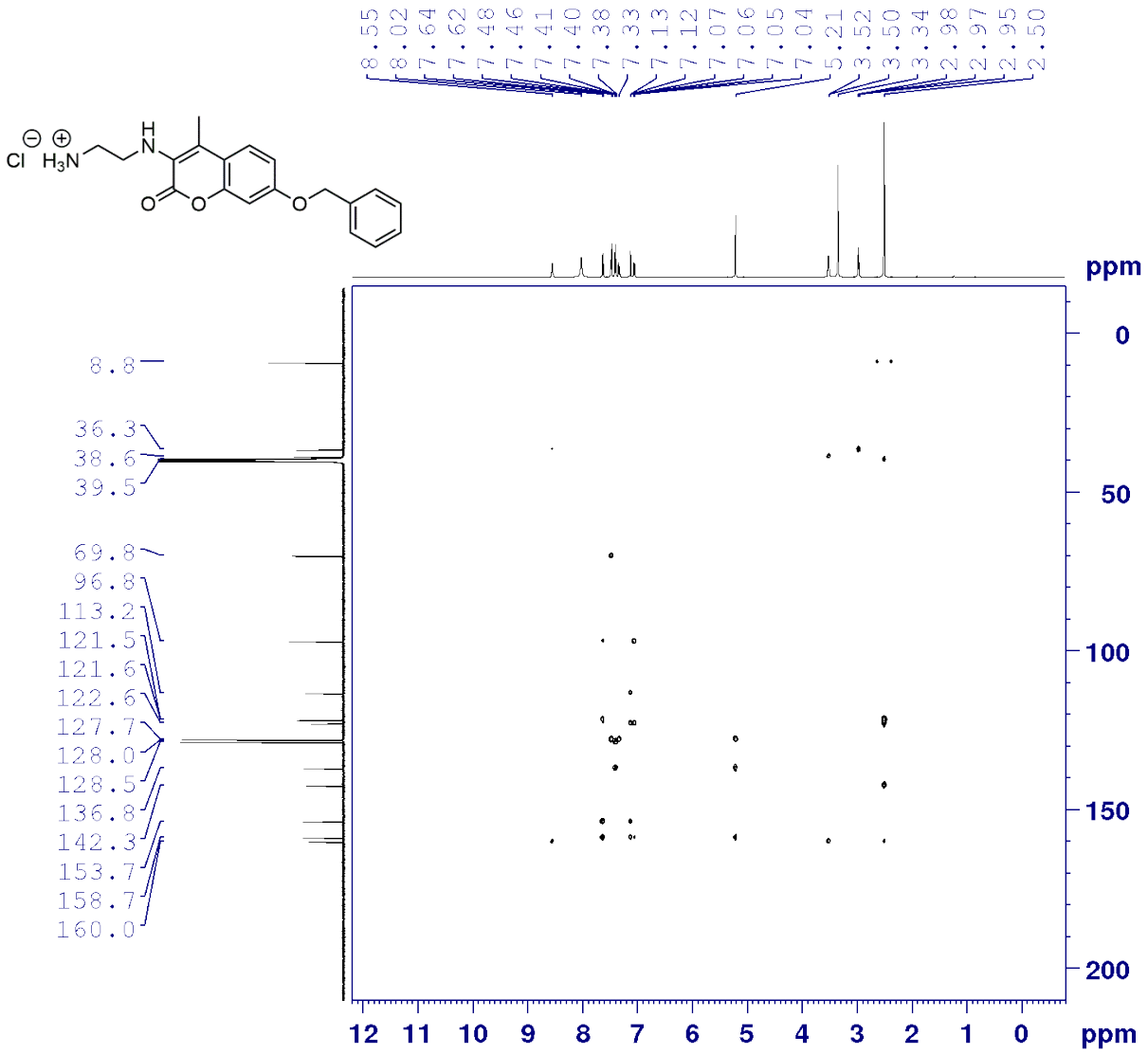

Figure S8: HMBC NMR (500 MHz) spectrum of coumarin **1** in DMSO-d_6.

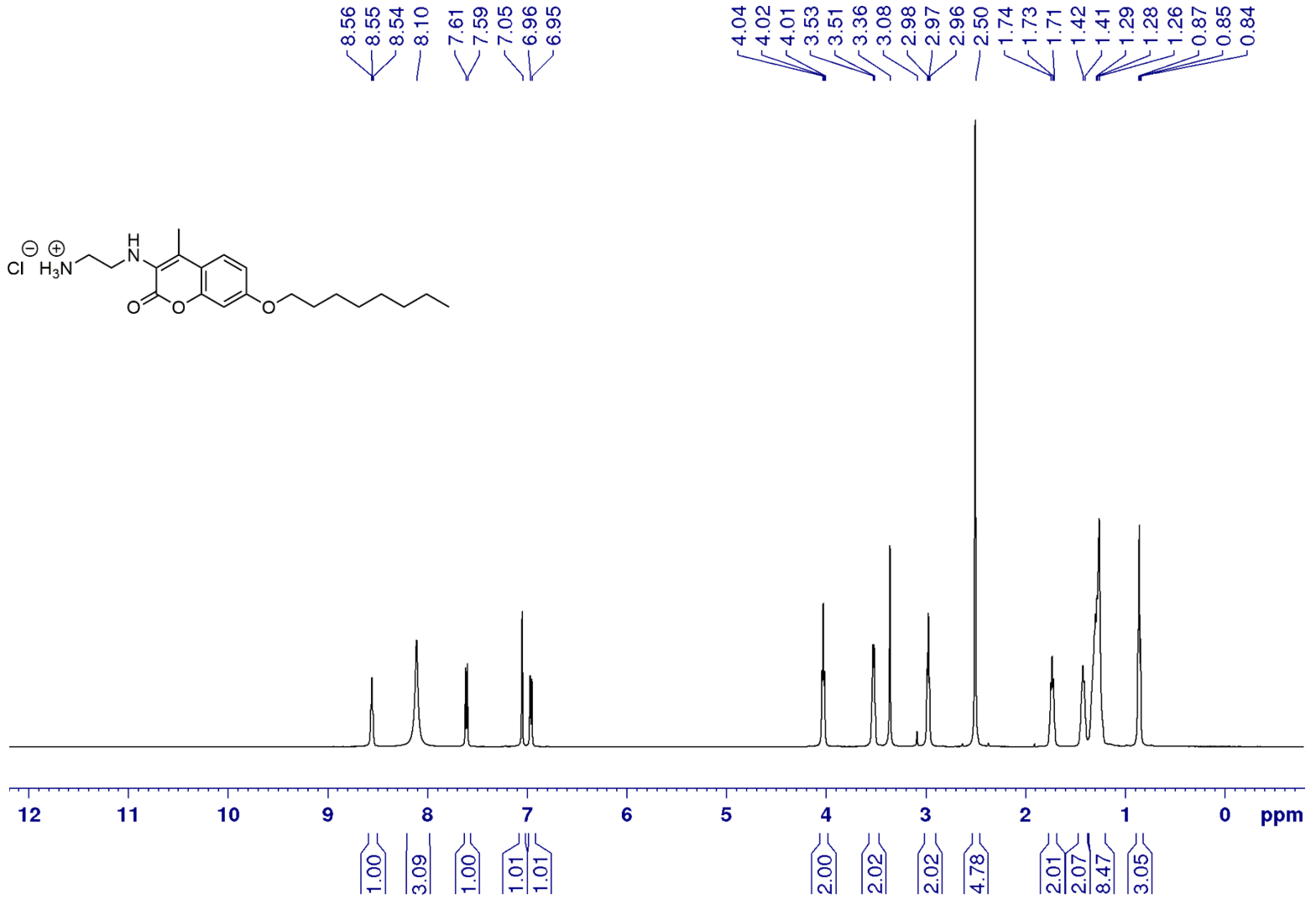

Figure S9: ^{1}H NMR (500 MHz) spectrum of coumarin **2** in DMSO-d_6.

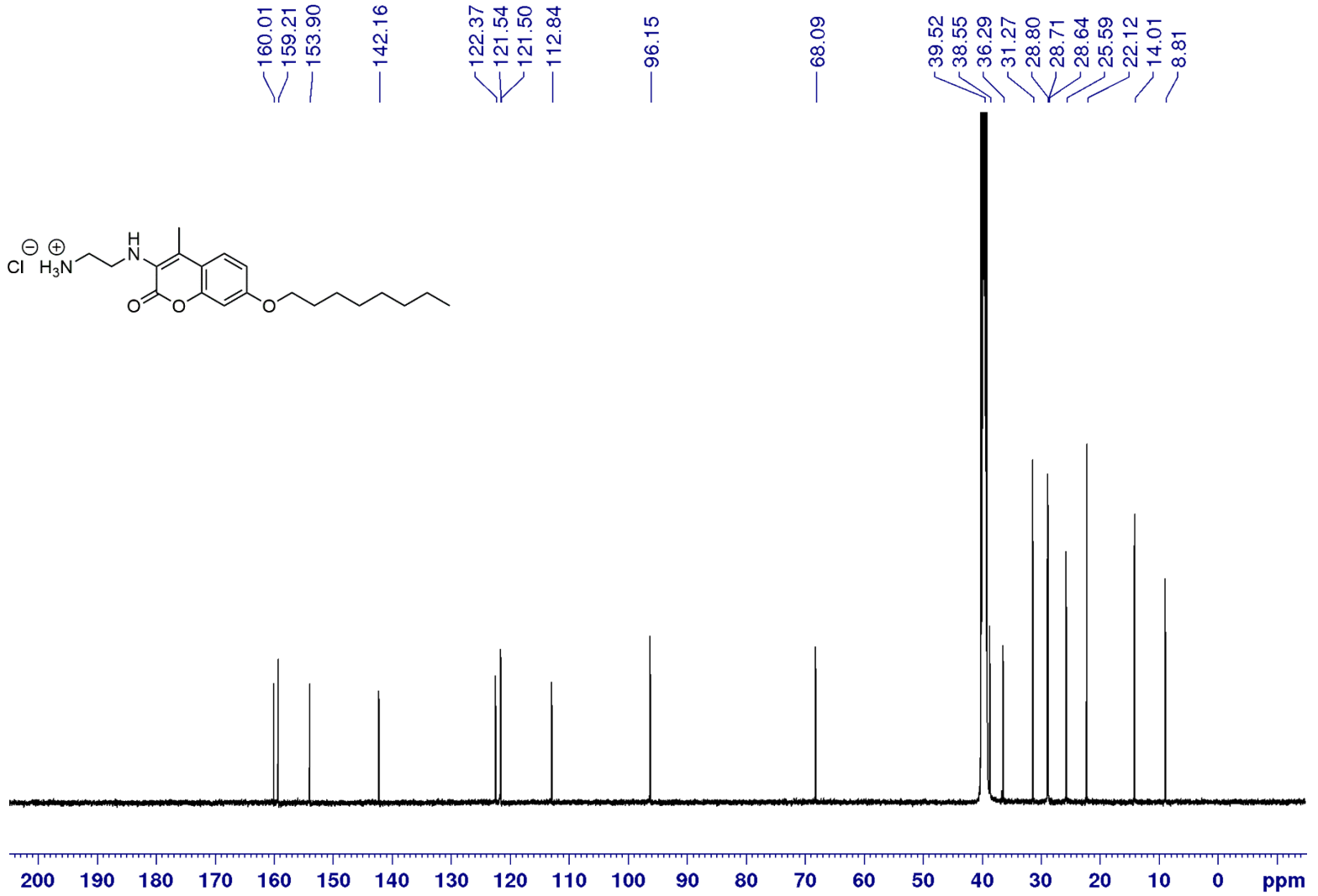

Figure S10: ^{13}C NMR (125 MHz) spectrum of coumarin **2** in DMSO-d_6.

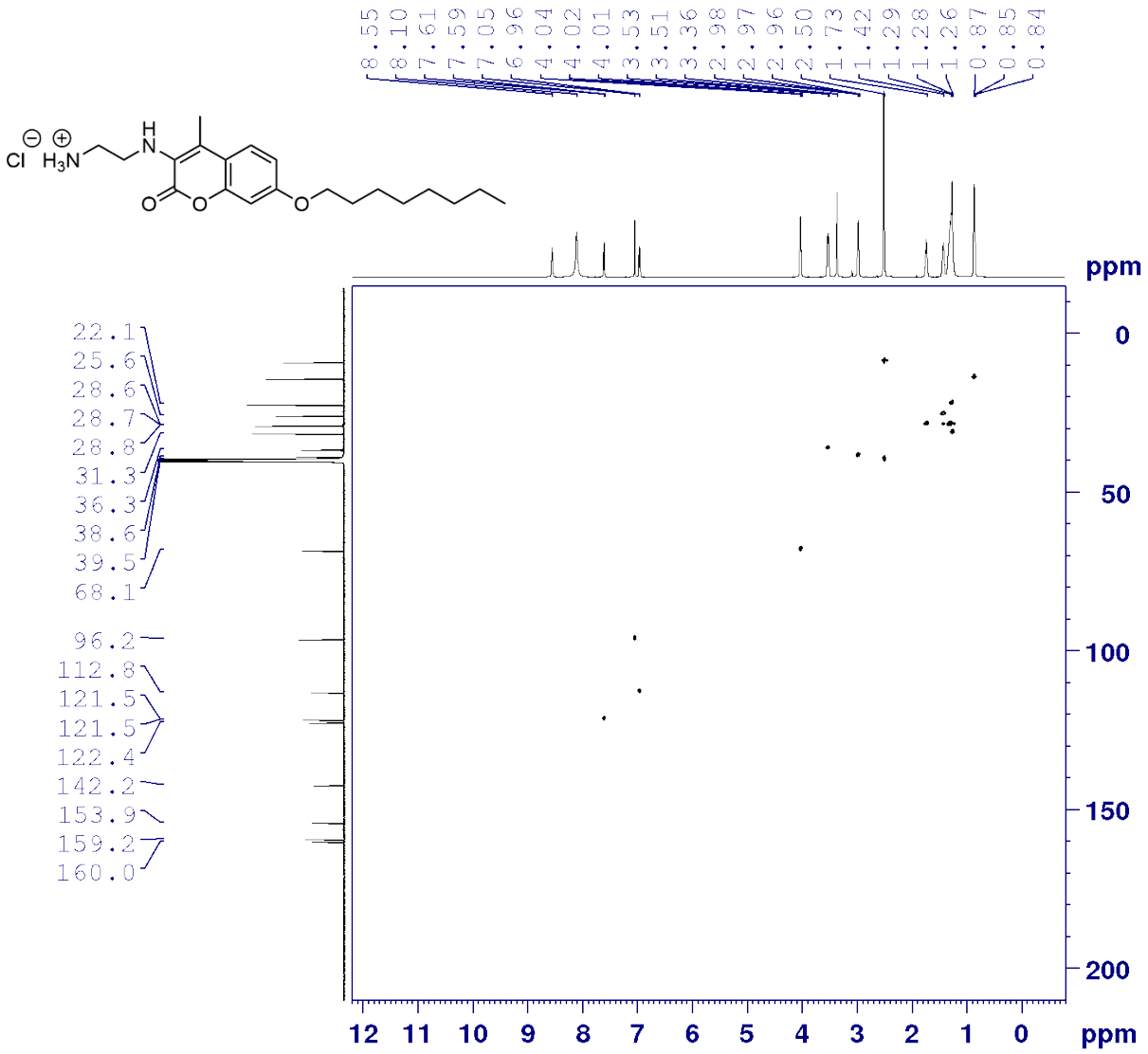

Figure S11: HSQC NMR (500 MHz) spectrum of coumarin **2** in DMSO-d_6.

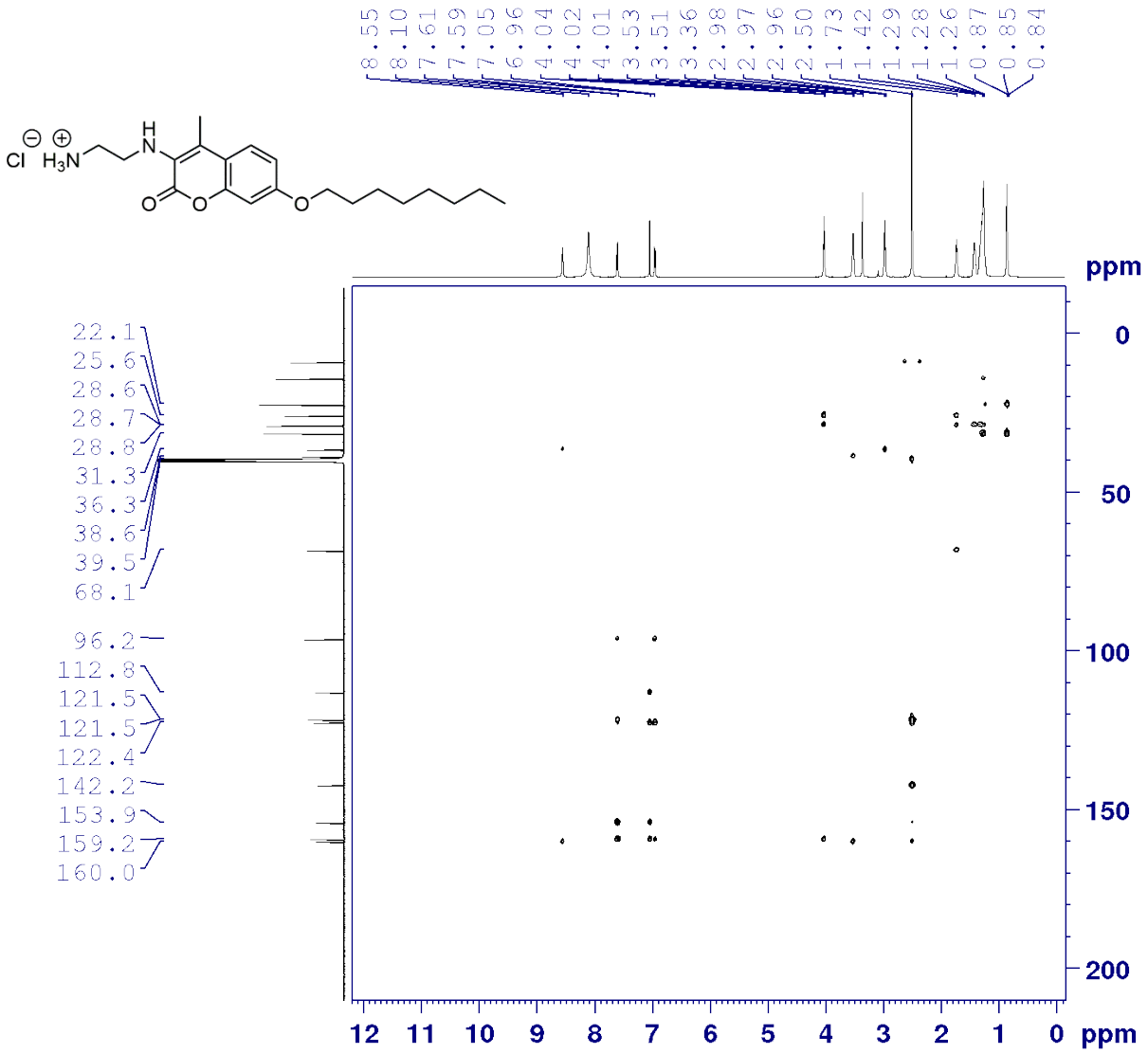

Figure S12: HMBC NMR (500 MHz) spectrum of coumarin **2** in DMSO-d_6.

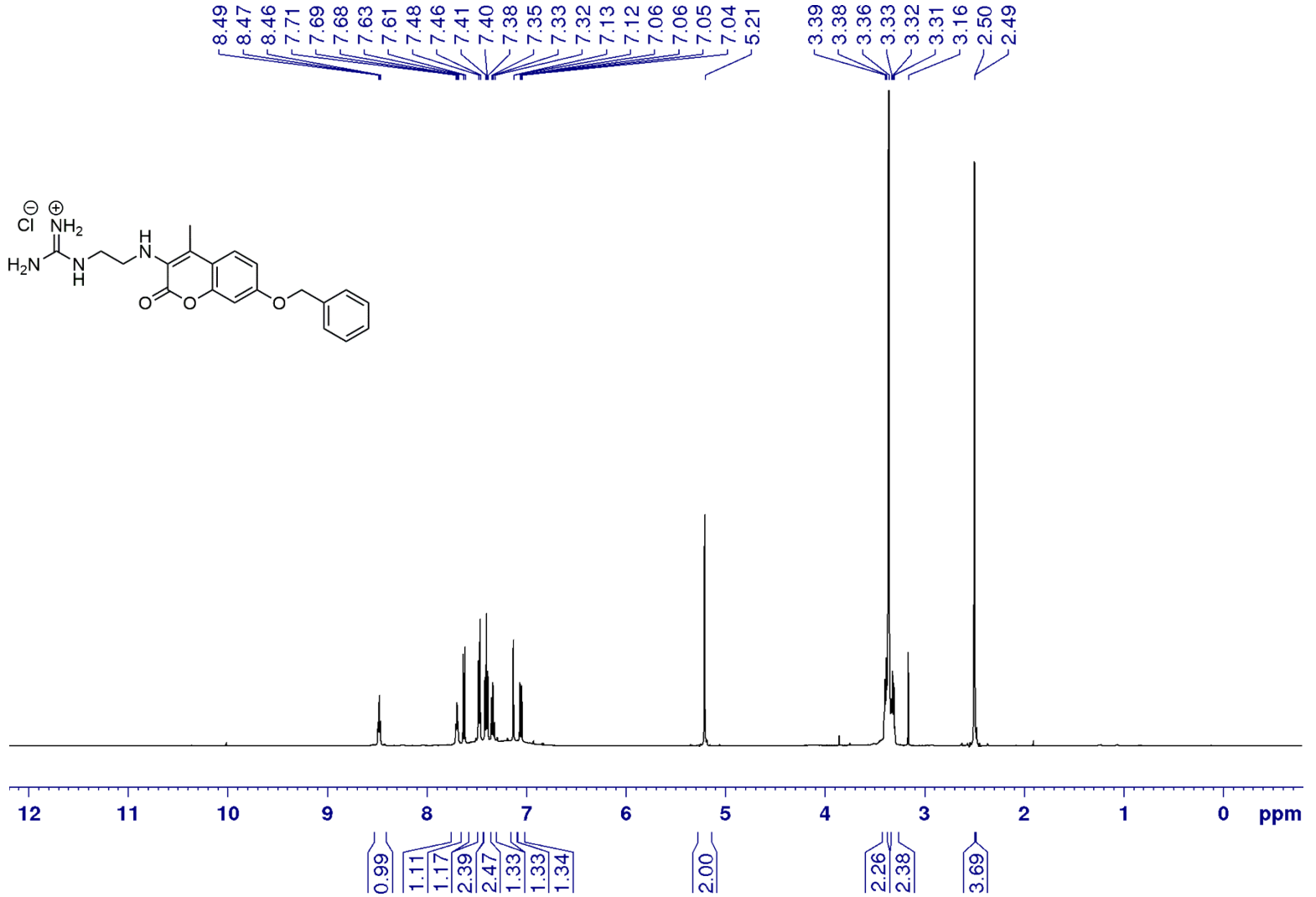

Figure S13: ^{1}H NMR (500 MHz) spectrum of coumarin **3** in DMSO-d_6.

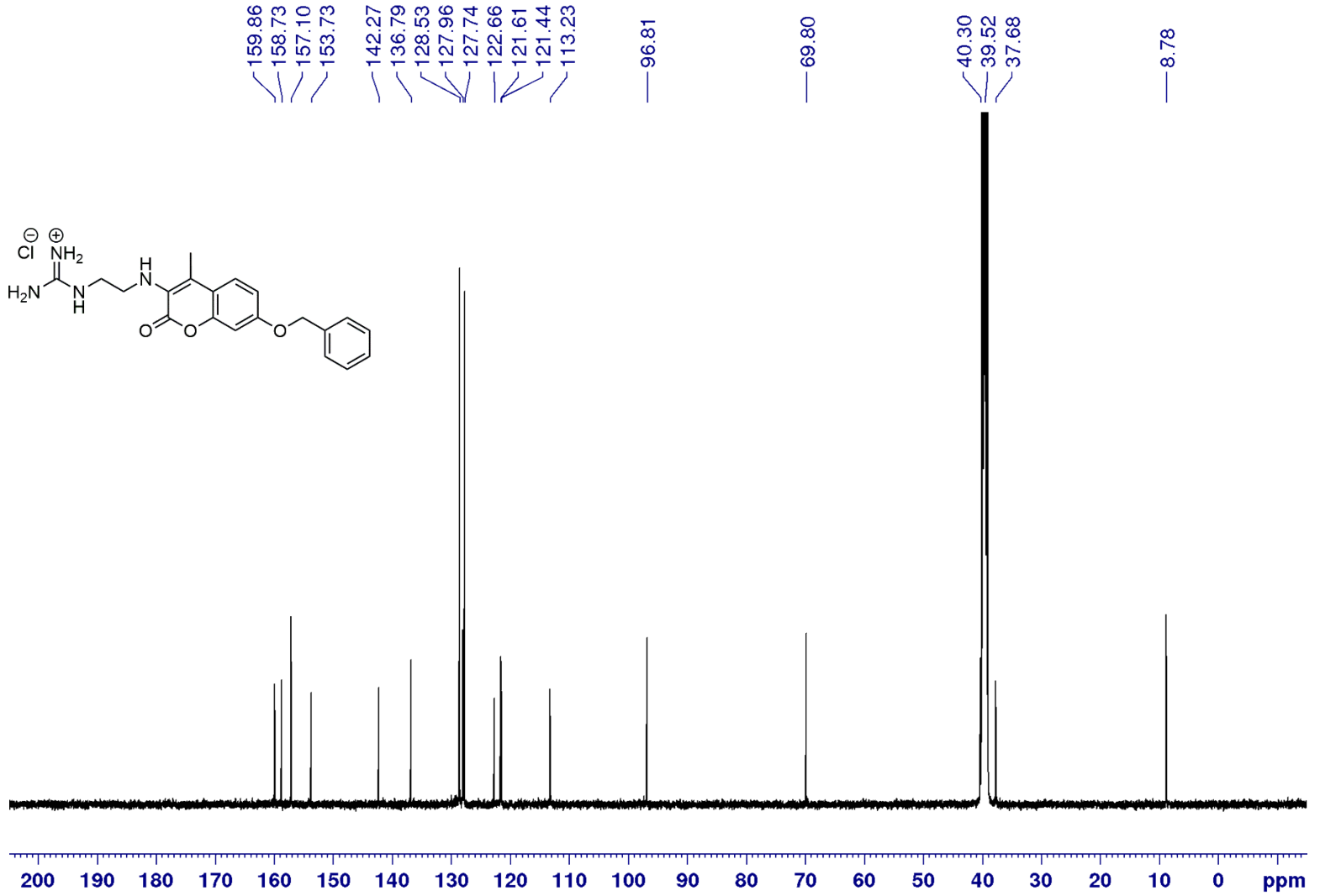

Figure S14: ^{13}C NMR (125 MHz) spectrum of coumarin **3** in DMSO-d_6.

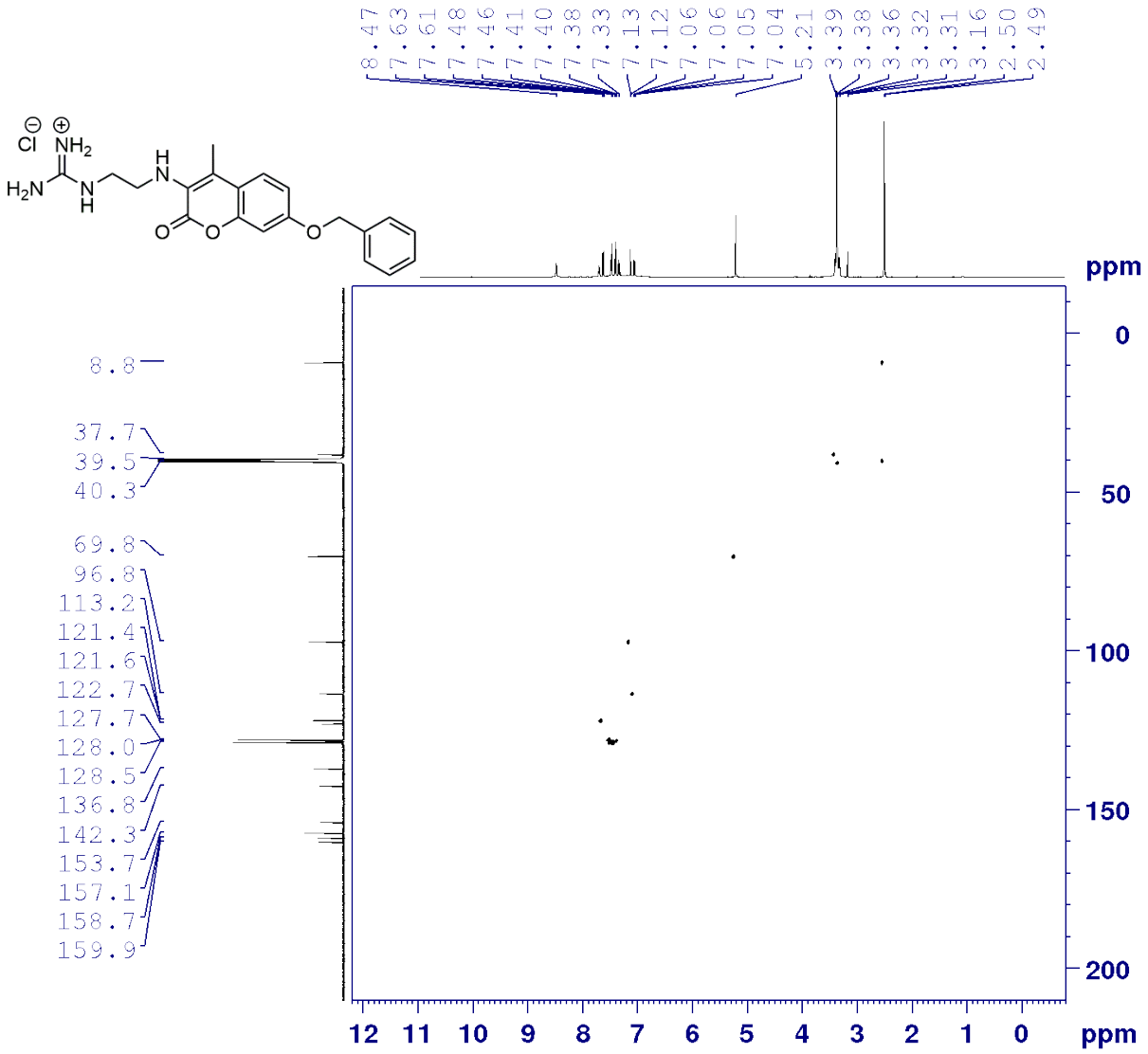

Figure S15: HSQC NMR (500 MHz) spectrum of coumarin **3** in DMSO-d_6.

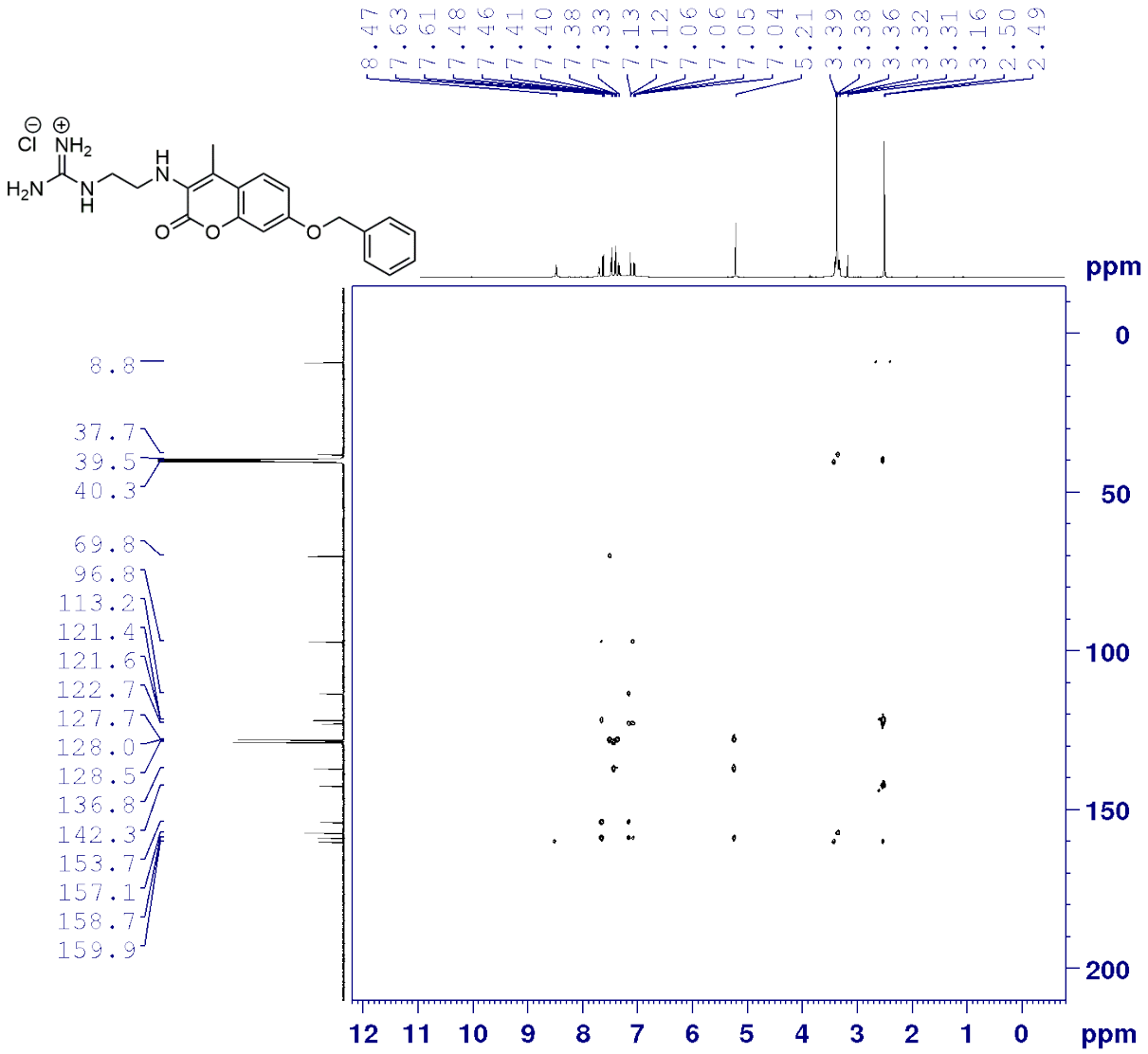

Figure S16: HMBC NMR (500 MHz) spectrum of coumarin **3** in DMSO-d_6.

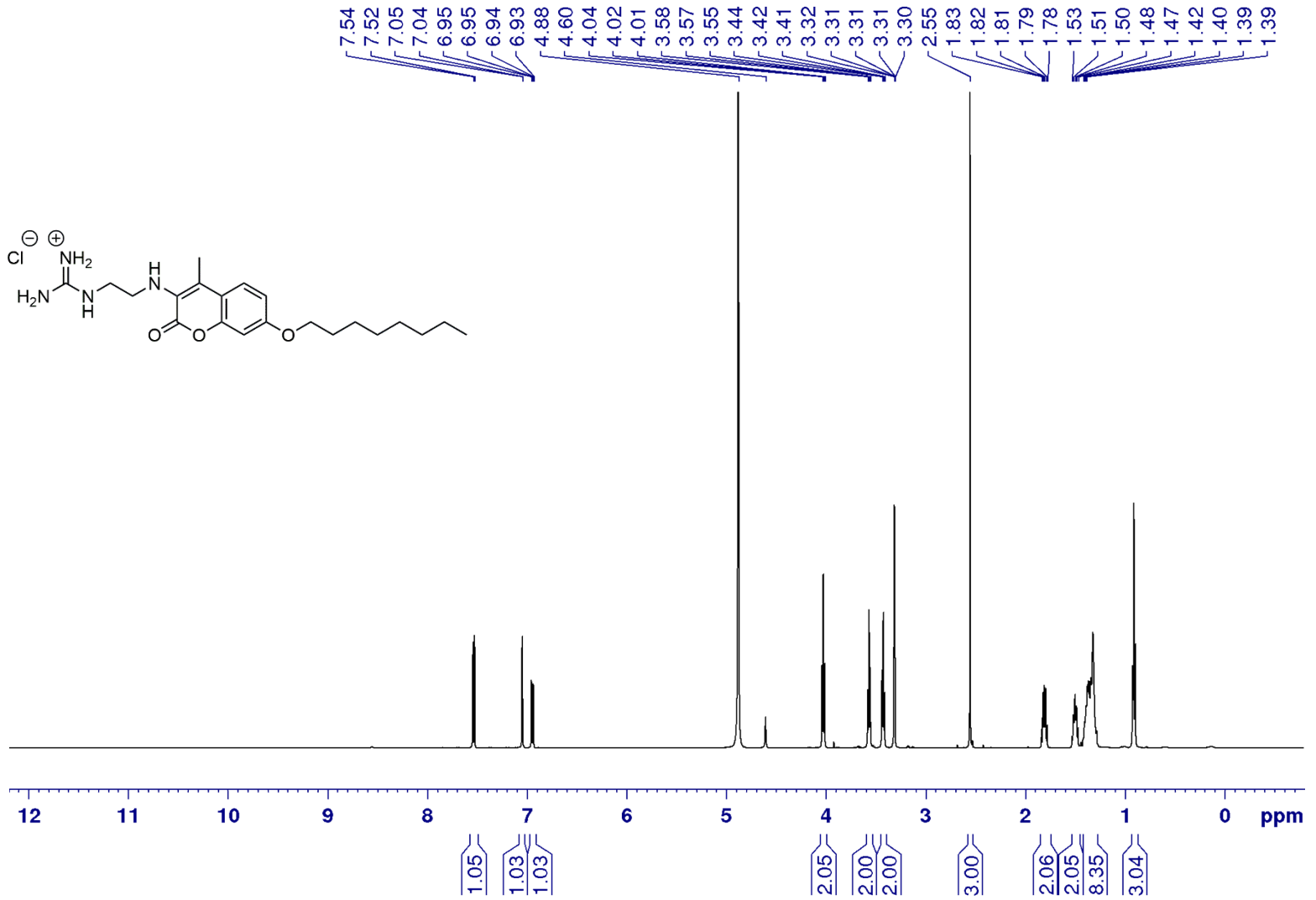

Figure S17: ^{1}H NMR (500 MHz) spectrum of coumarin **4** in MeOD.

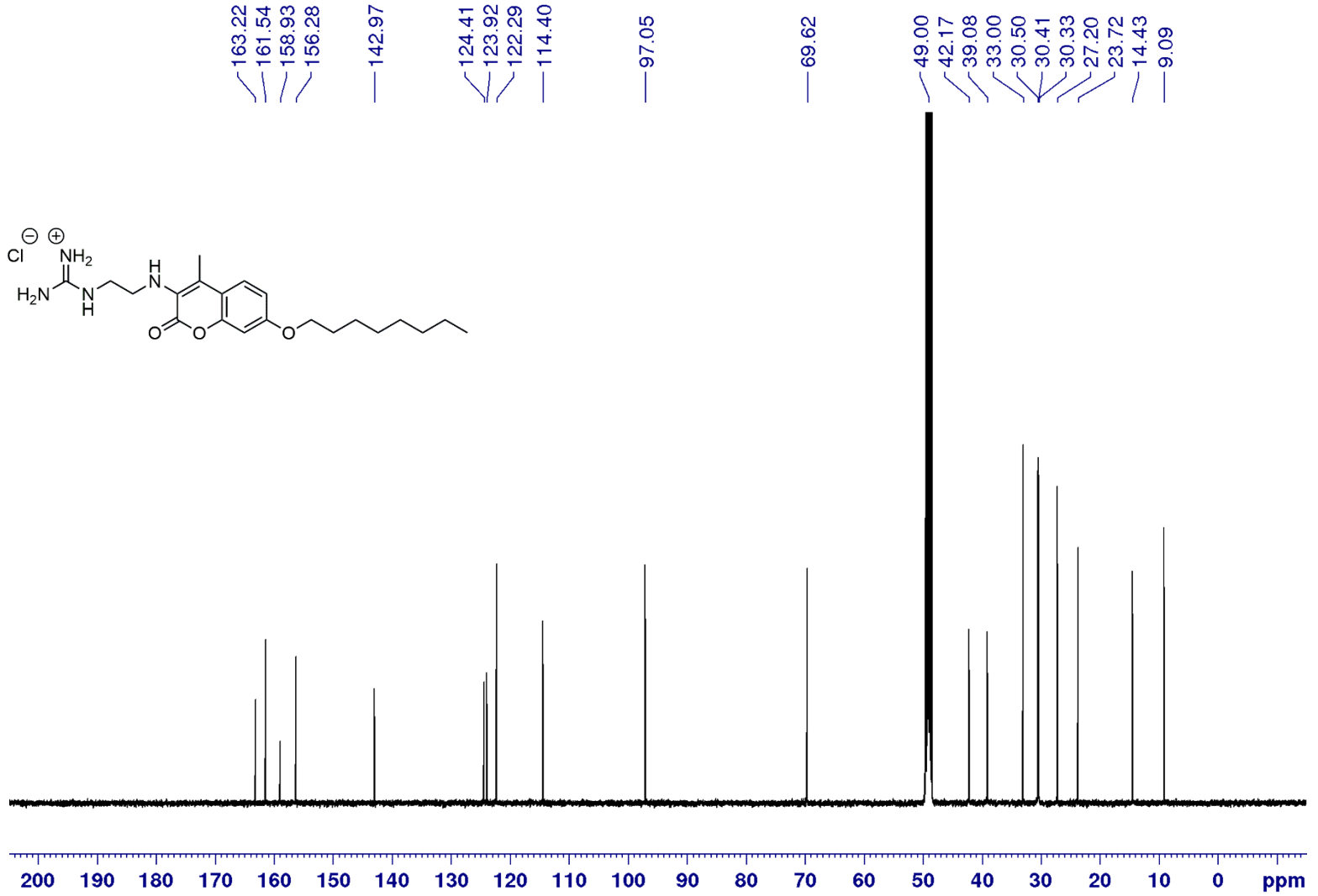

Figure S18: ^{13}C NMR (125 MHz) spectrum of coumarin **4** in MeOD.

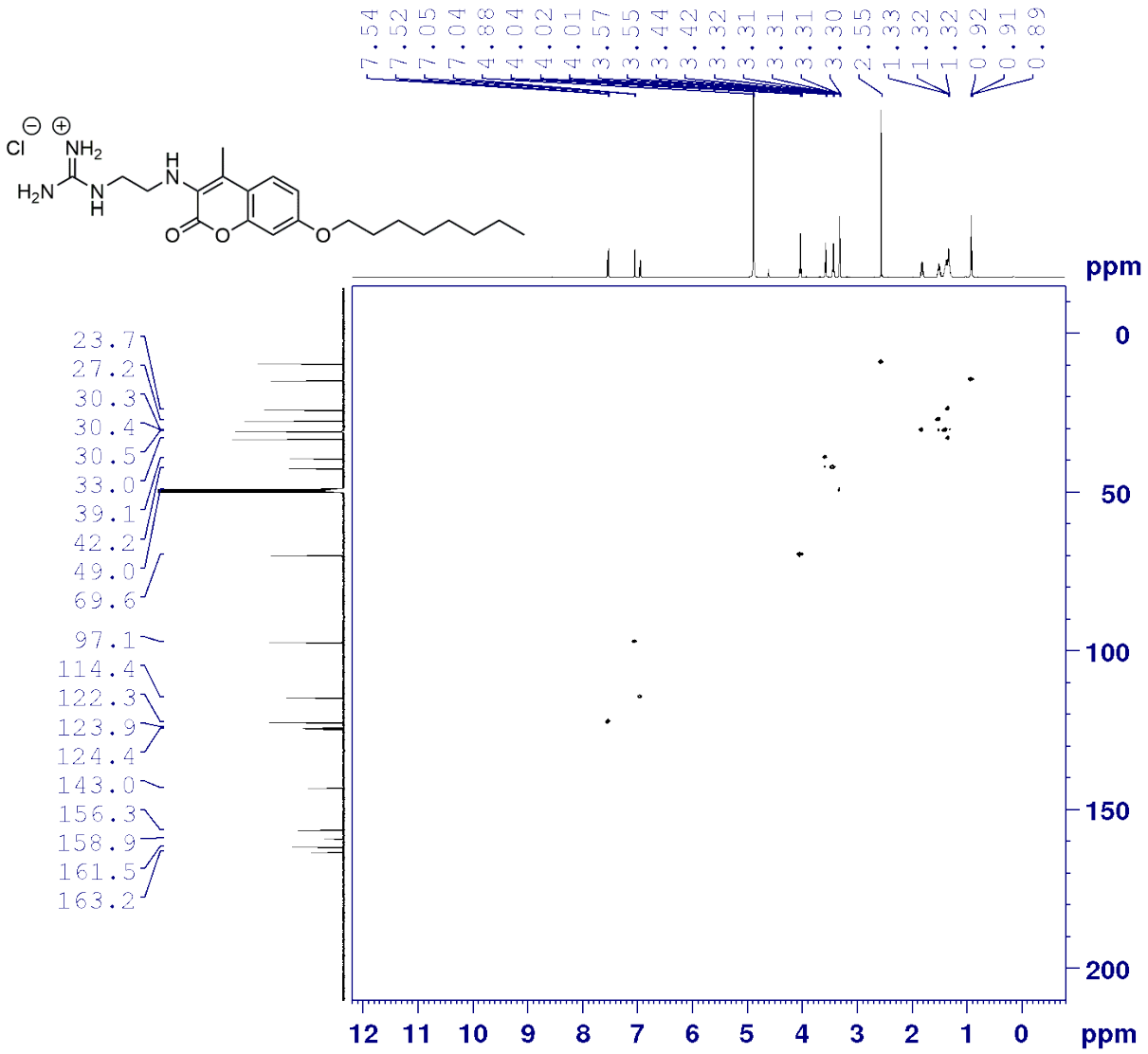

Figure S19: HSQC NMR (500 MHz) spectrum of coumarin **4** in MeOD.

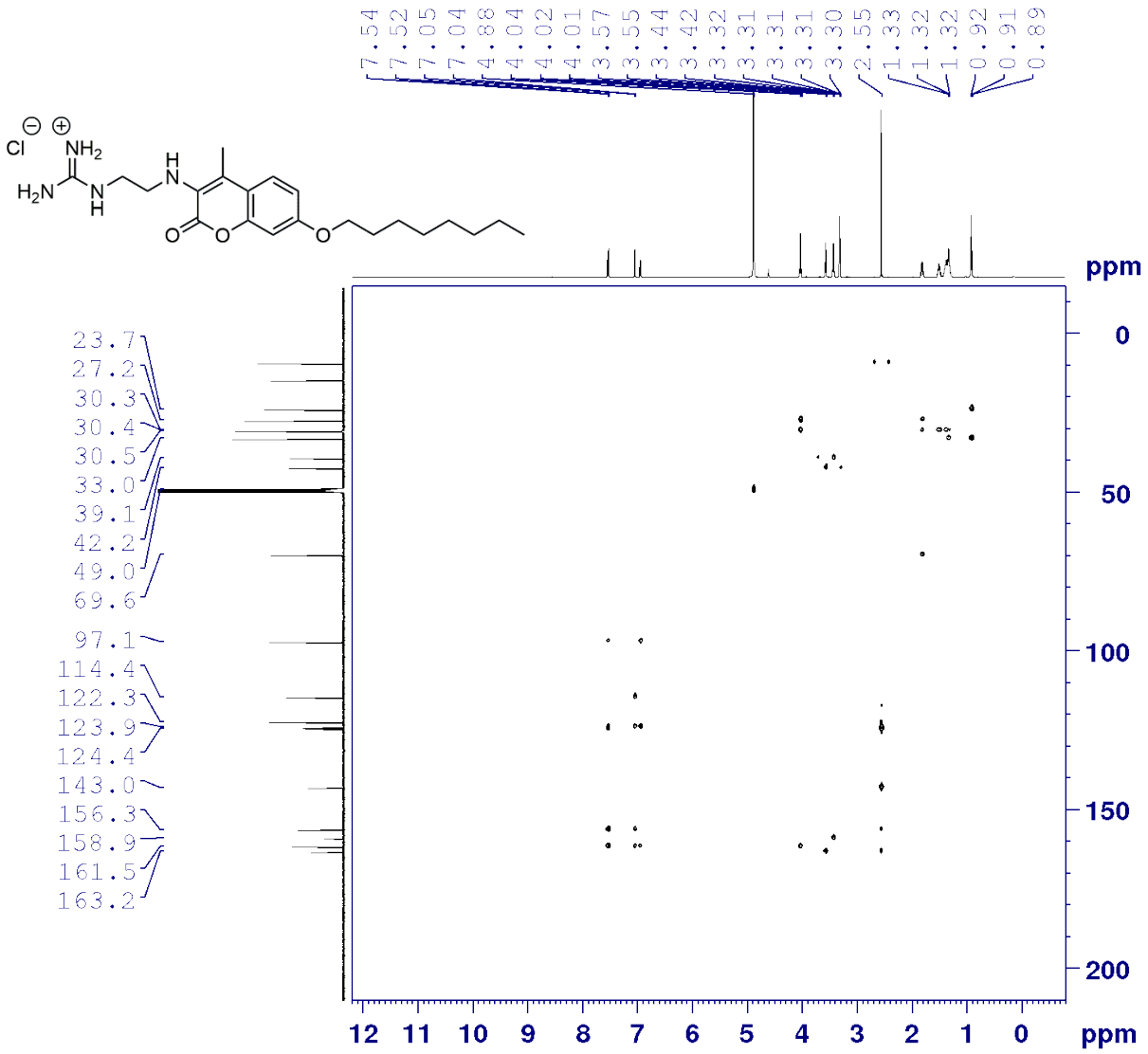

Figure S20: HMBC NMR (500 MHz) spectrum of coumarin **4** in MeOD.

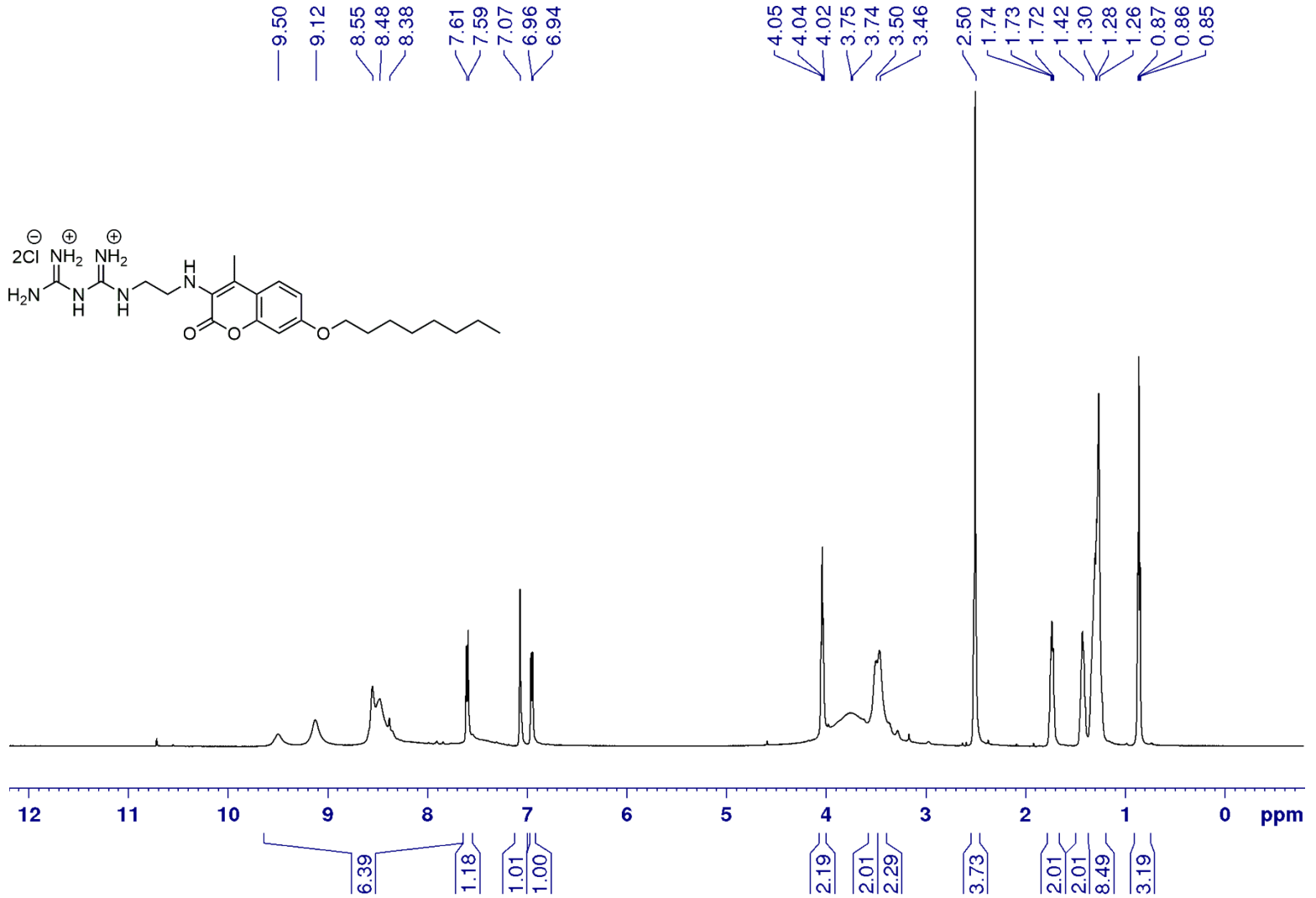

Figure S21: ^{1}H NMR (500 MHz) spectrum of coumarin **5** in DMSO-d_6.

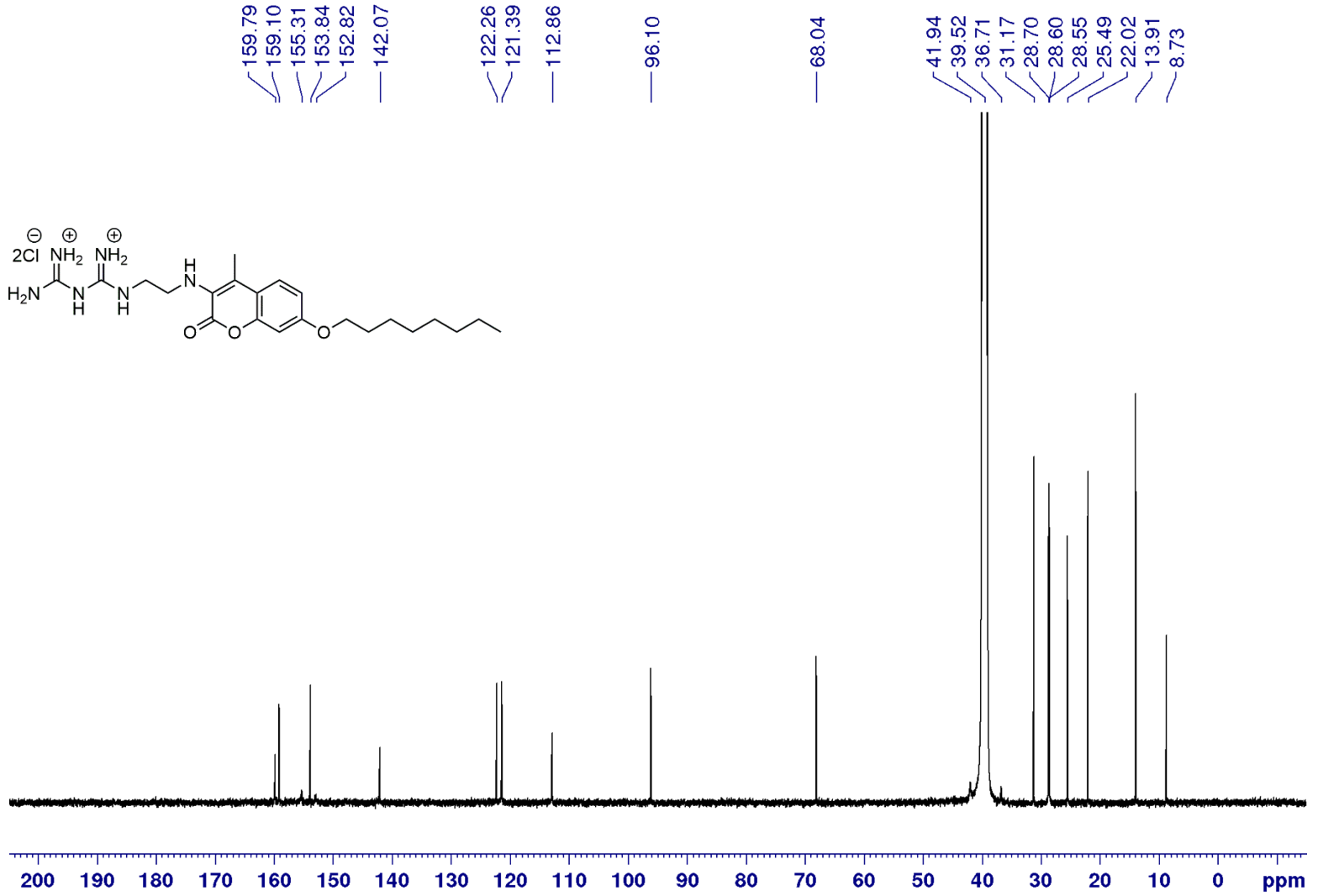

Figure S22: ^{13}C NMR (125 MHz) spectrum of coumarin **5** in DMSO-d_6.

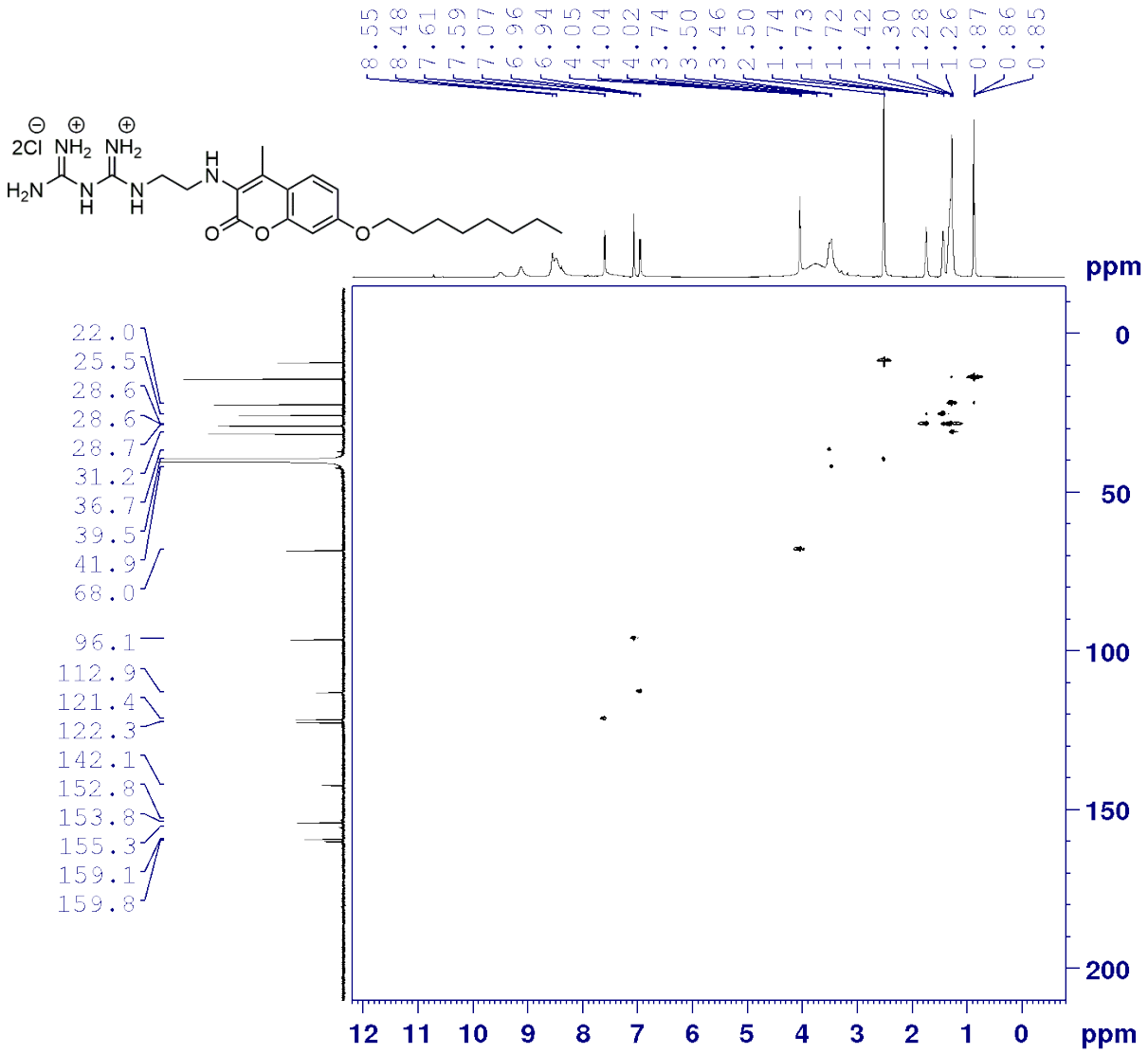

Figure S23: HSQC NMR (500 MHz) spectrum of coumarin **5** in DMSO-d_6.

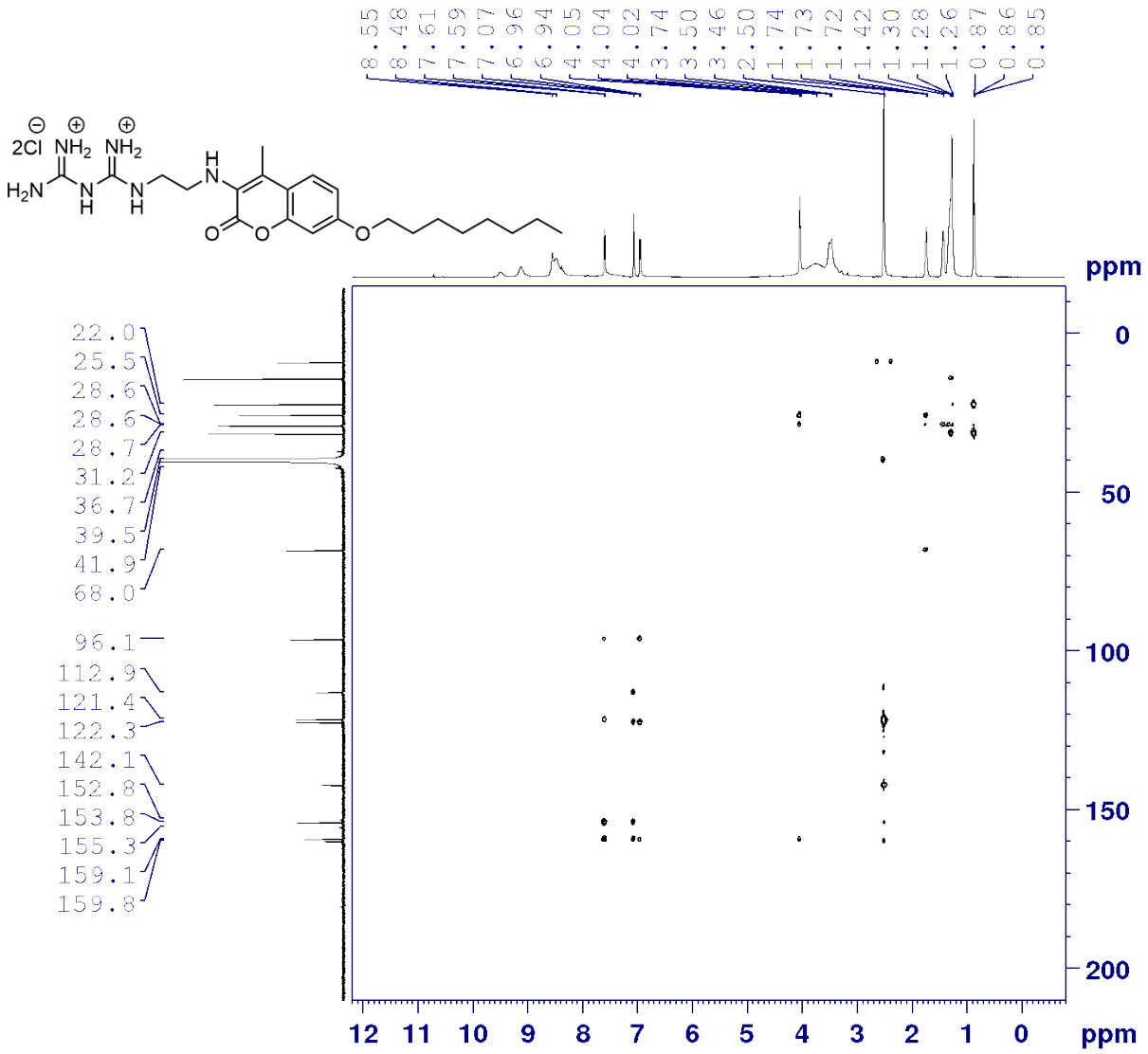

Figure S24: HMBC NMR (500 MHz) spectrum of coumarin **5** in DMSO-d_6.

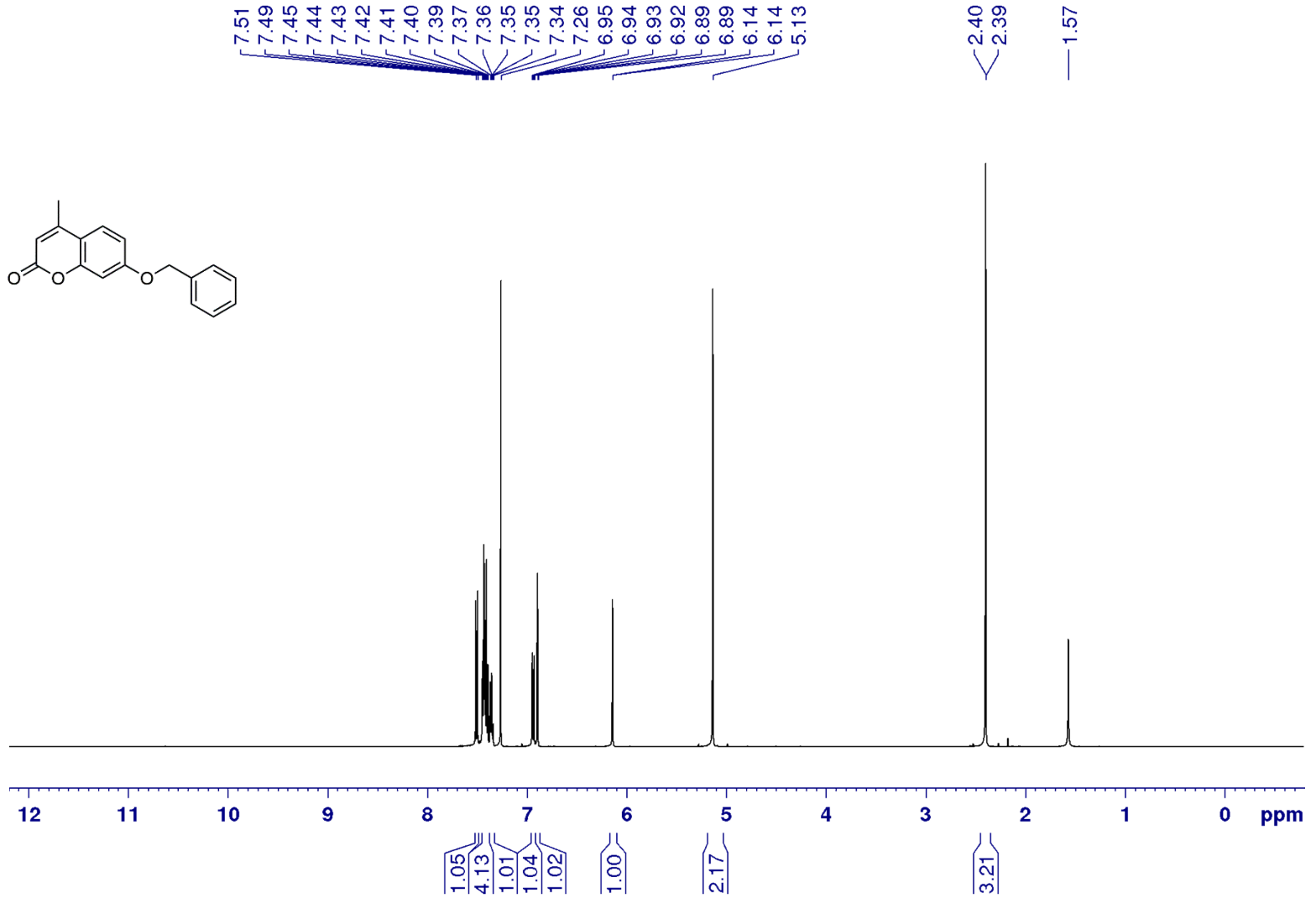

Figure S25: ^{1}H NMR (500 MHz) spectrum of coumarin **S2a** in $CDCl_3$.

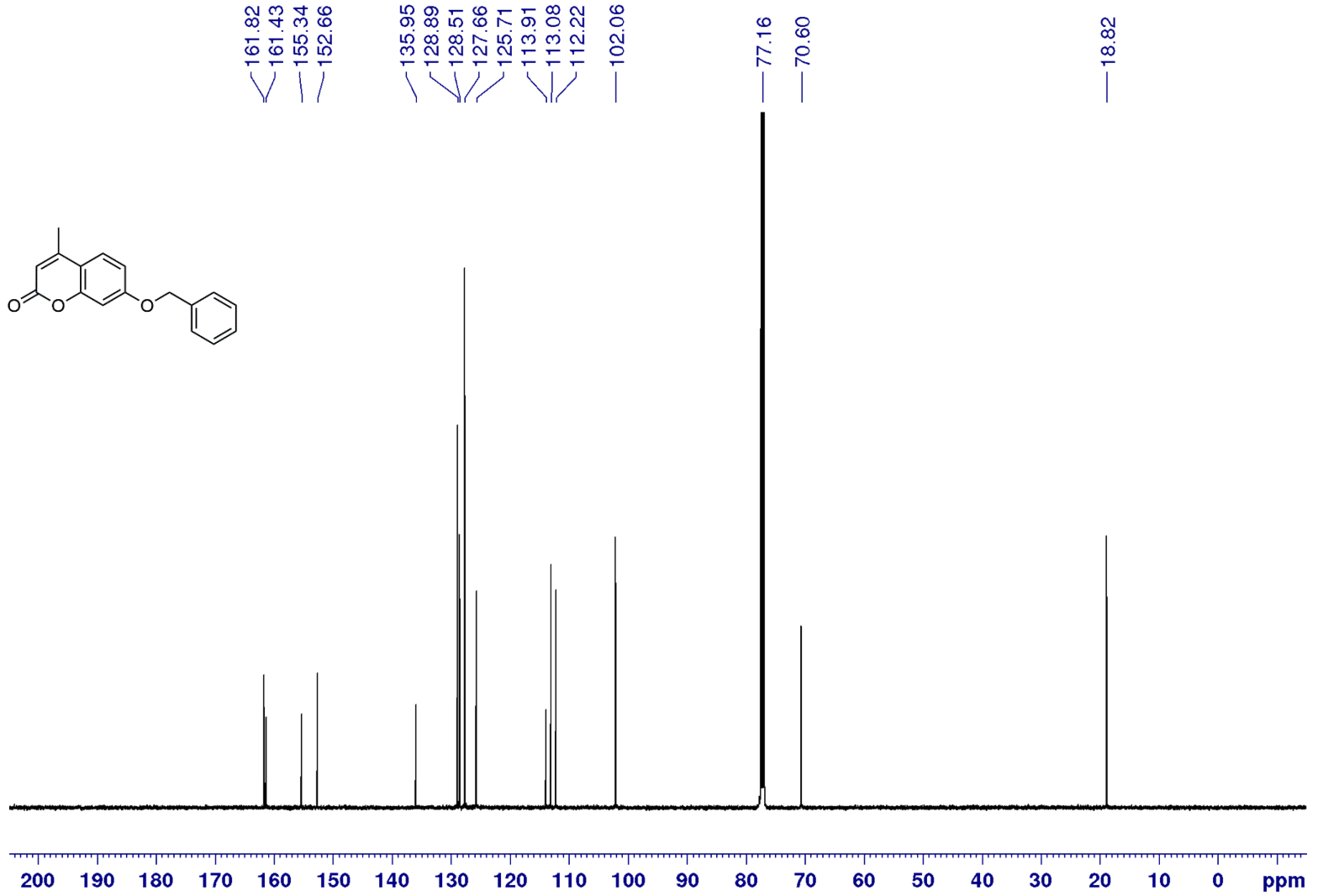

Figure S26: ^{13}C NMR (125 MHz) spectrum of coumarin **S2a** in $CDCl_3$.

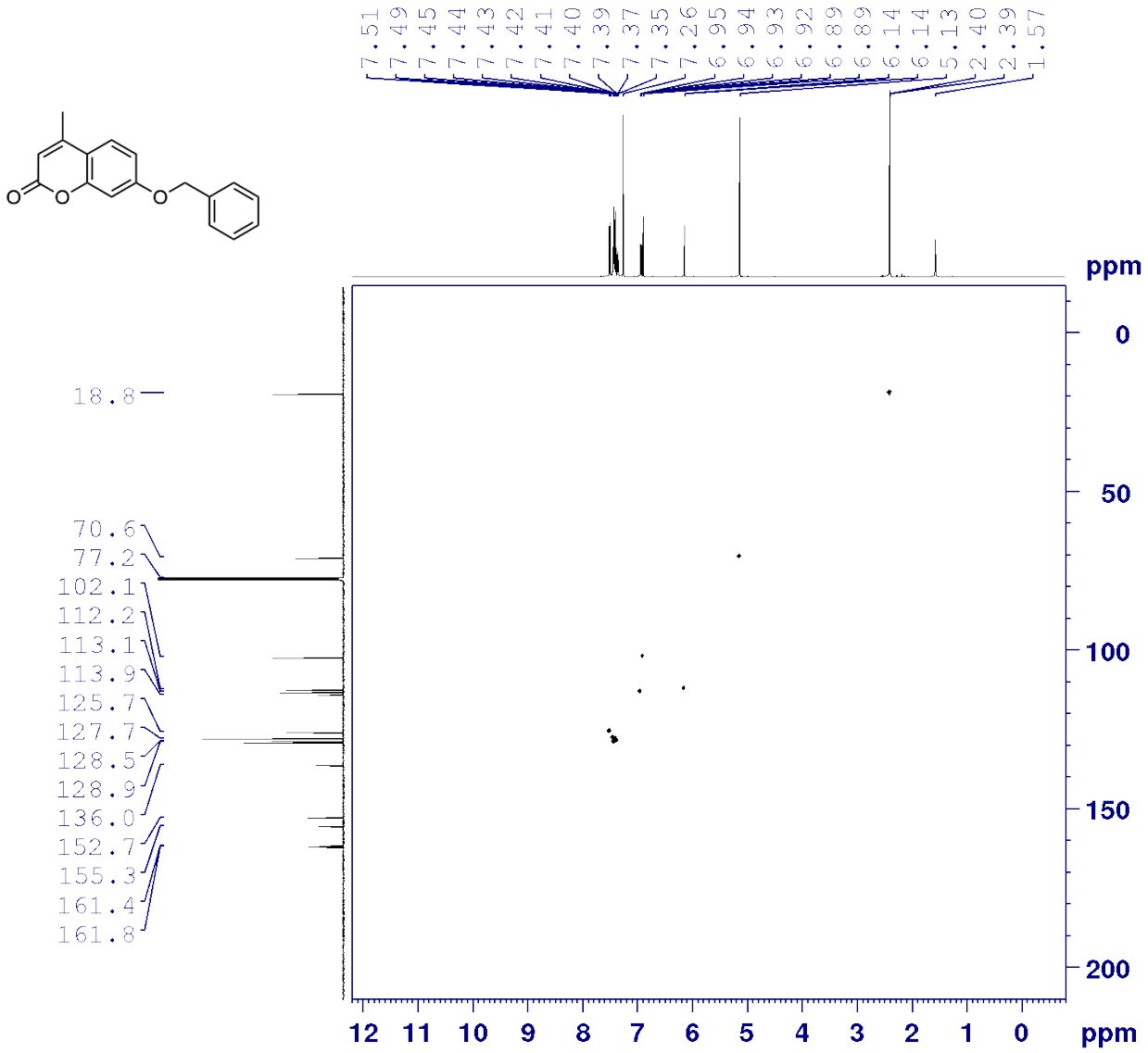

Figure S27: HSQC NMR (500 MHz) spectrum of coumarin **S2a** in $CDCl_3$.

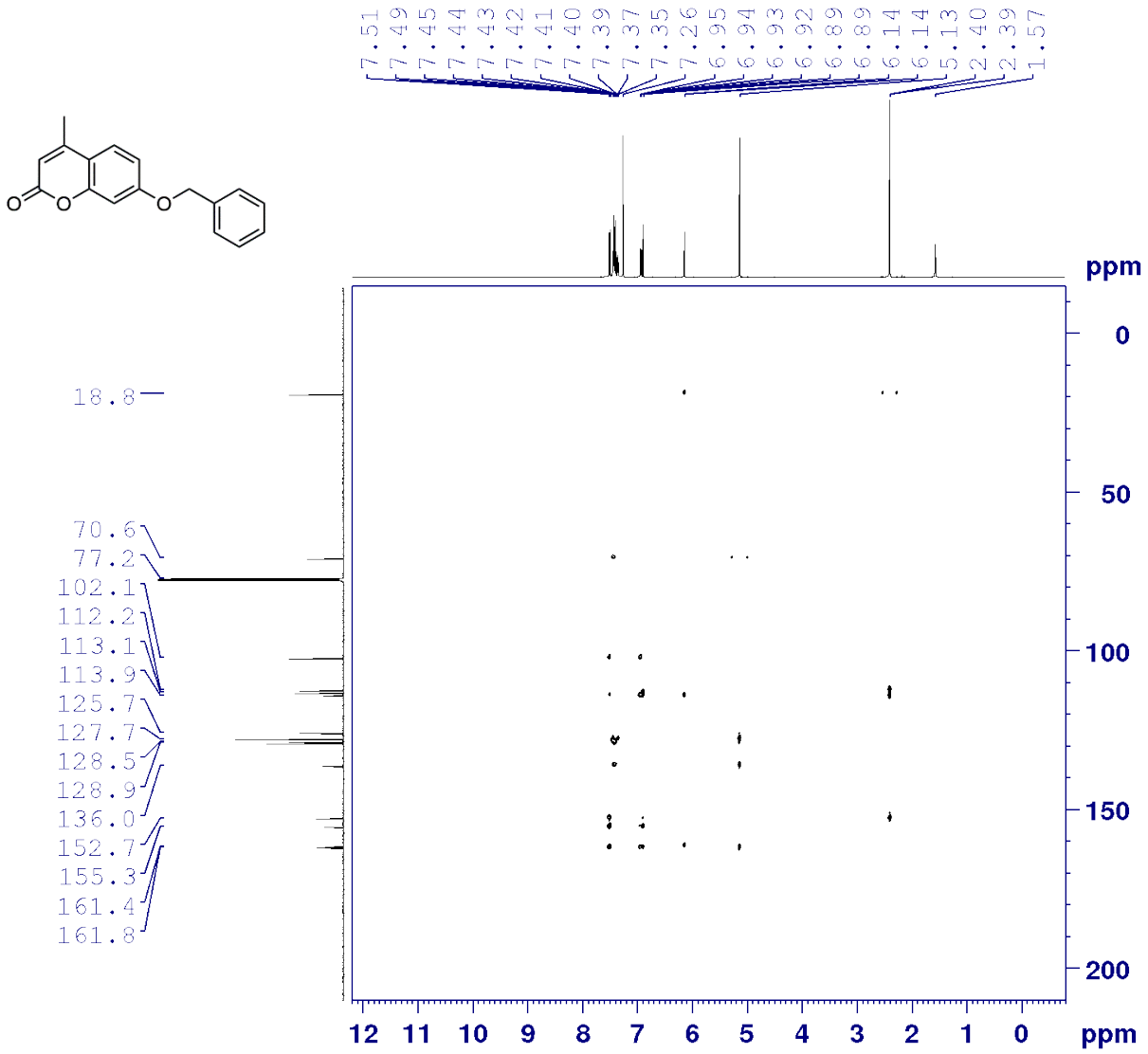

Figure S28: HMBC NMR (500 MHz) spectrum of coumarin **S2a** in $CDCl_3$.

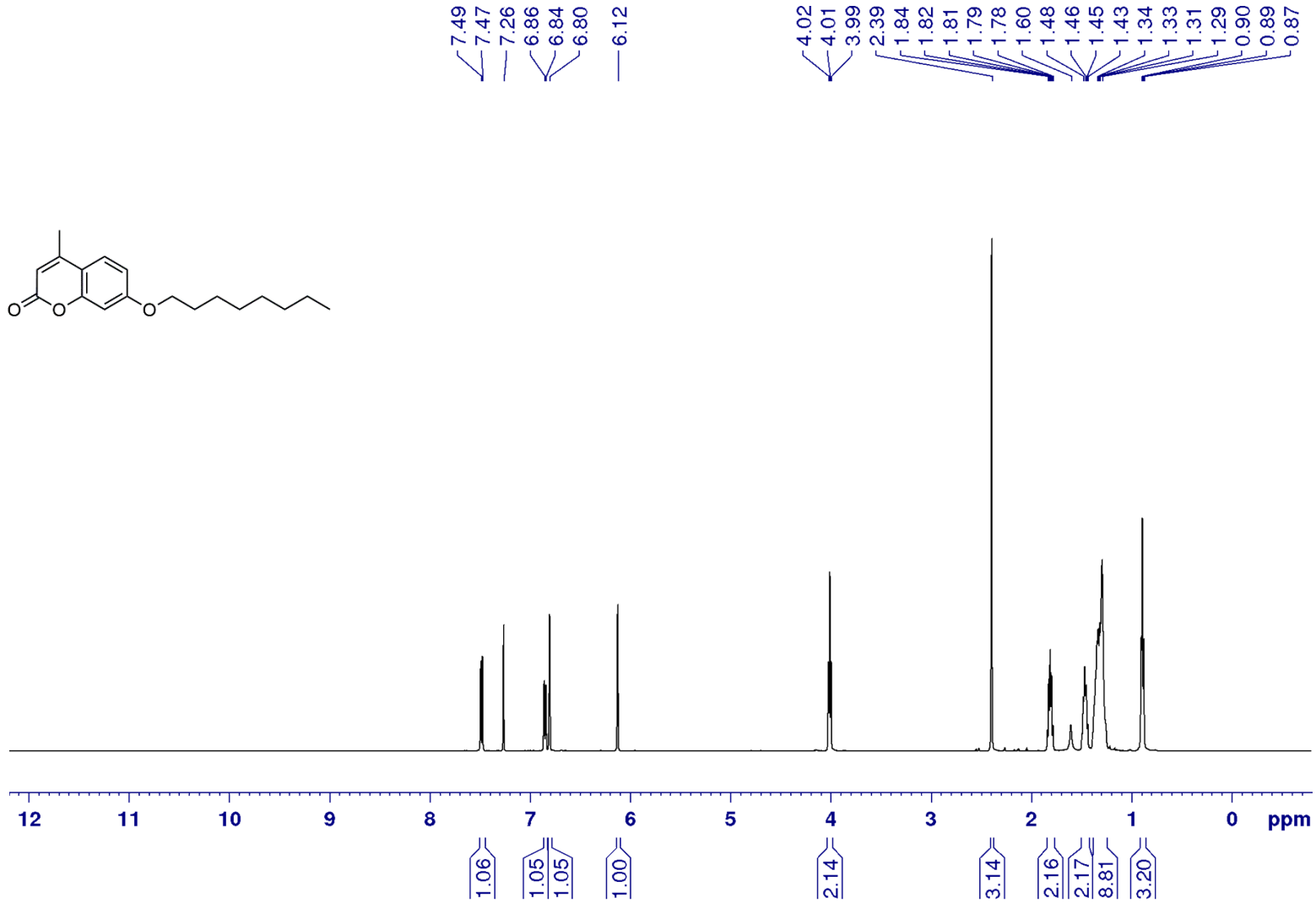

Figure S29: ^{1}H NMR (500 MHz) spectrum of coumarin **S2b** in $CDCl_3$.

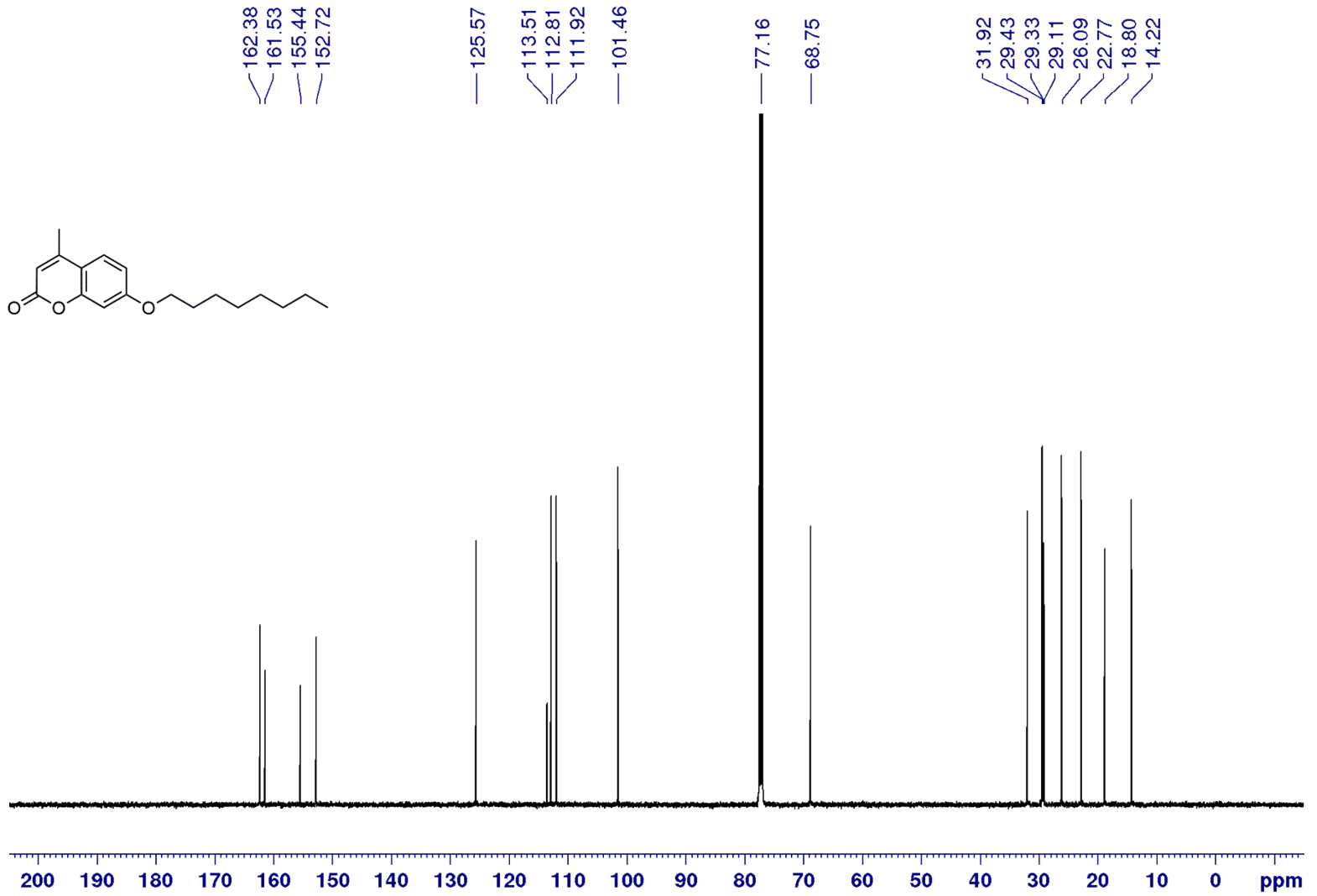

Figure S30: ^{13}C NMR (125 MHz) spectrum of coumarin **S2b** in $CDCl_3$.

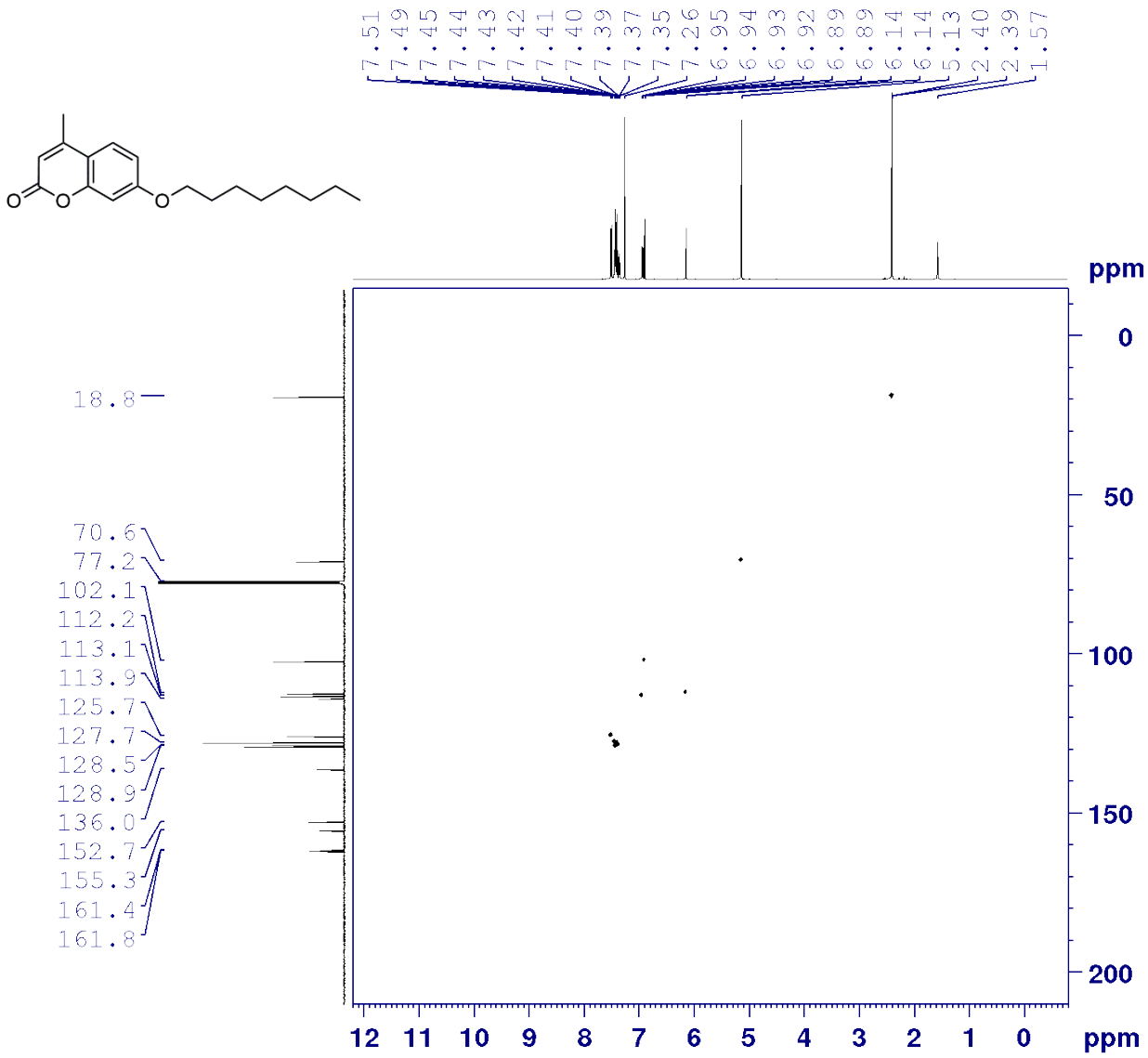

Figure S31: HSQC NMR (500 MHz) spectrum of coumarin **S2b** in $CDCl_3$.

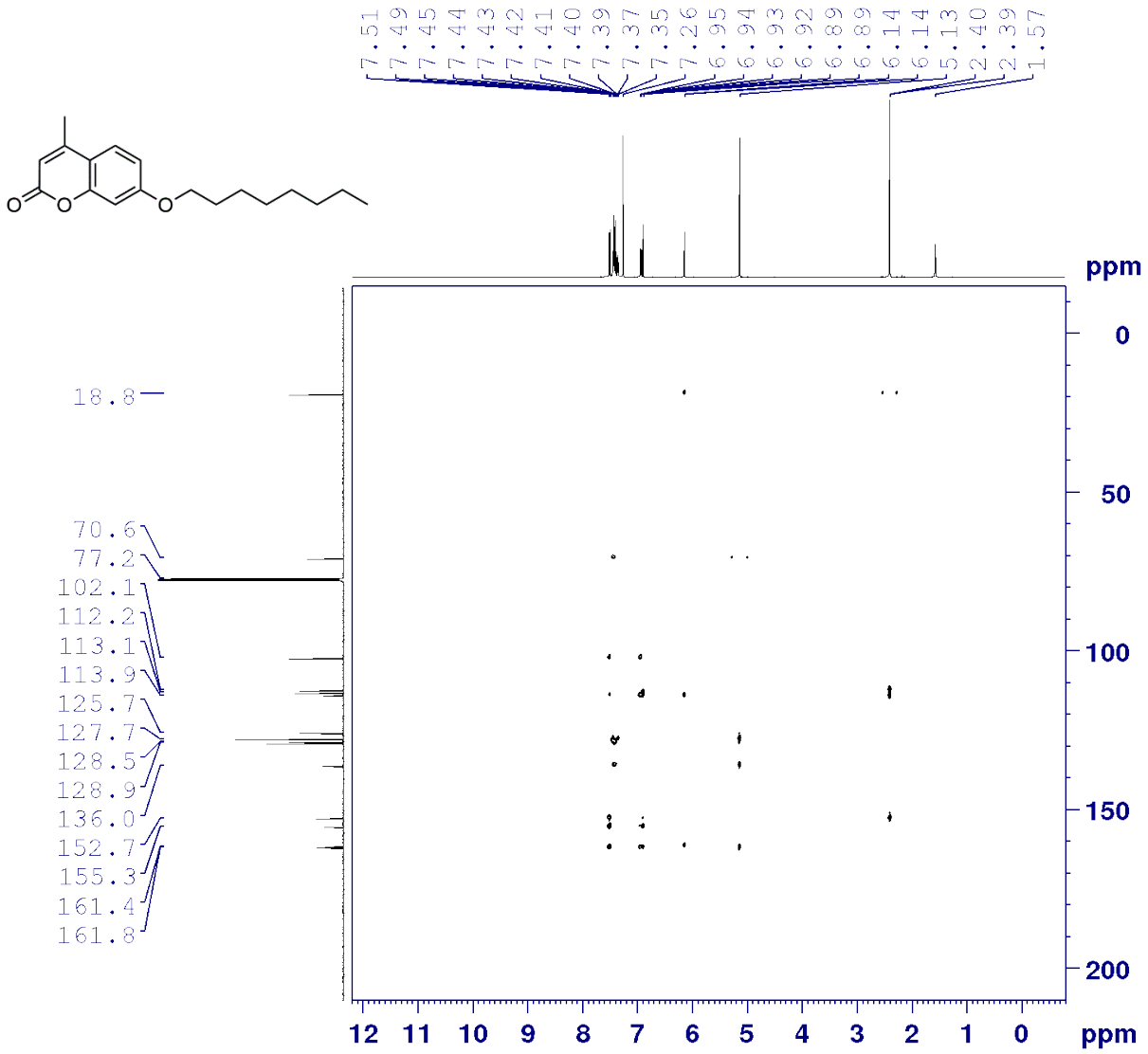

Figure S32: HMBC NMR (500 MHz) spectrum of coumarin **S2b** in $CDCl_3$.

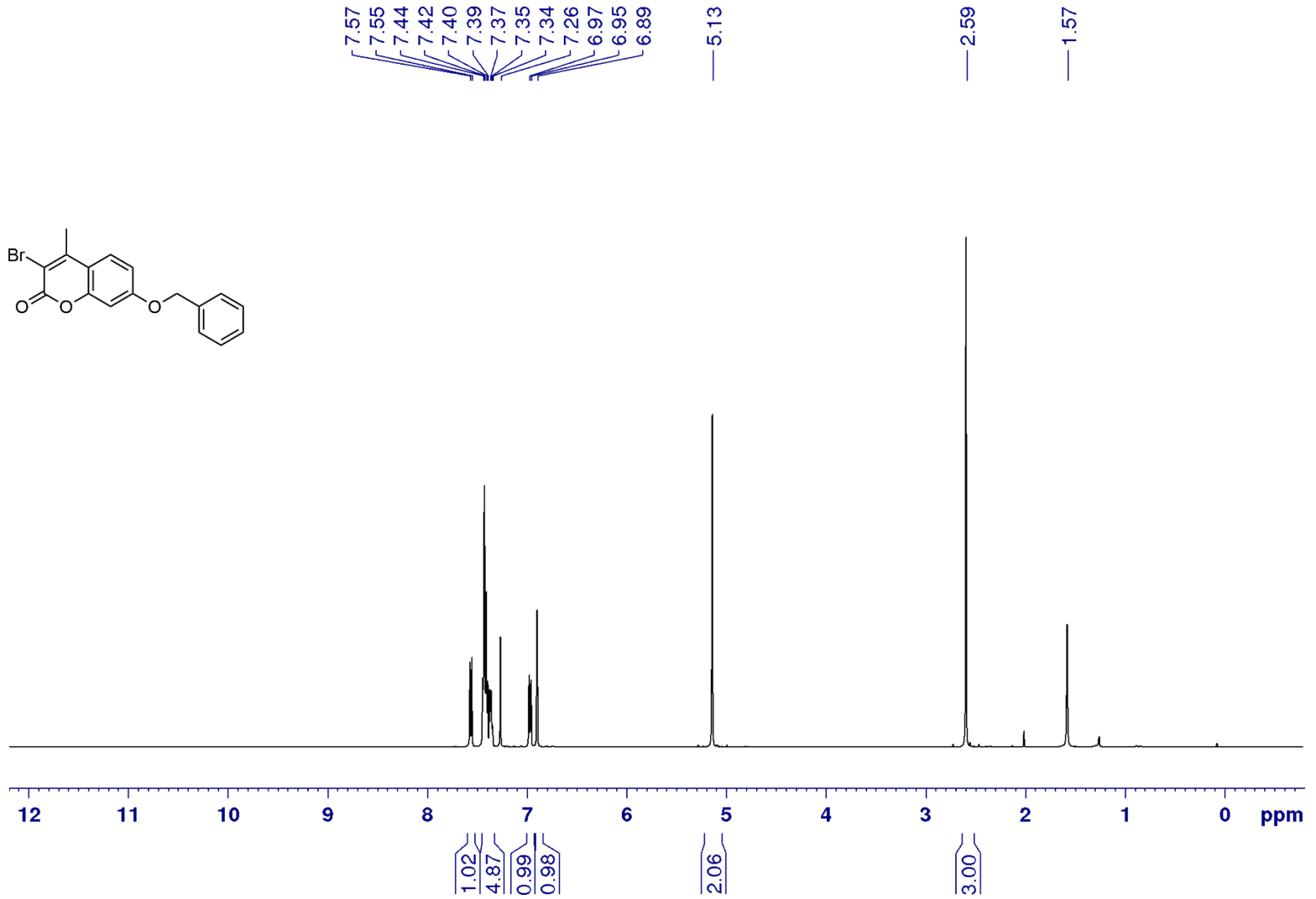

Figure S33: ^{1}H NMR (500 MHz) spectrum of coumarin **S3a** in $CDCl_3$.

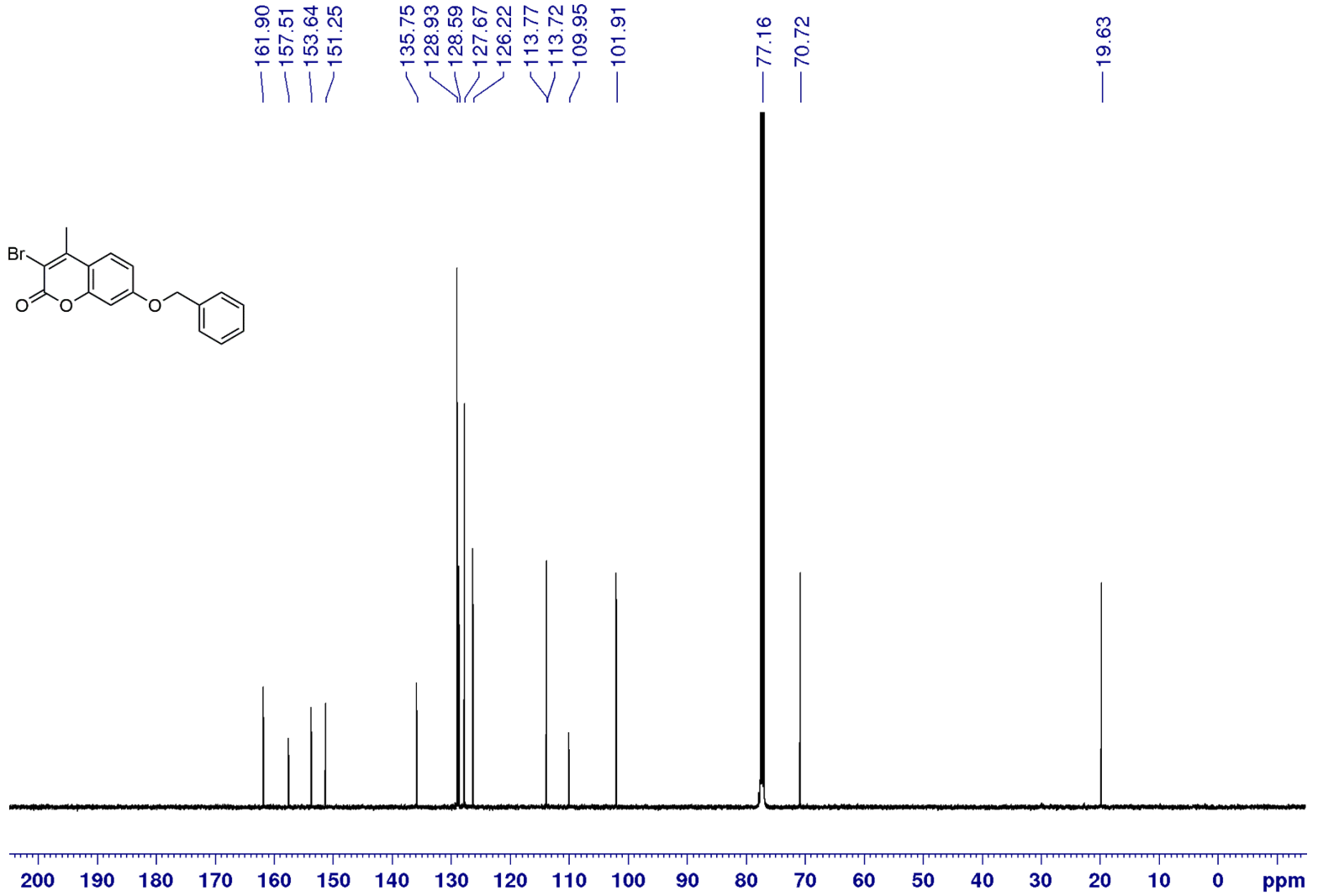

Figure S34: ^{13}C NMR (125 MHz) spectrum of coumarin **S3a** in $CDCl_3$.

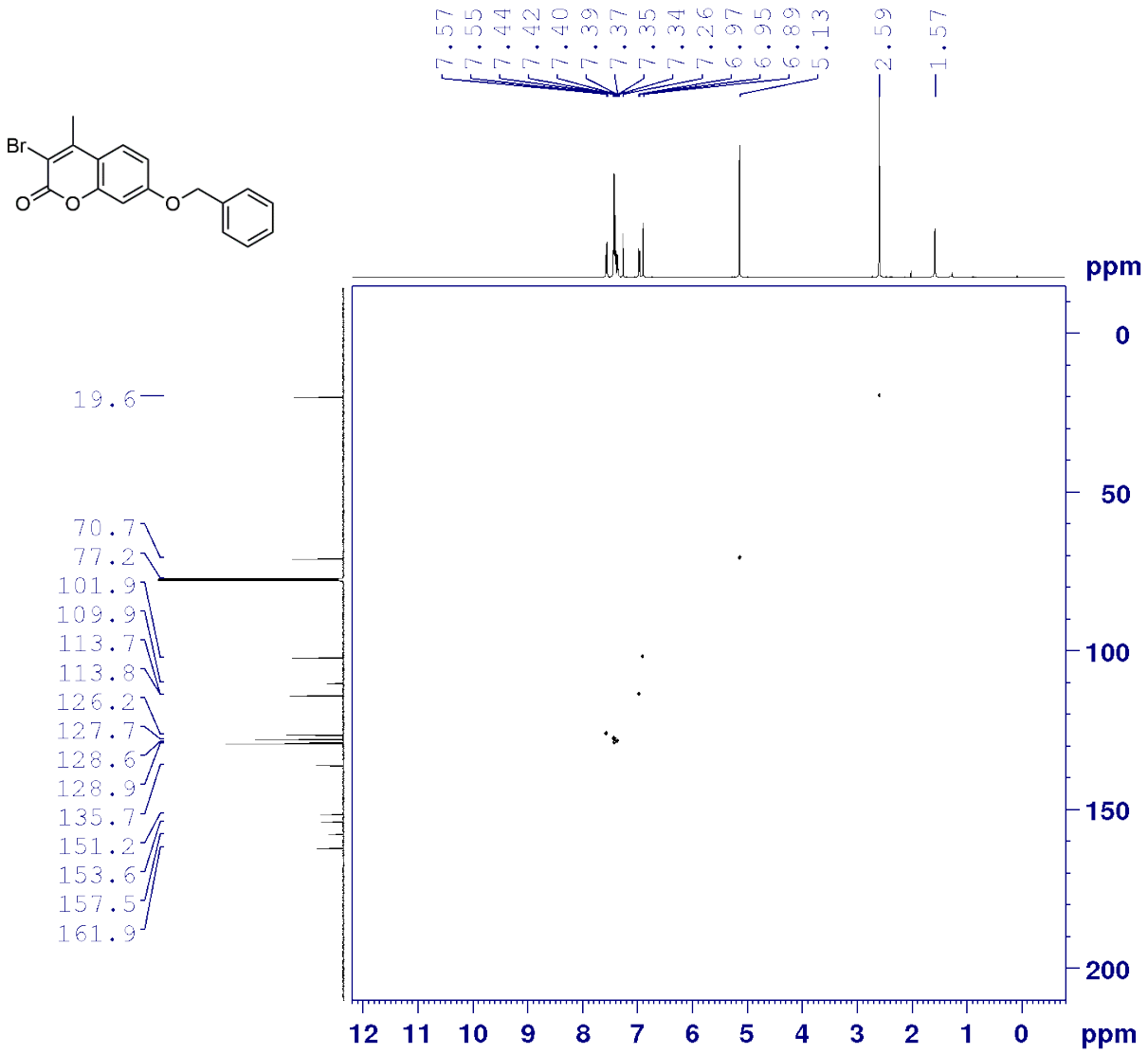

Figure S35: HSQC NMR (500 MHz) spectrum of coumarin **S3a** in $CDCl_3$.

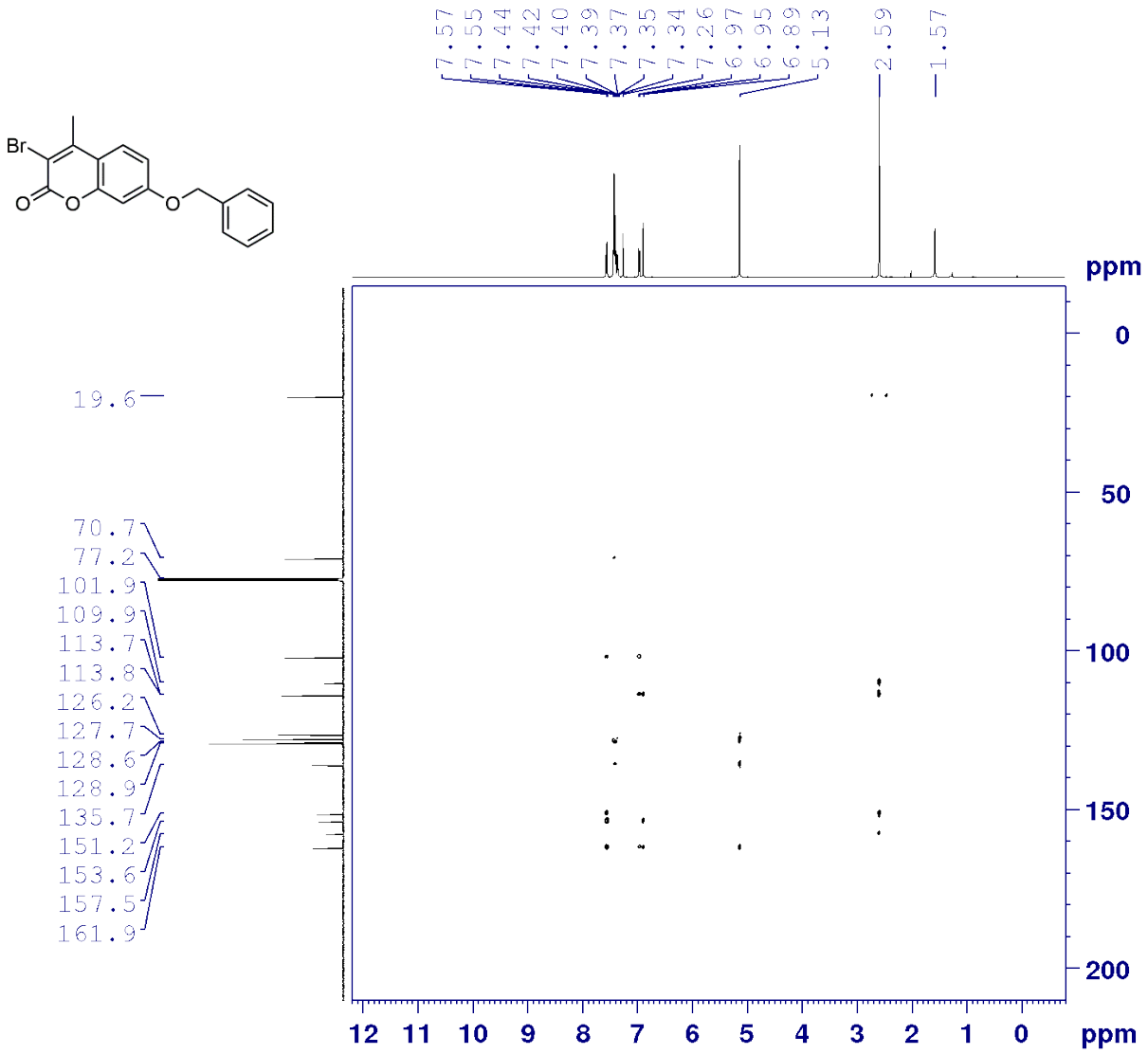

Figure S36: HMBC NMR (500 MHz) spectrum of coumarin **S3a** in $CDCl_3$.

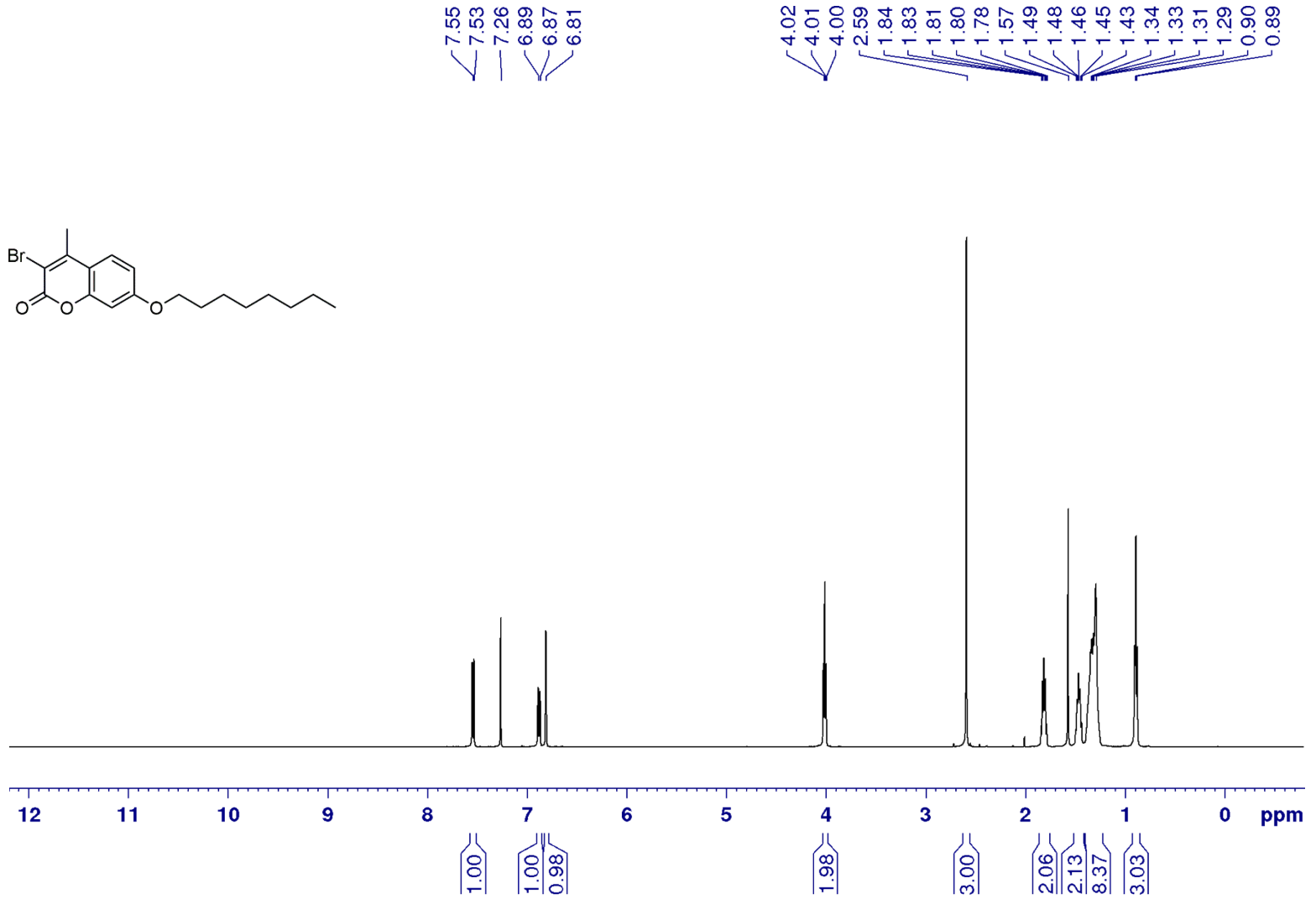

Figure S37: ^{1}H NMR (500 MHz) spectrum of coumarin **S3b** in $CDCl_3$.

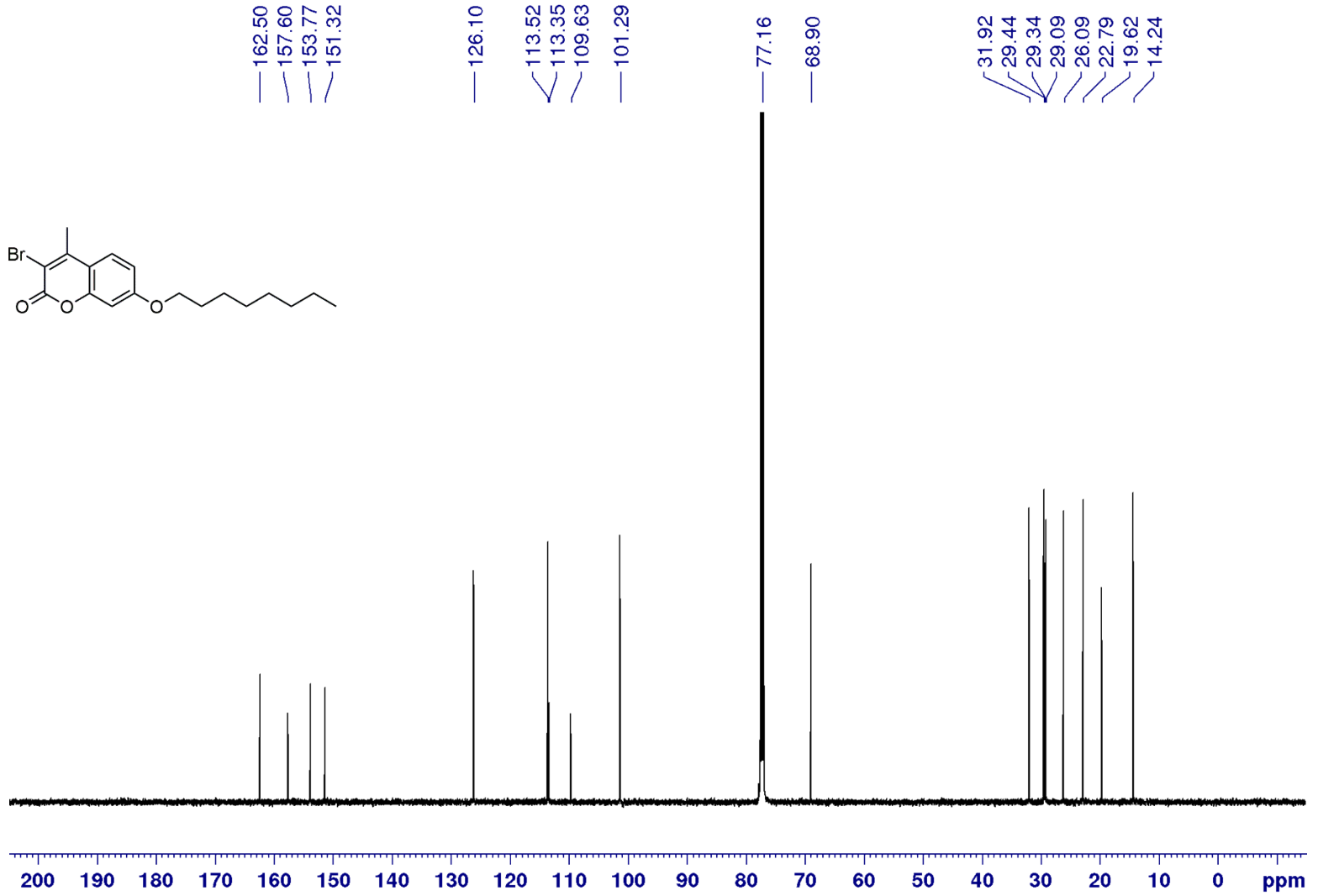

Figure S38: ^{13}C NMR (125 MHz) spectrum of coumarin **S3b** in $CDCl_3$.

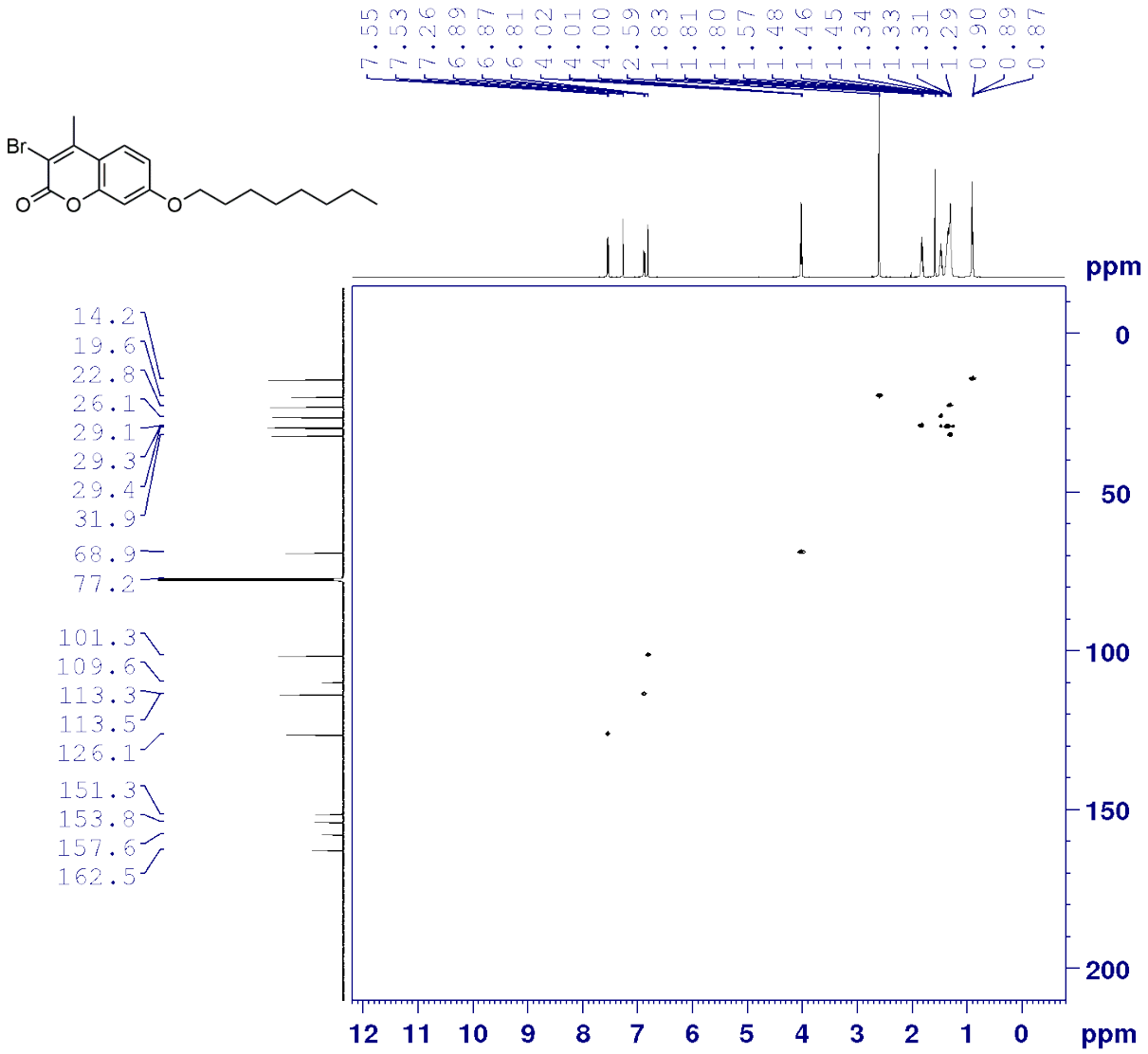

Figure S39: HSQC NMR (500 MHz) spectrum of coumarin **S3b** in $CDCl_3$.

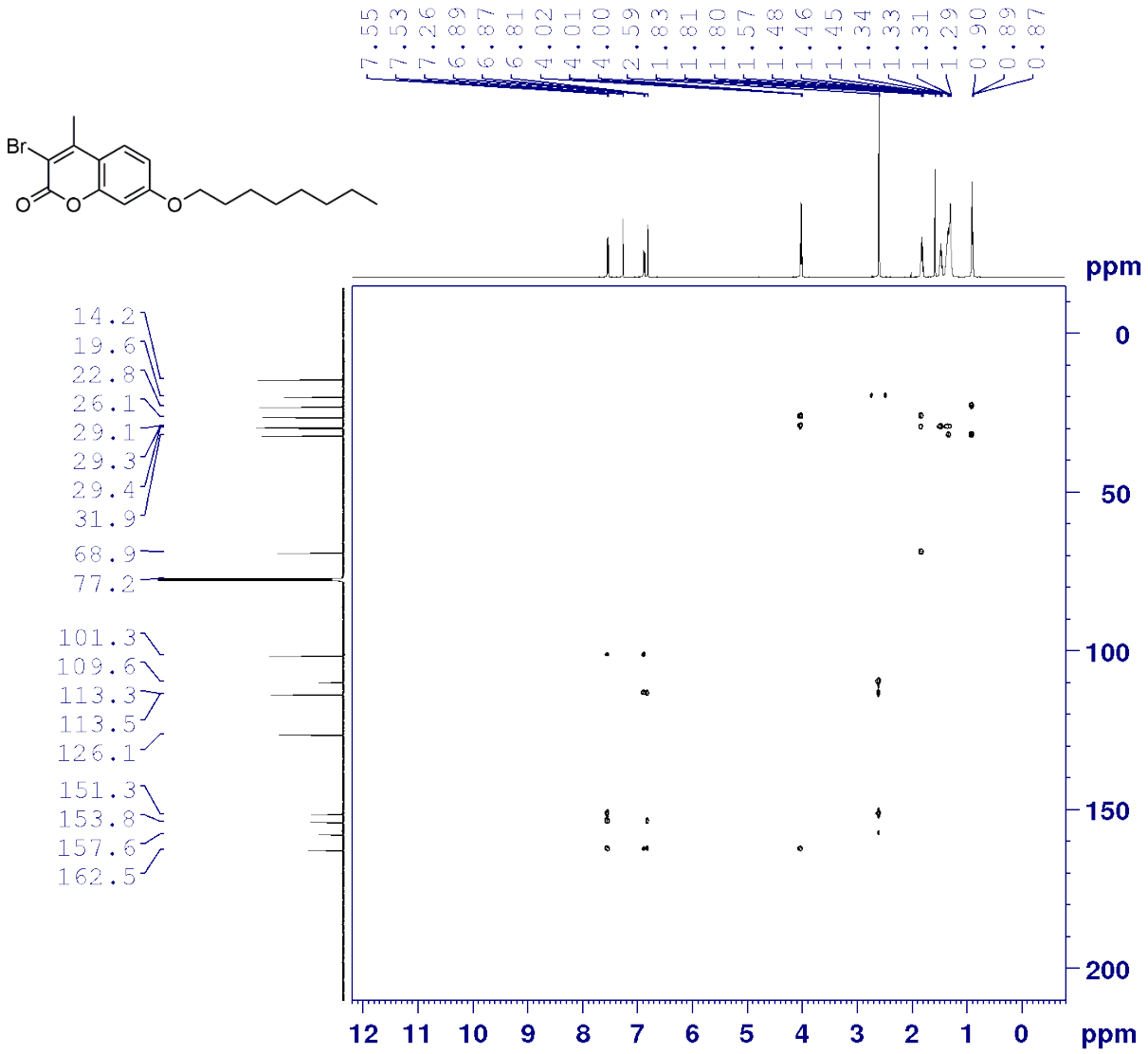

Figure S40: HMBC NMR (500 MHz) spectrum of coumarin **S3b** in $CDCl_3$.

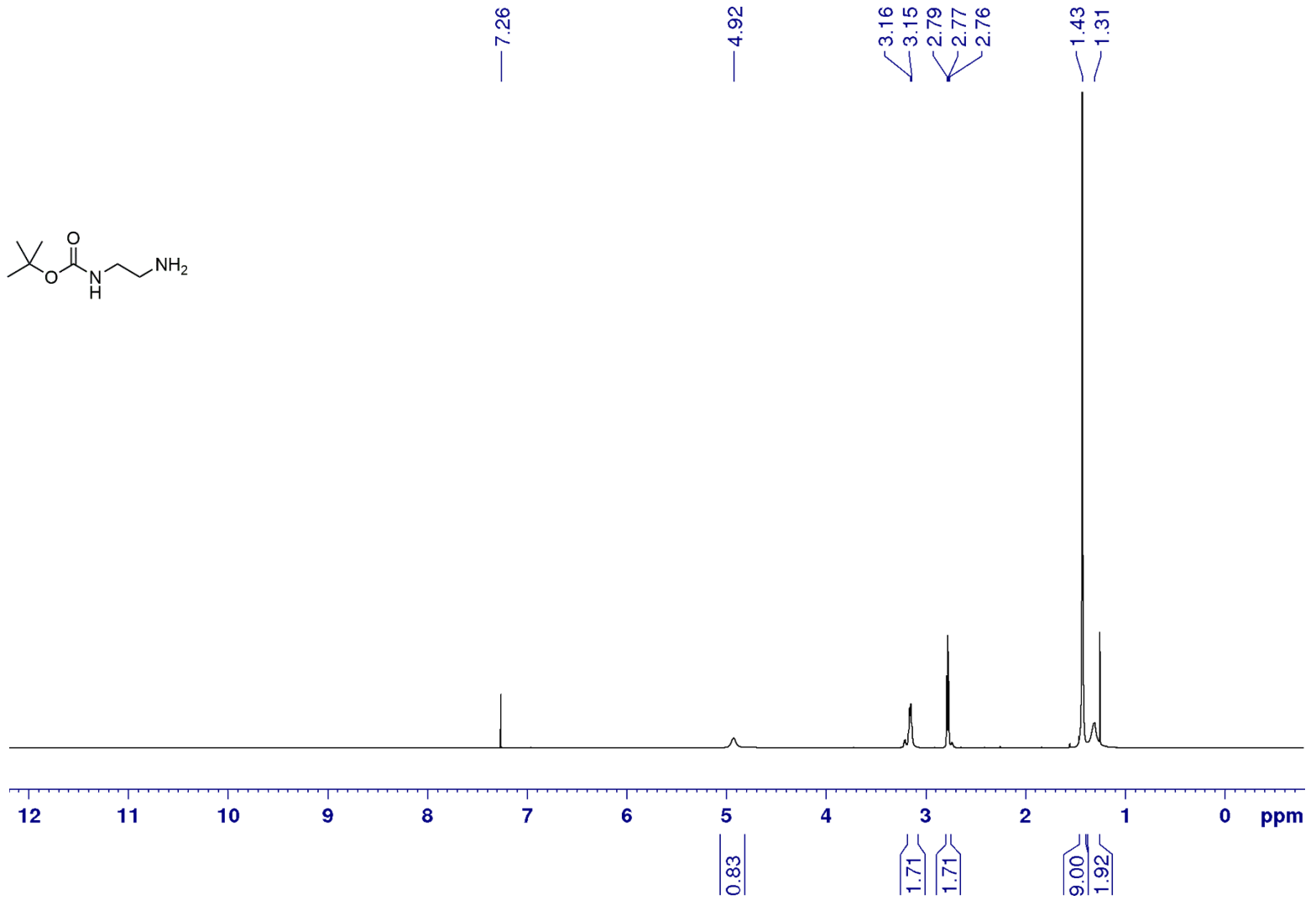

Figure S41: ^{1}H NMR (500 MHz) spectrum of compound **S4** in $CDCl_3$.

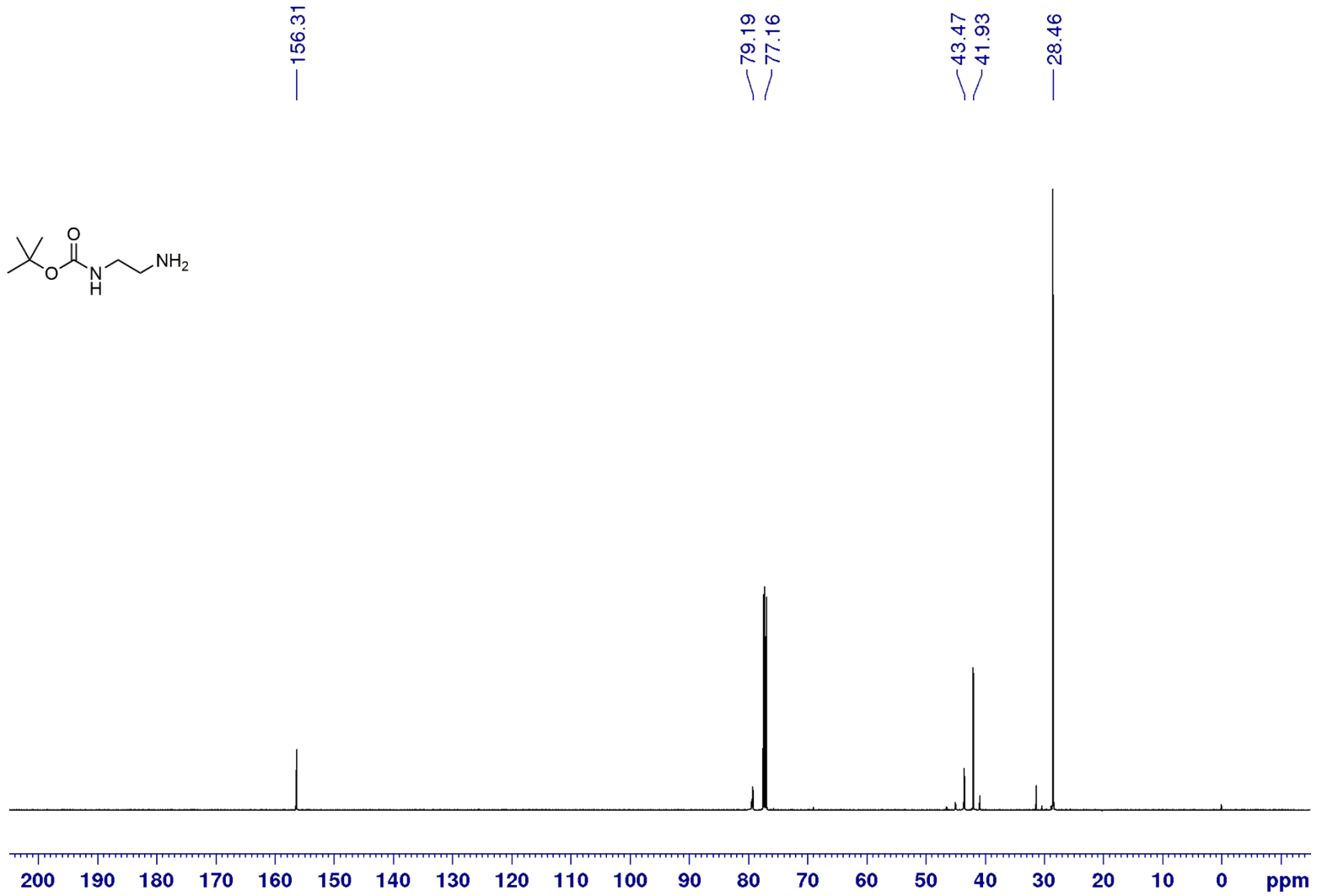

Figure S42: ^{13}C NMR (125 MHz) spectrum of compound **S4** in $CDCl_3$.

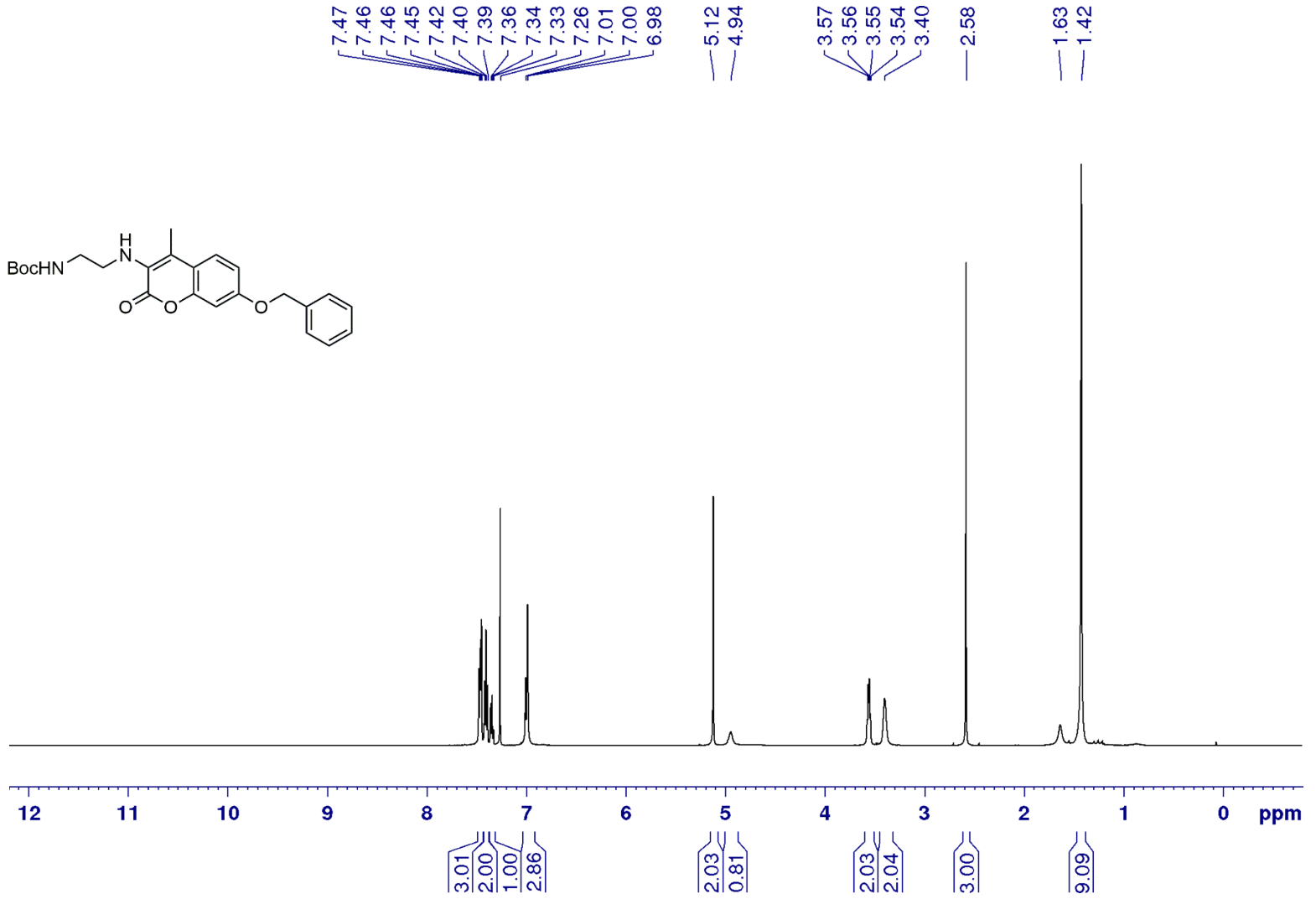

Figure S43: ^{1}H NMR (500 MHz) spectrum of coumarin **S5a** in $CDCl_3$.

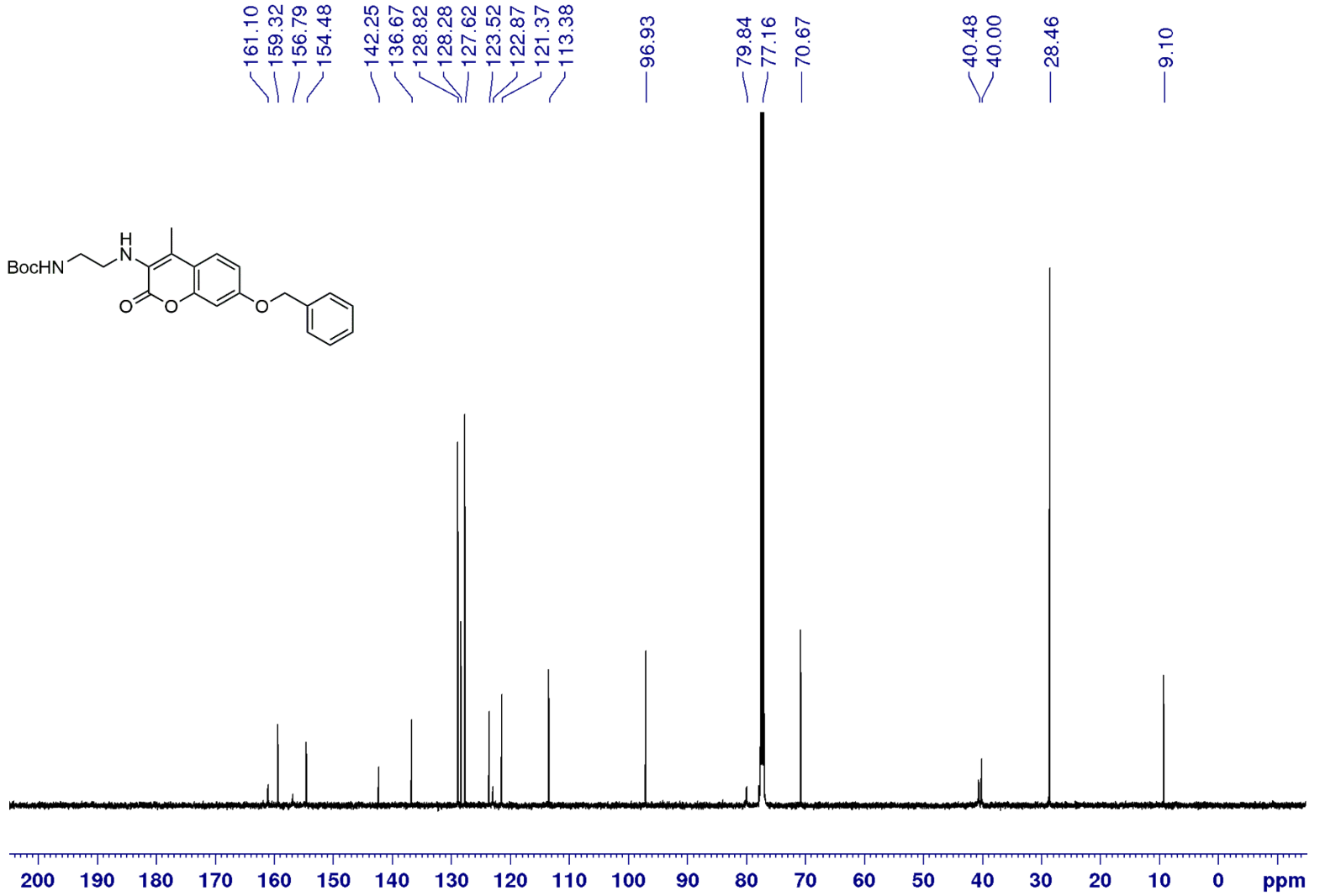

Figure S44: ^{13}C NMR (125 MHz) spectrum of coumarin **S5a** in $CDCl_3$.

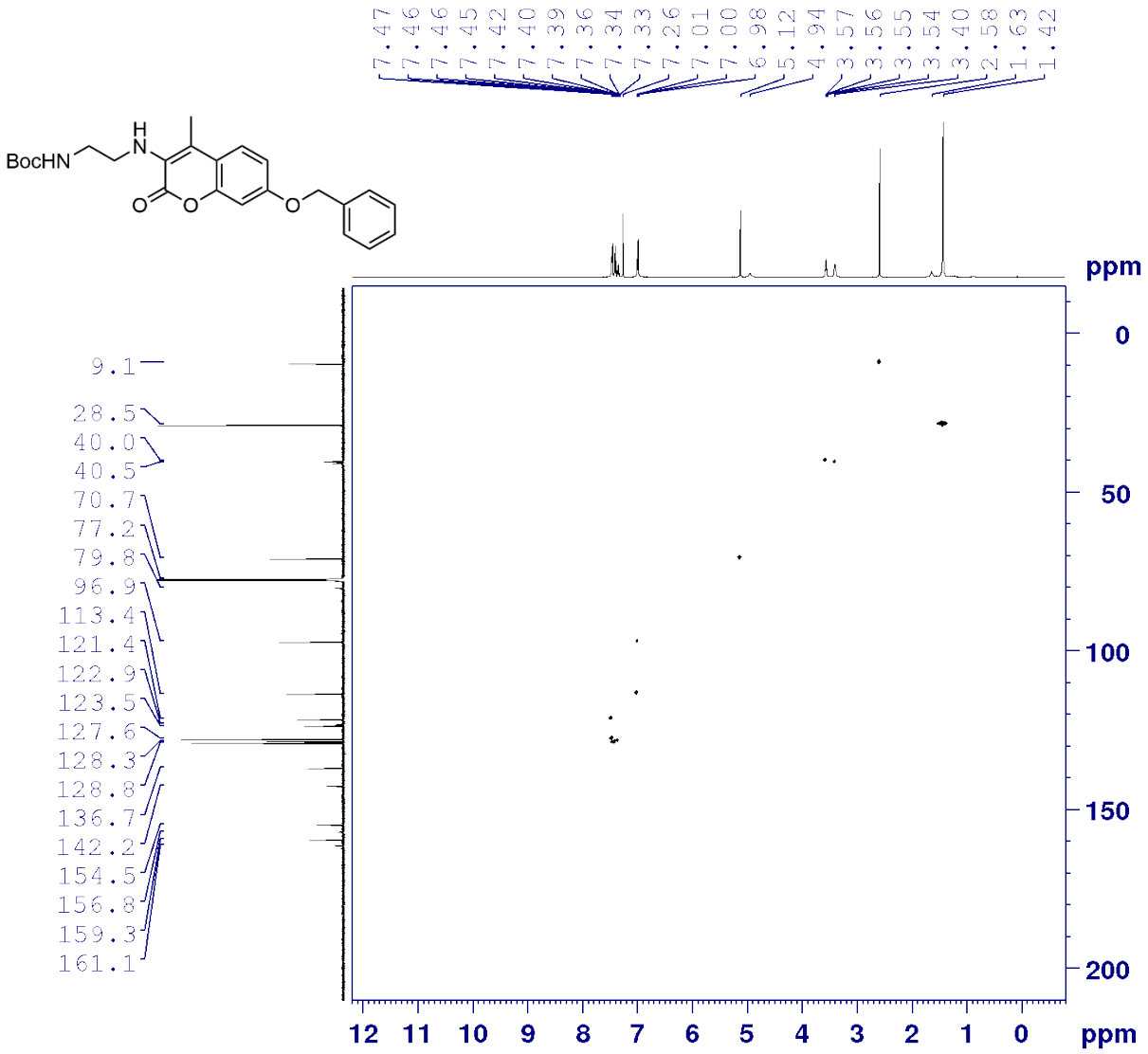

Figure S45: HSQC NMR (500 MHz) spectrum of coumarin **S5a** in $CDCl_3$.

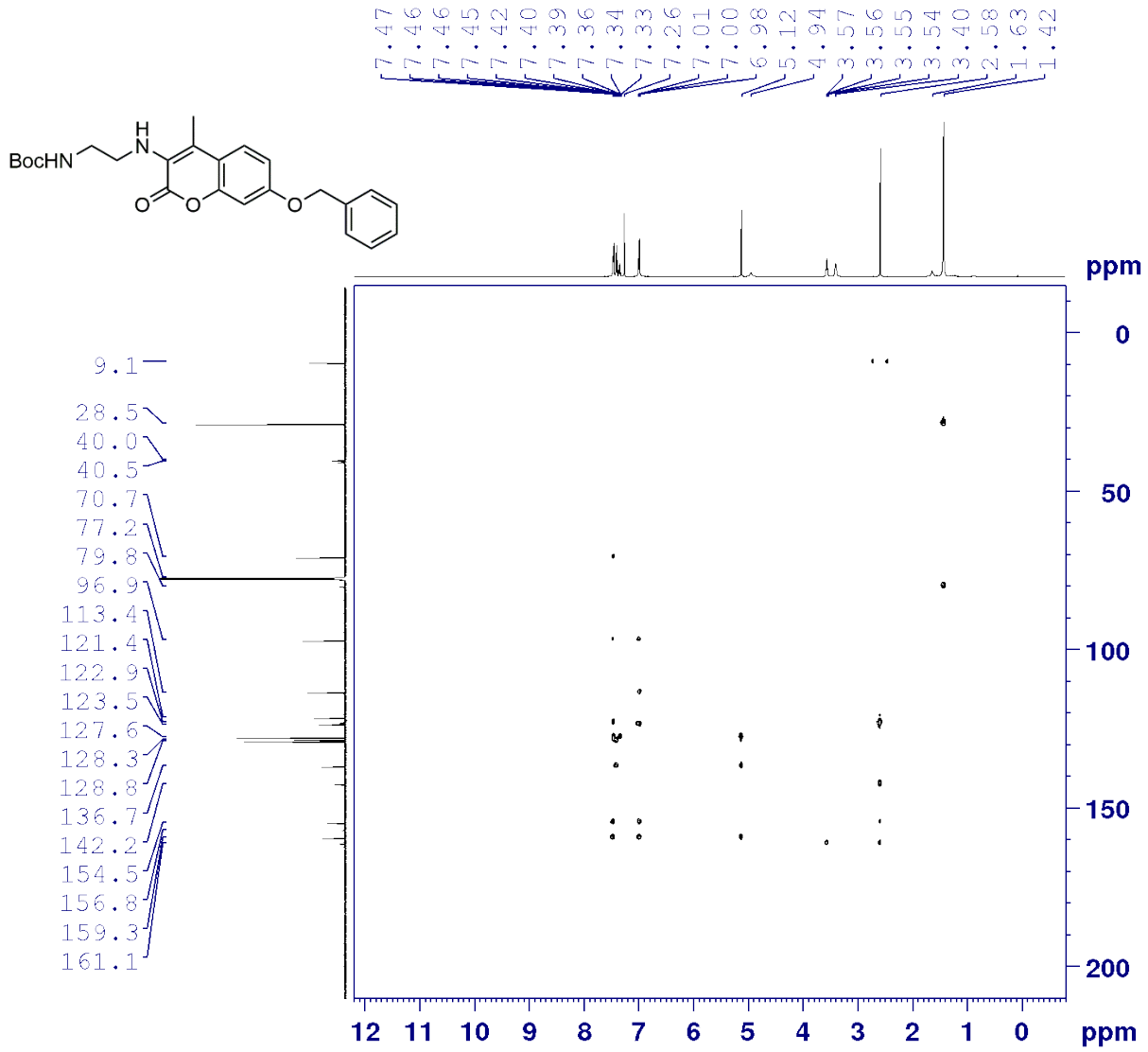

Figure S46: HMBC NMR (500 MHz) spectrum of coumarin **S5a** in $CDCl_3$.

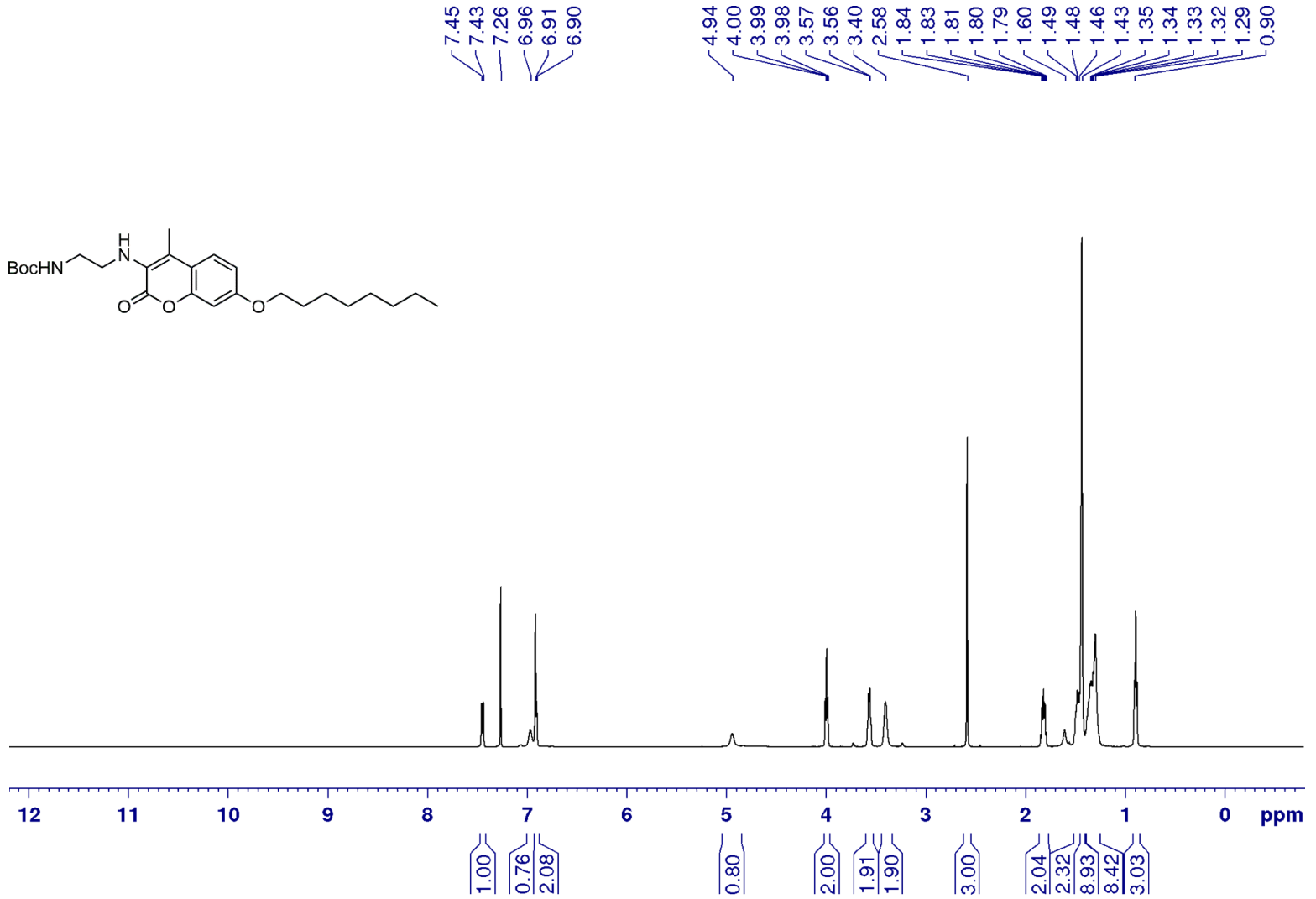

Figure S47: ^{1}H NMR (500 MHz) spectrum of coumarin **S5b** in $CDCl_3$.

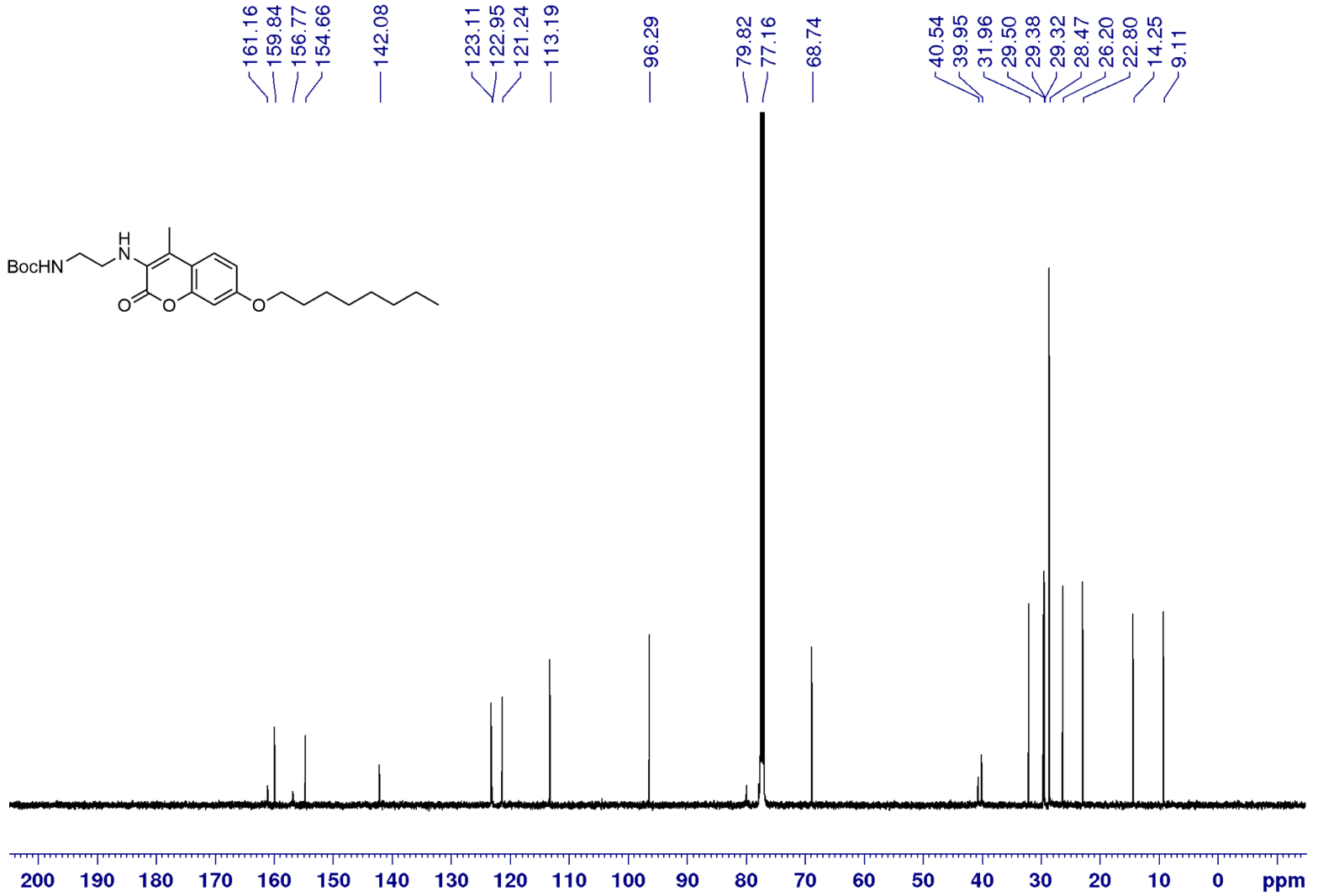

Figure S48: ^{13}C NMR (125 MHz) spectrum of coumarin **S5b** in $CDCl_3$.

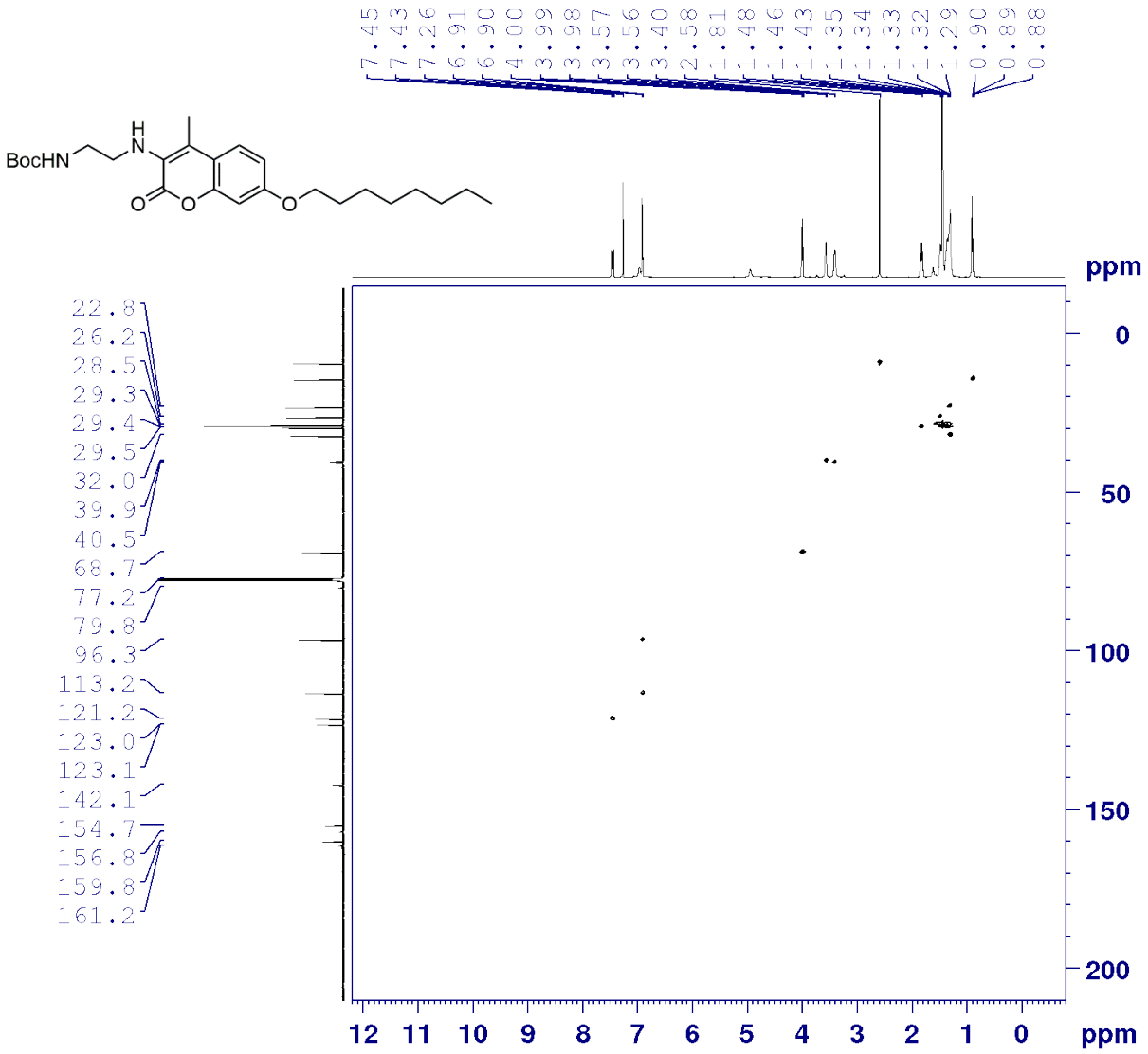

Figure S49: HSQC NMR (500 MHz) spectrum of coumarin **S5b** in $CDCl_3$.

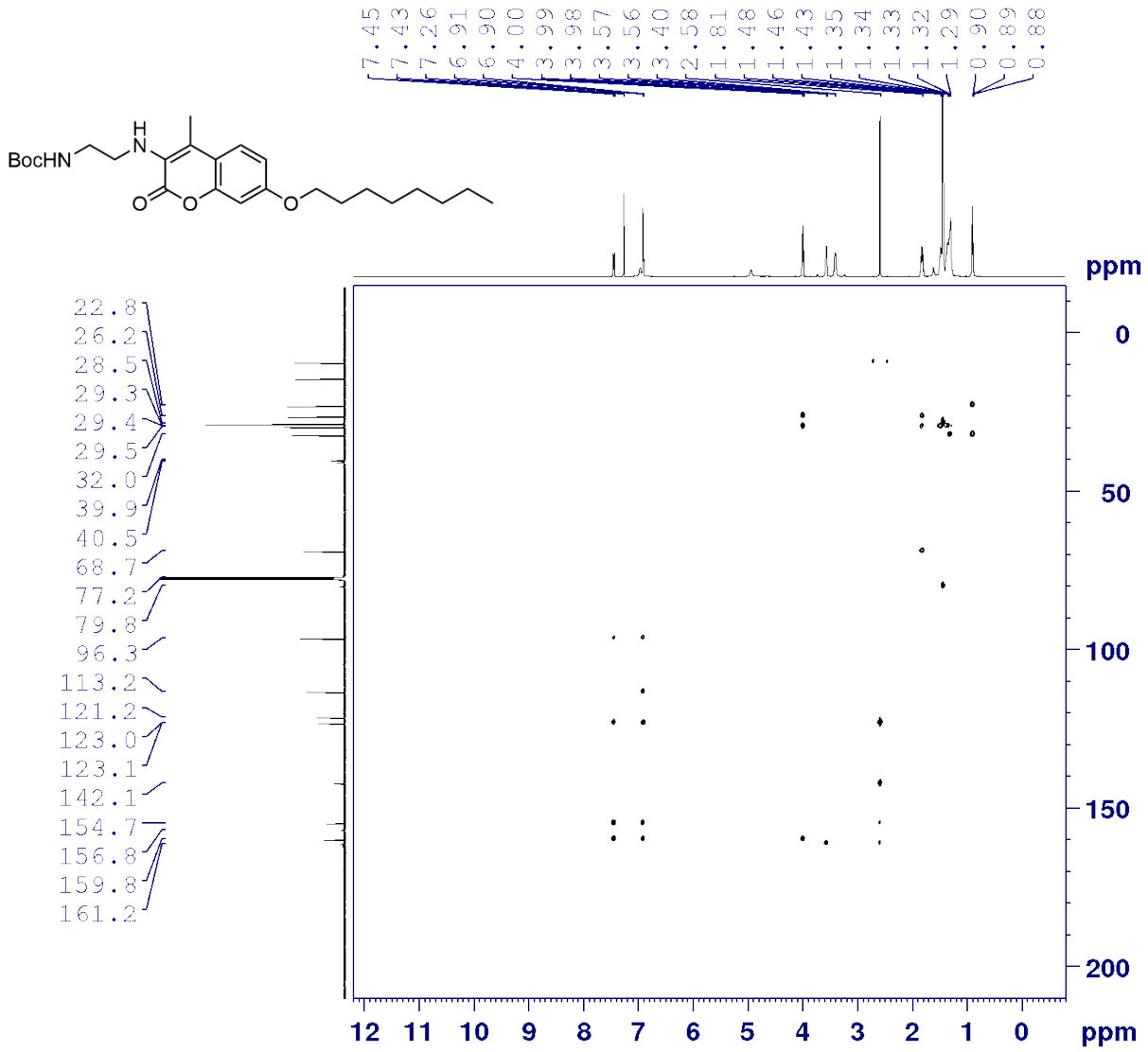

Figure S50: HMBC NMR (500 MHz) spectrum of coumarin **S5b** in $CDCl_3$.

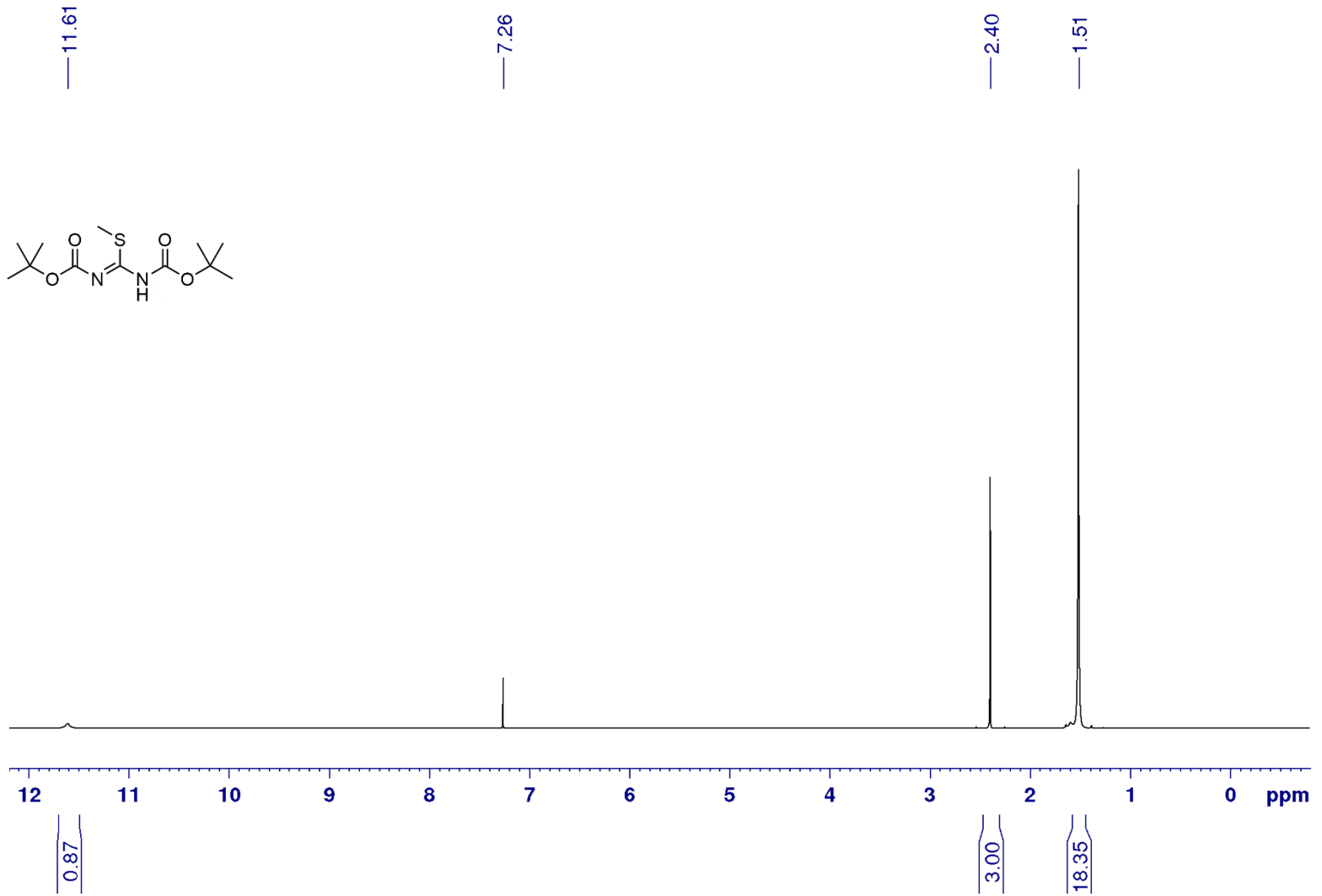

Figure S51: ^{1}H NMR (500 MHz) spectrum of compound **S7** in $CDCl_3$.

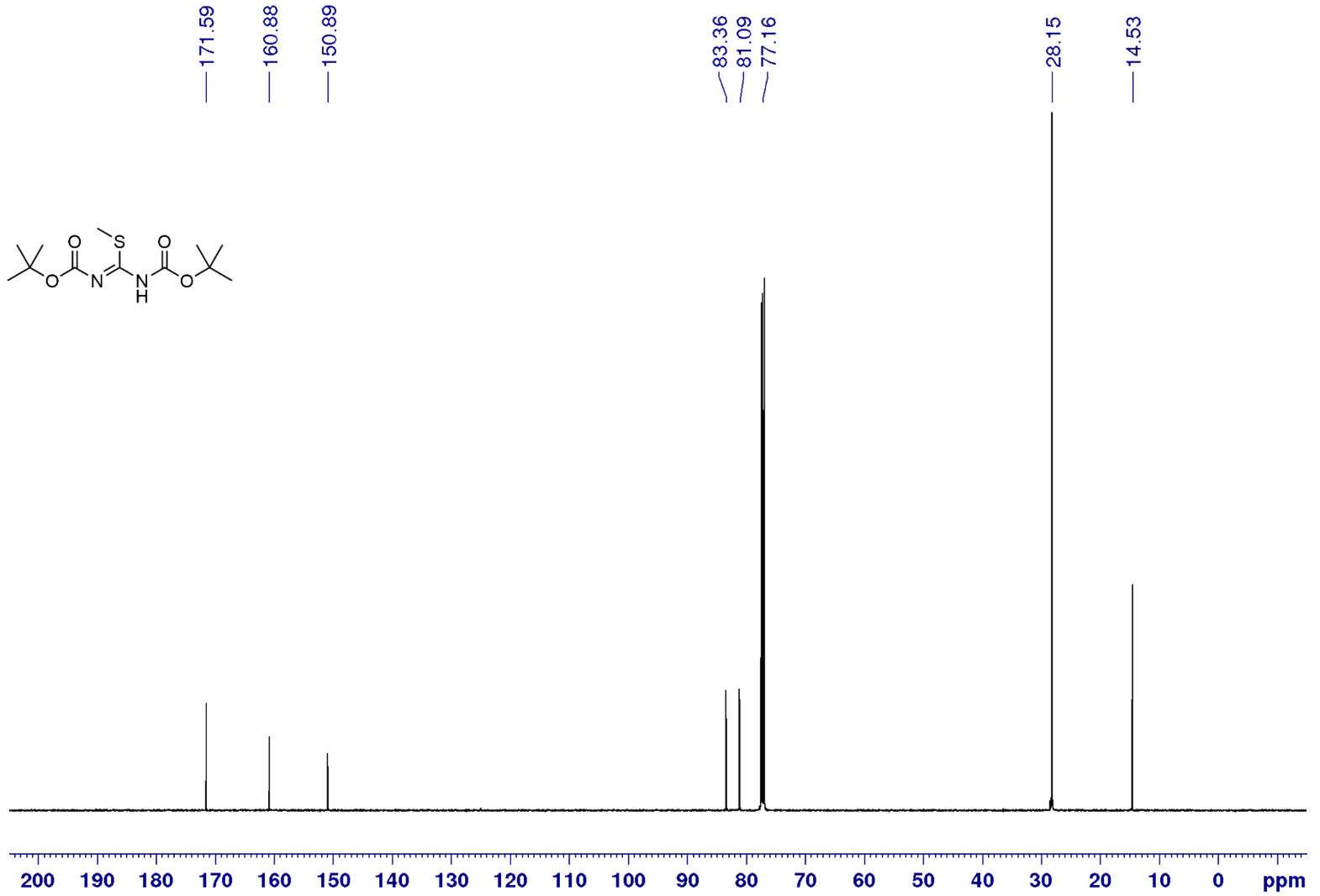

Figure S52: ^{13}C NMR (125 MHz) spectrum of compound **S7** in $CDCl_3$.

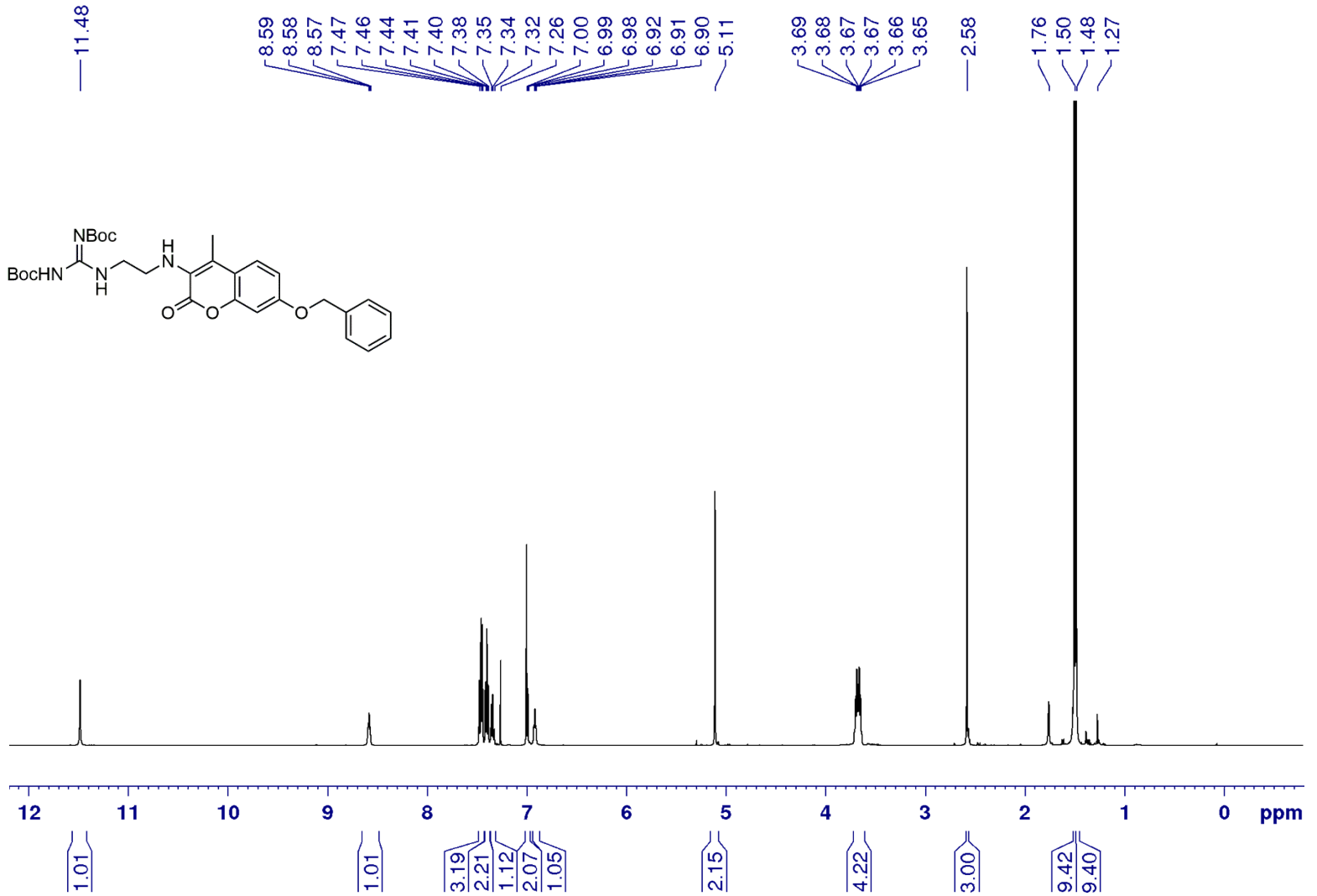

Figure S53: ^{1}H NMR (500 MHz) spectrum of coumarin **S8a** in $CDCl_3$.

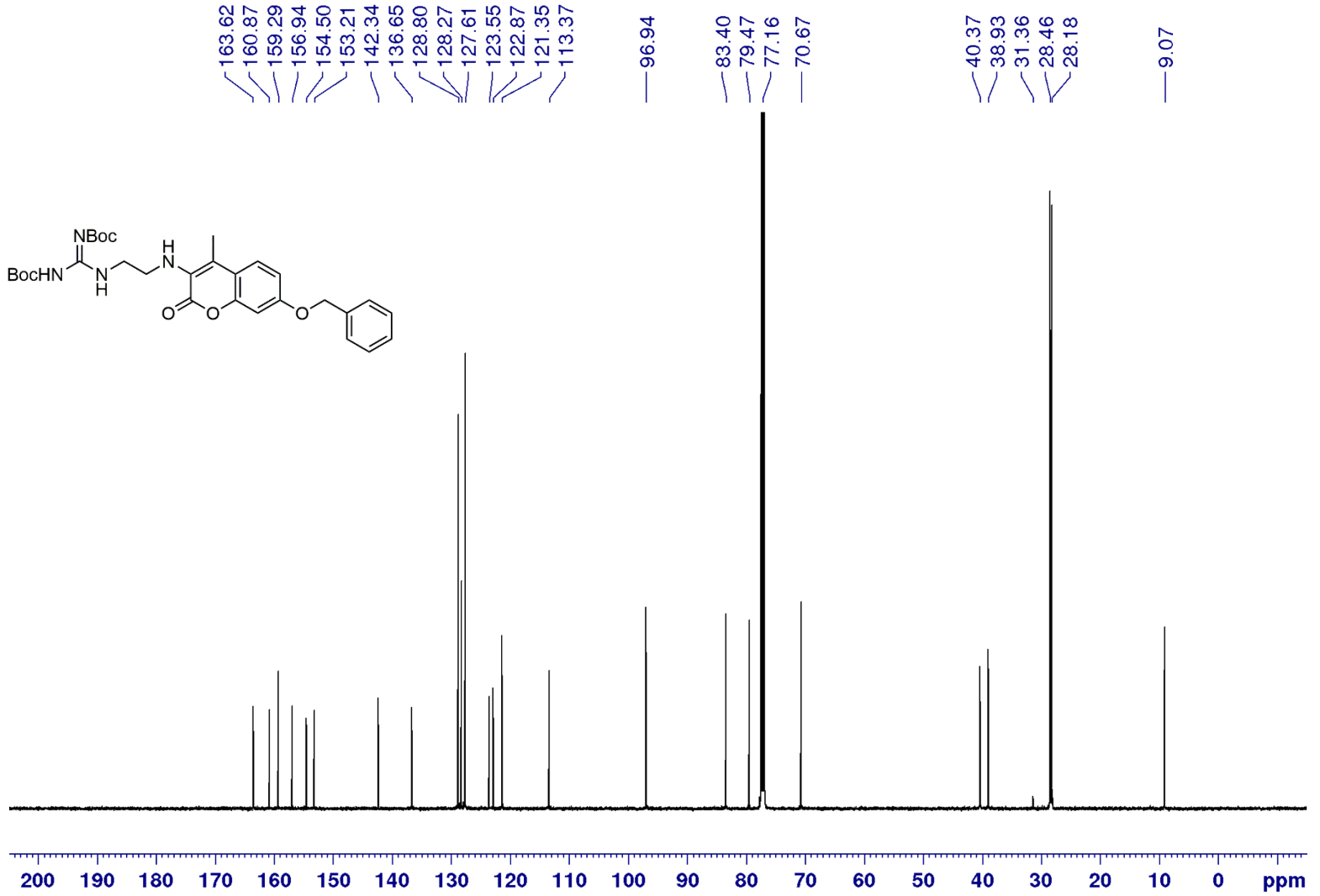

Figure S54: ^{13}C NMR (125 MHz) spectrum of coumarin **S8a** in $CDCl_3$.

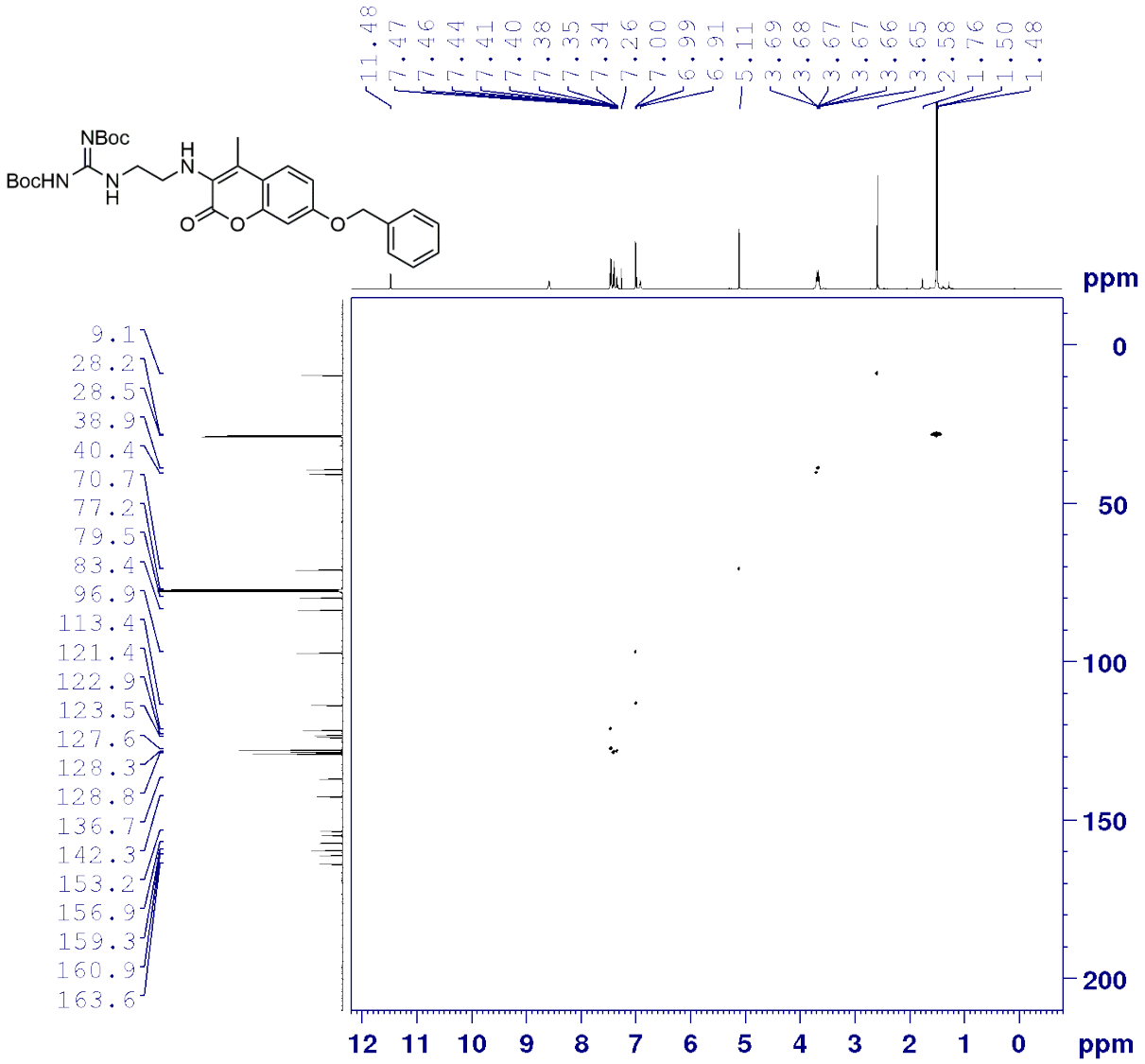

Figure S55: HSQC NMR (500 MHz) spectrum of coumarin **S8a** in $CDCl_3$.

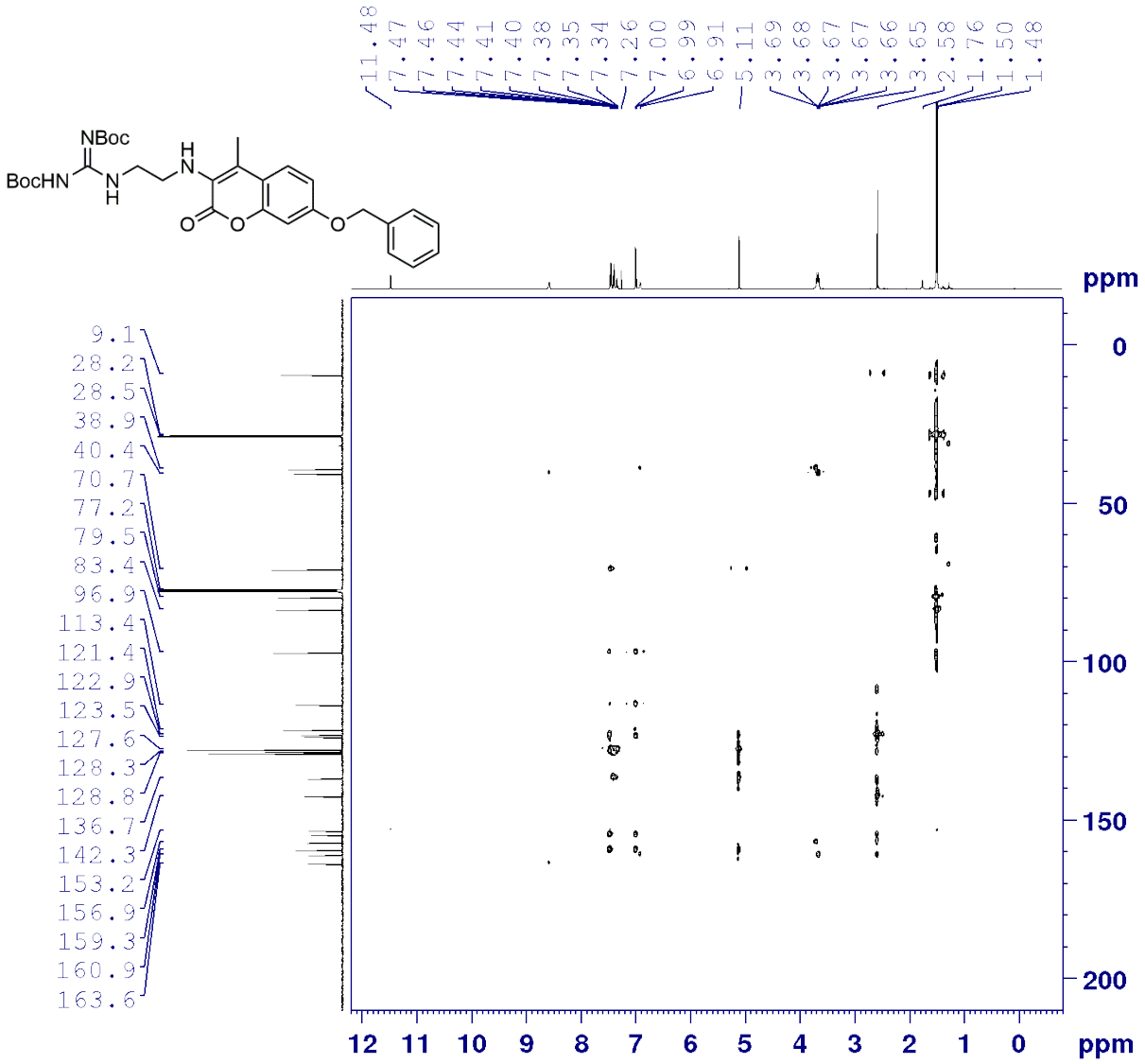

Figure S56: HMBC NMR (500 MHz) spectrum of coumarin **S8a** in $CDCl_3$.

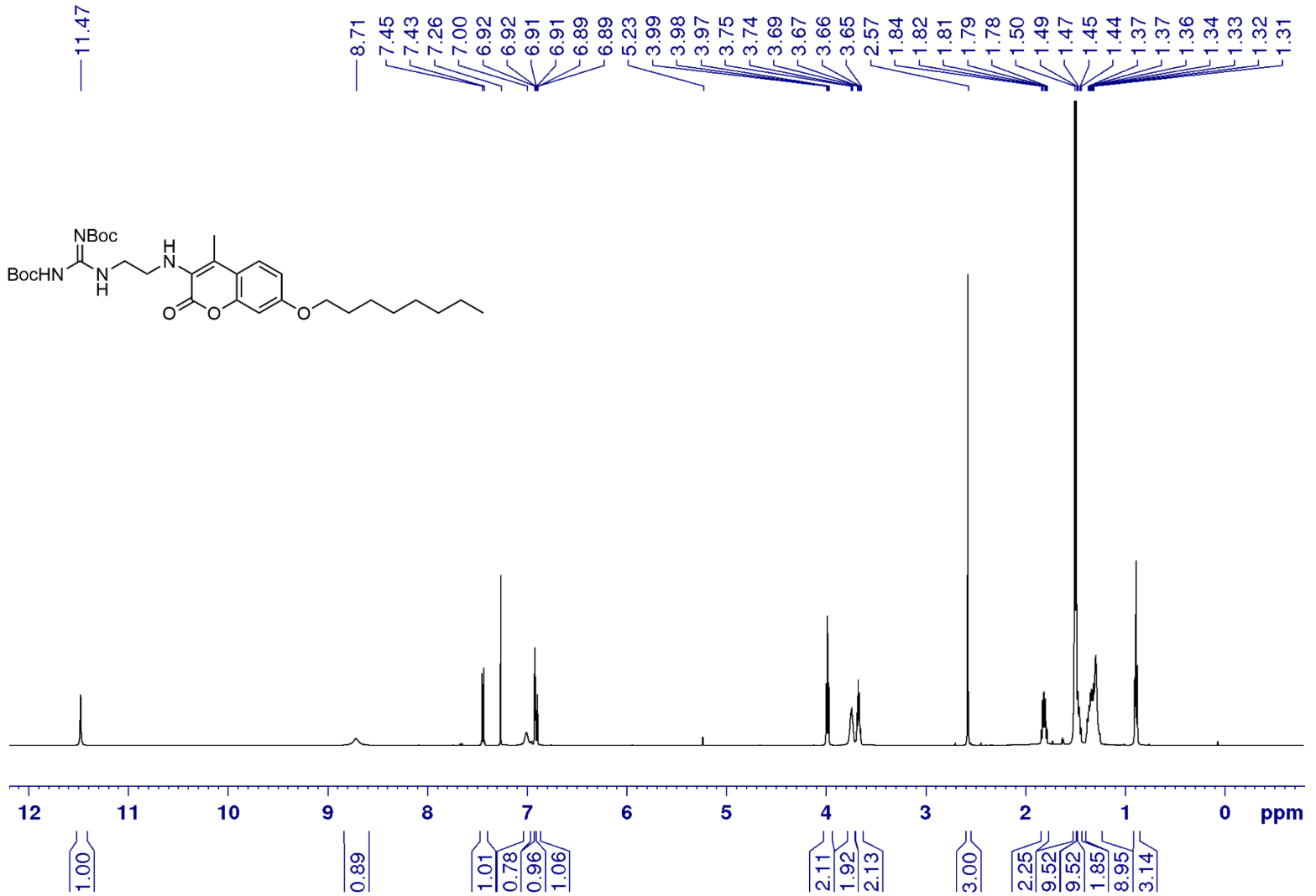

Figure S57: ^{1}H NMR (500 MHz) spectrum of coumarin **S8b** in $CDCl_3$.

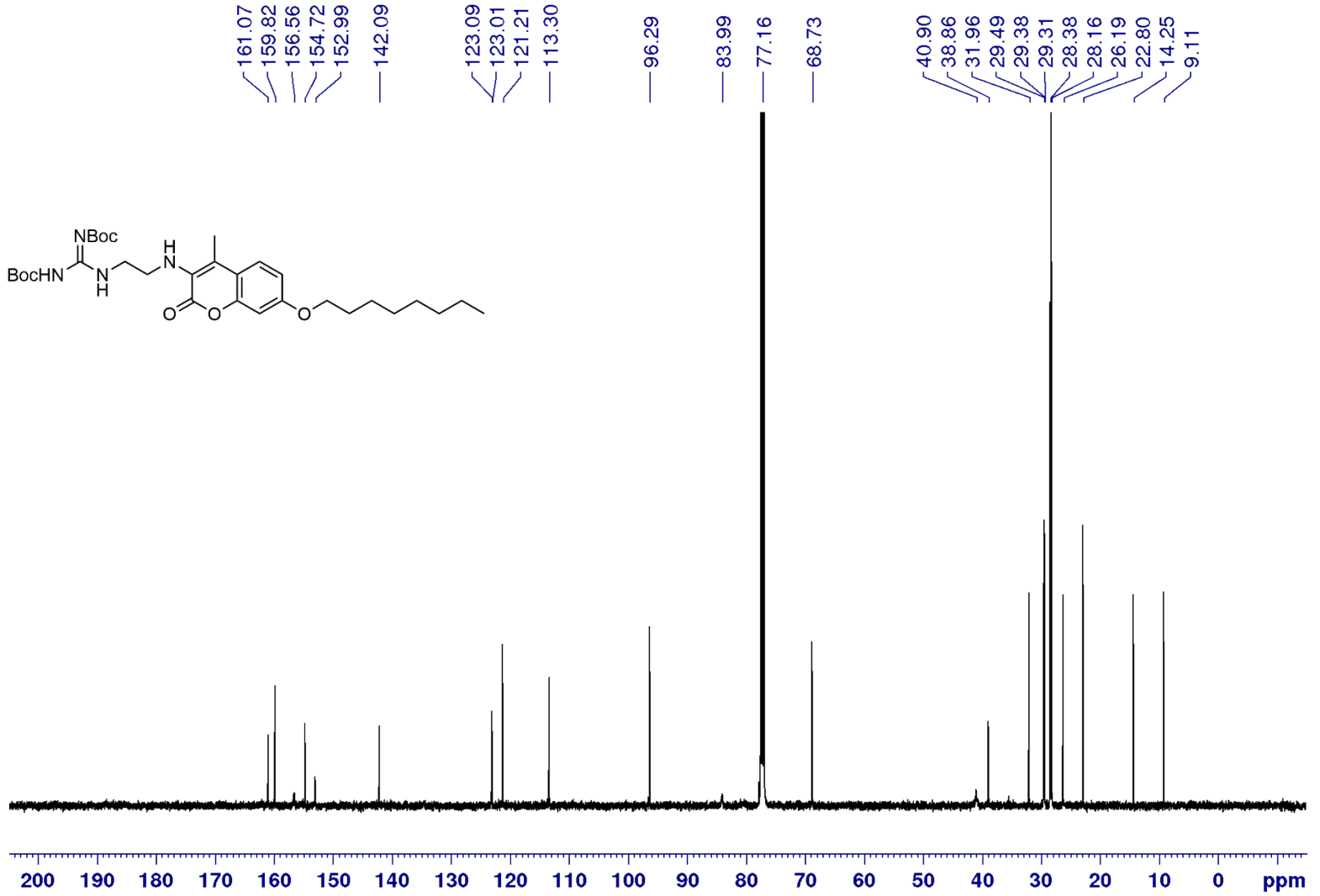

Figure S58: ^{13}C NMR (125 MHz) spectrum of coumarin **S8b** in $CDCl_3$.

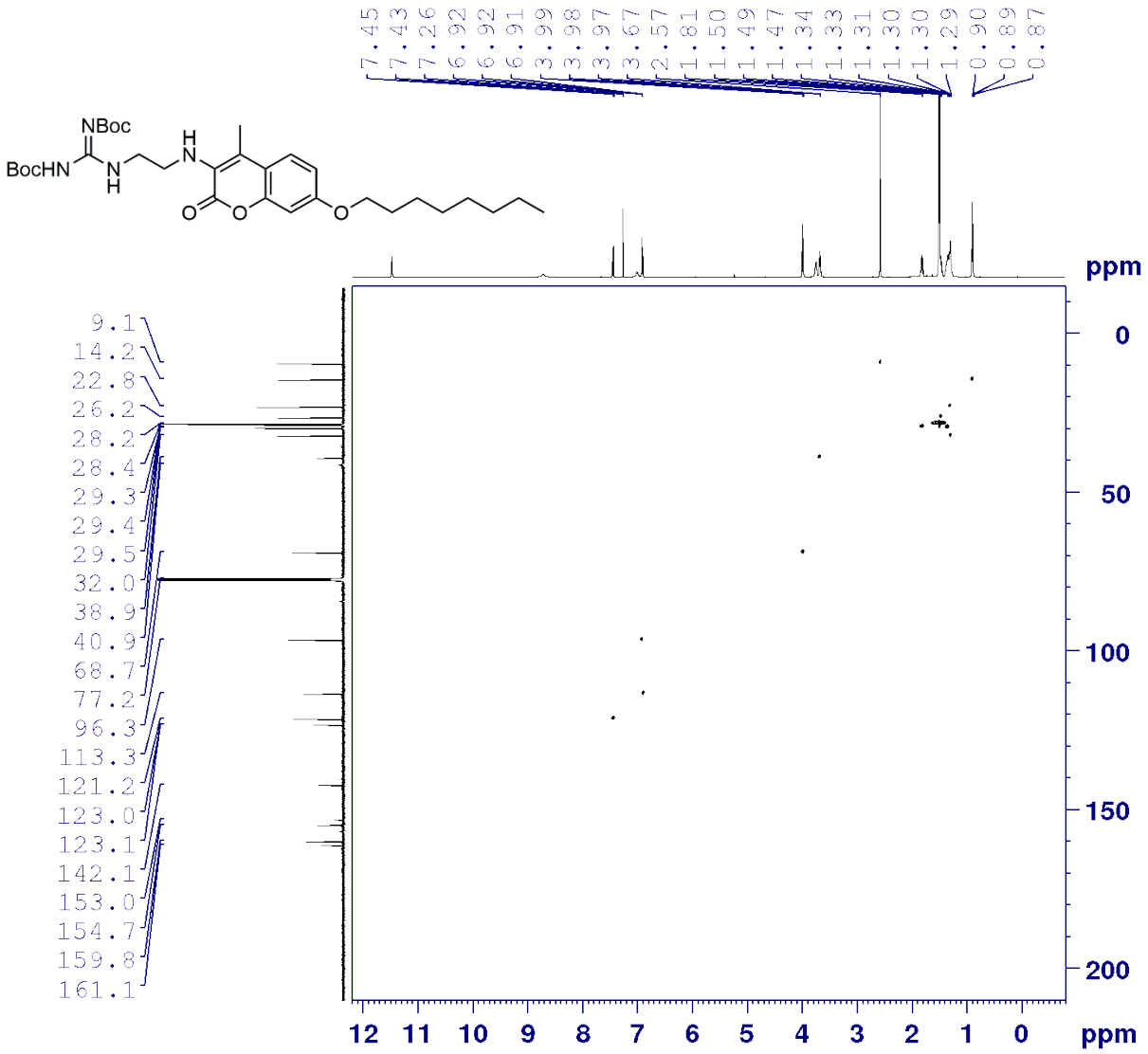

Figure S59: HSQC NMR (500 MHz) spectrum of coumarin **S8b** in $CDCl_3$.

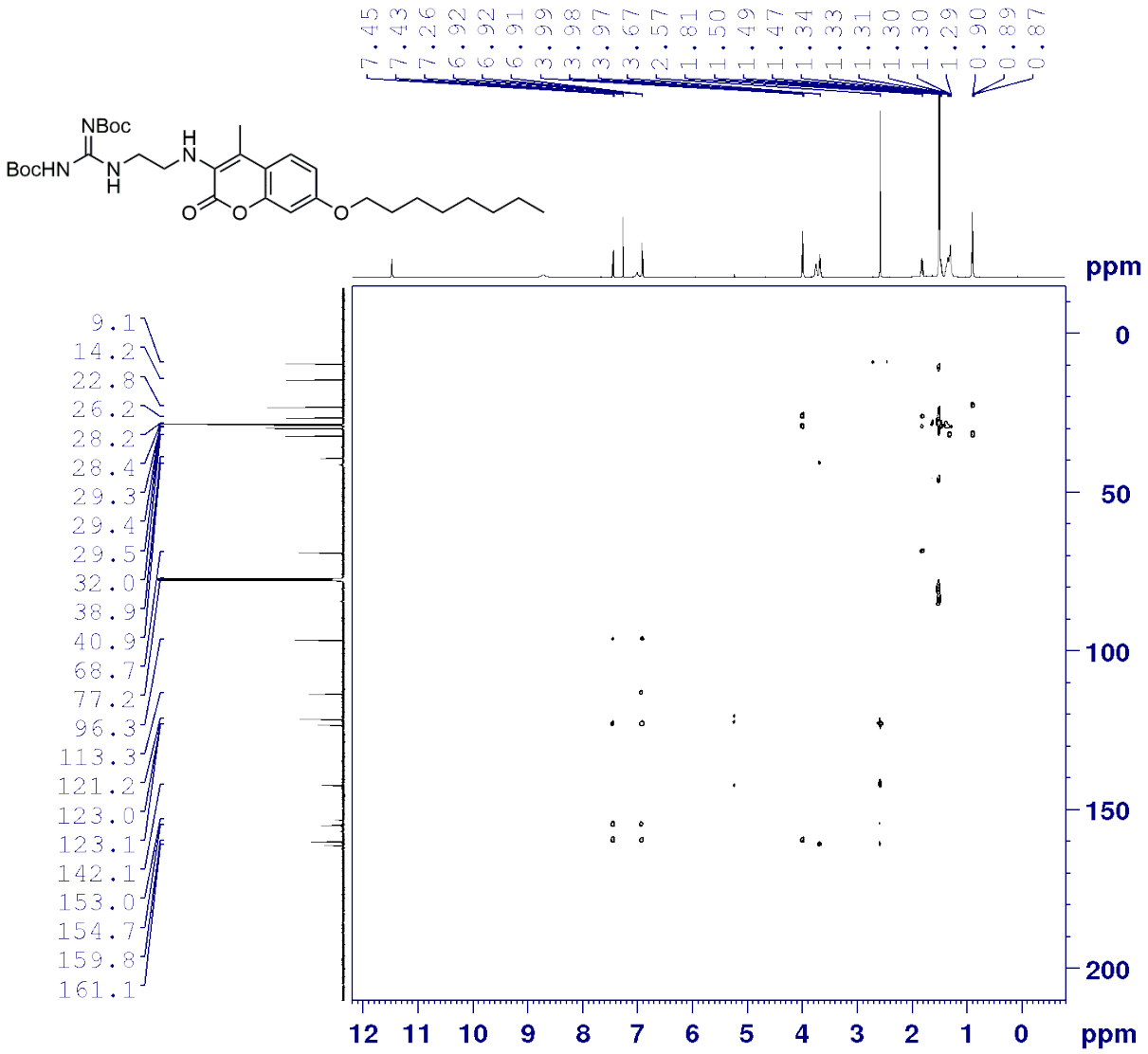

Figure S60: HMBC NMR (500 MHz) spectrum of coumarin **S8b** in $CDCl_3$.

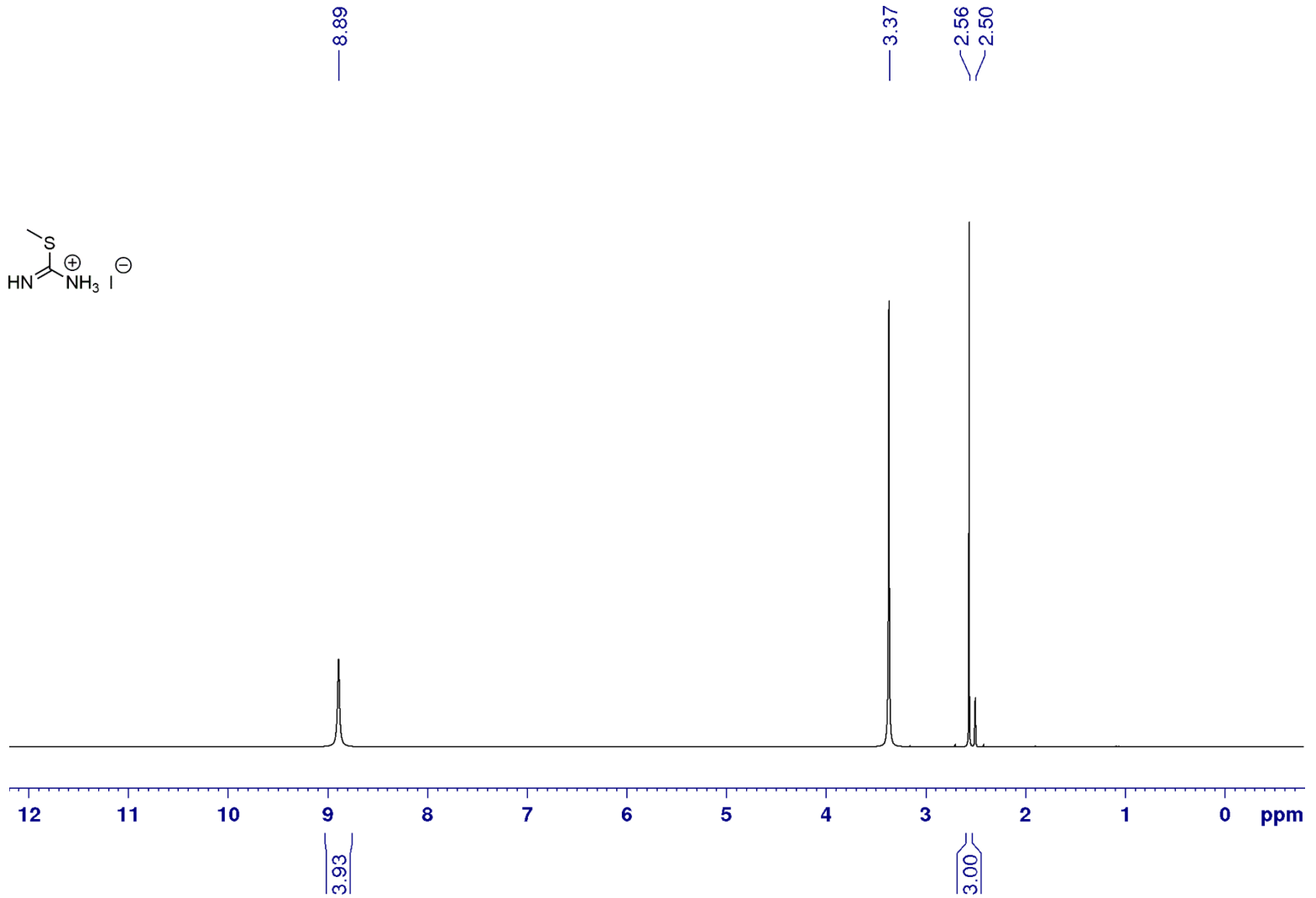

Figure S61: ^{1}H NMR (500 MHz) spectrum of compound **S9** in DMSO-d_6.

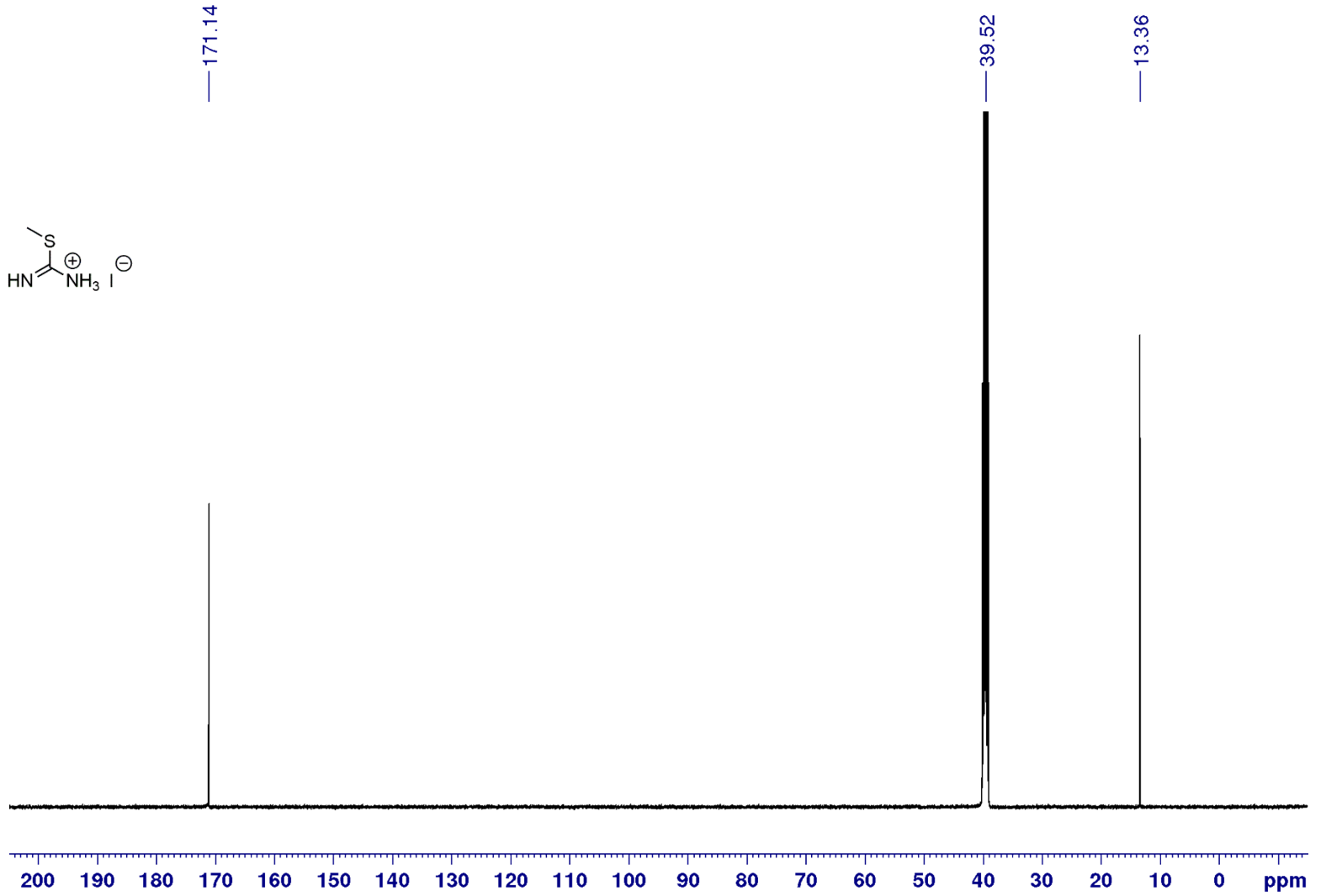

Figure S62: ^{13}C NMR (125 MHz) spectrum of compound **S9** in DMSO-d_6.

High-Resolution Mass Spectrometry Data

ESI-TOF mass spectra chromatograms were acquired and processed using Sciex Analyst TF 1.8.0.

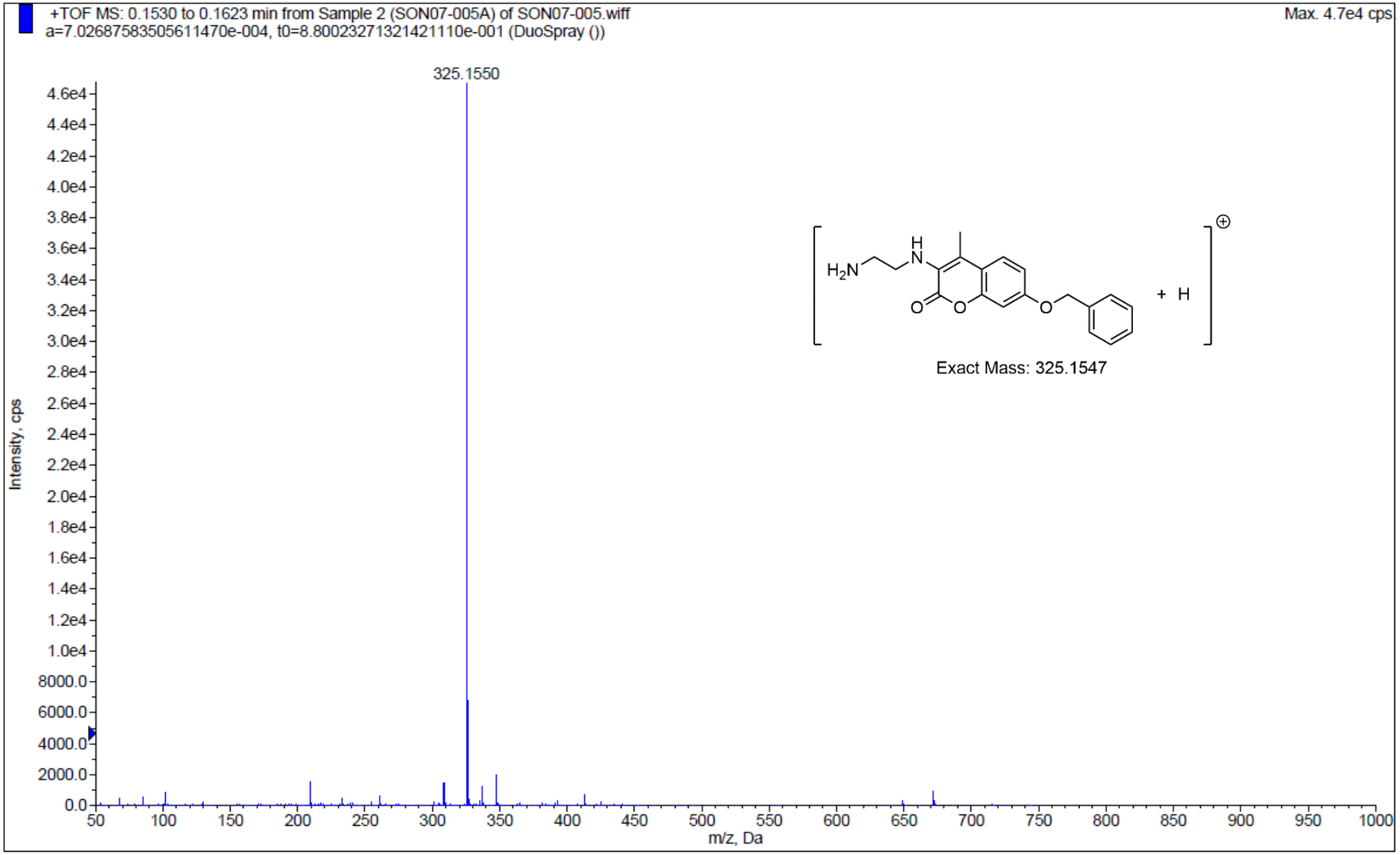

Figure S63: ESI-TOF mass spectrum of coumarin **1**.

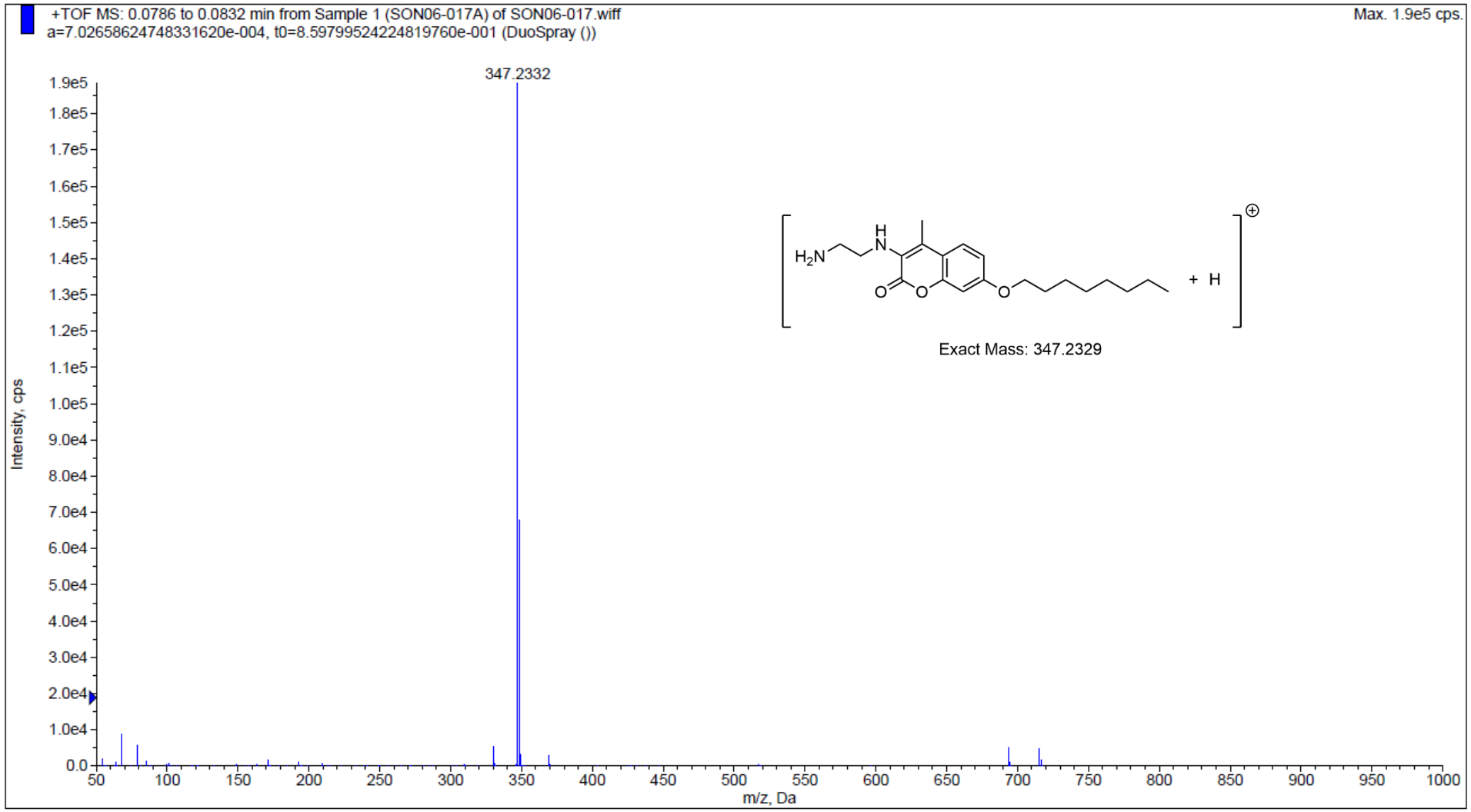

Figure S64: ESI-TOF mass spectrum of coumarin **2**.

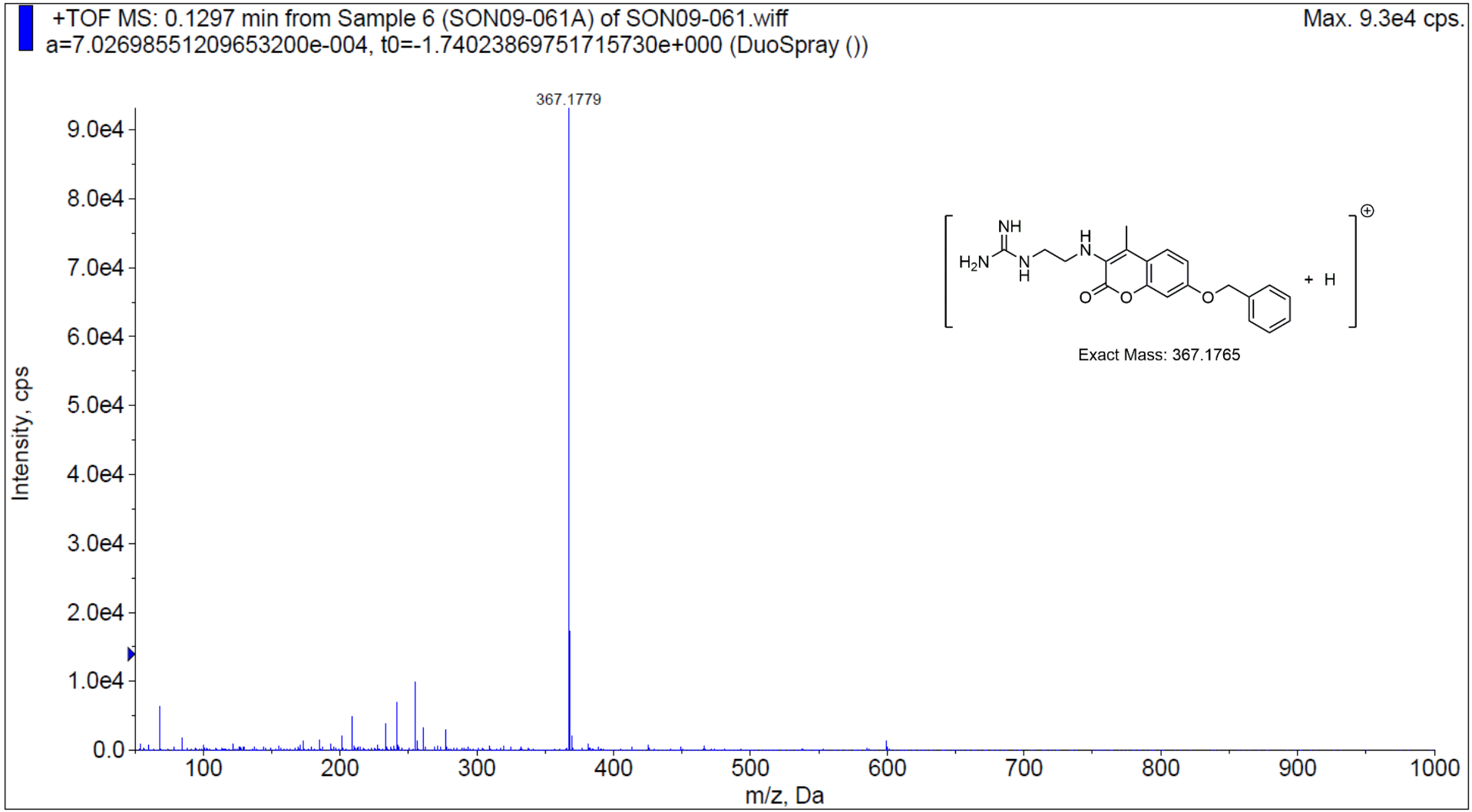

Figure S65: ESI-TOF mass spectrum of coumarin **3**.

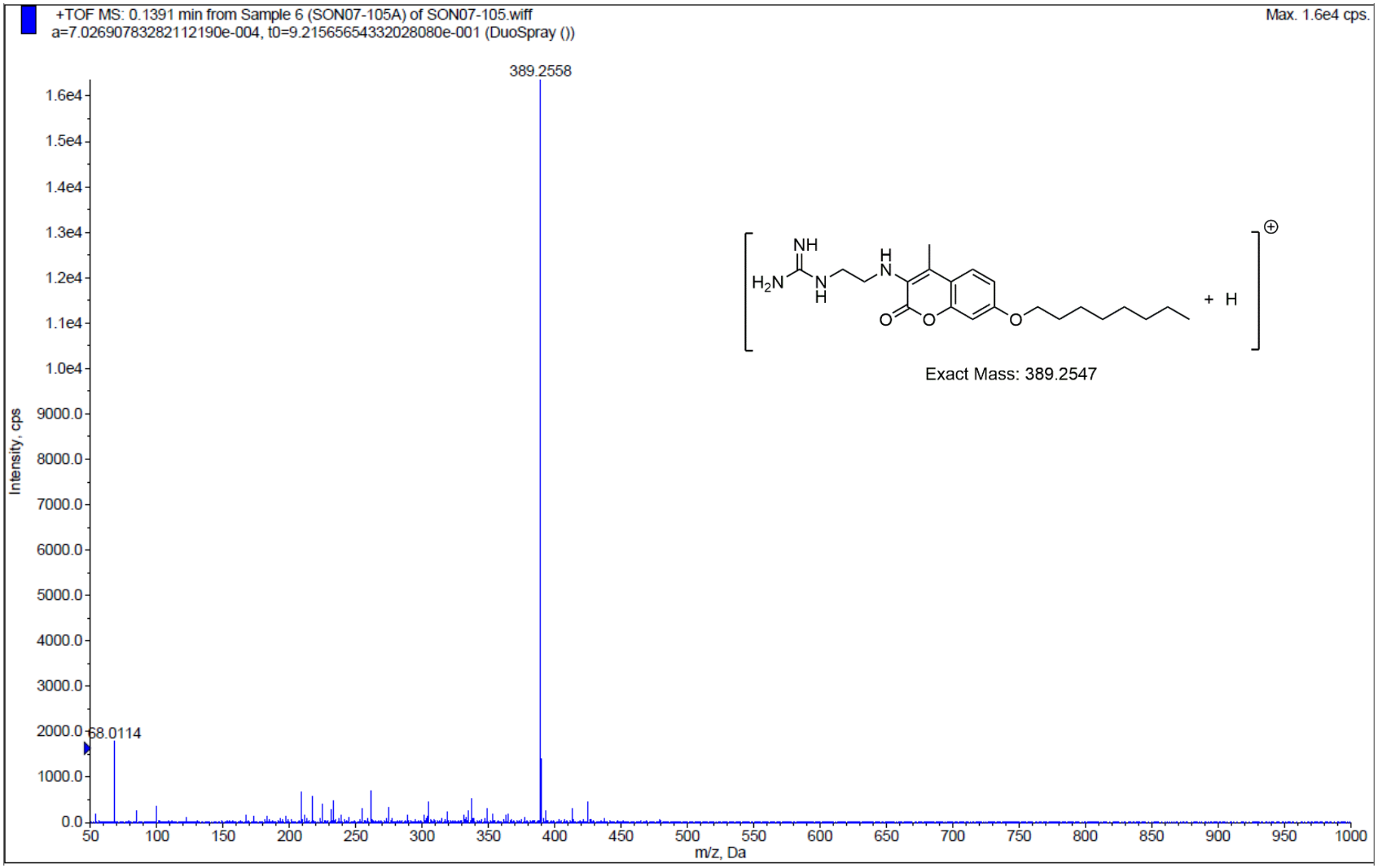

Figure S66: ESI-TOF mass spectrum of coumarin **4**.

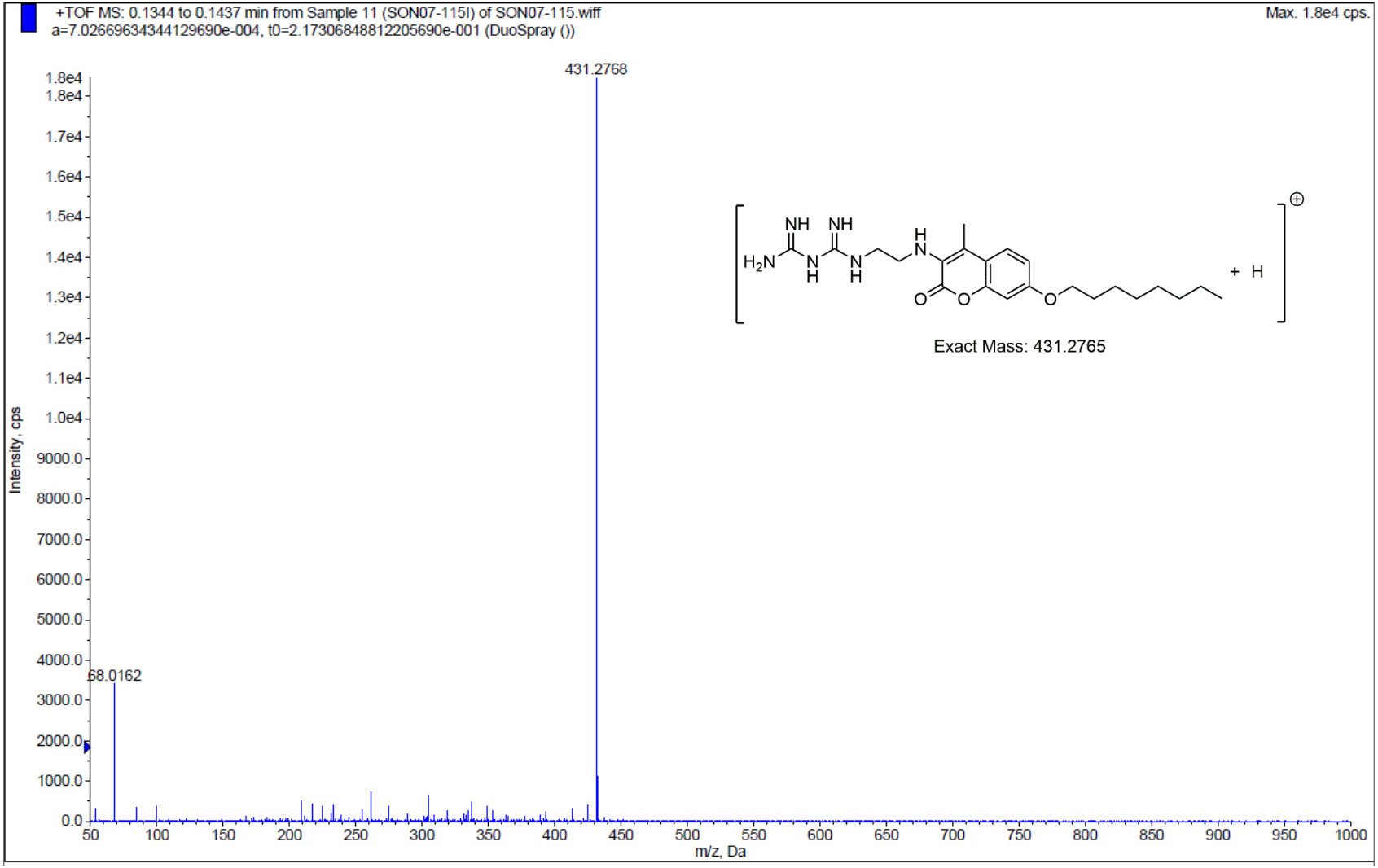

Figure S67: ESI-TOF mass spectrum of coumarin **5**.

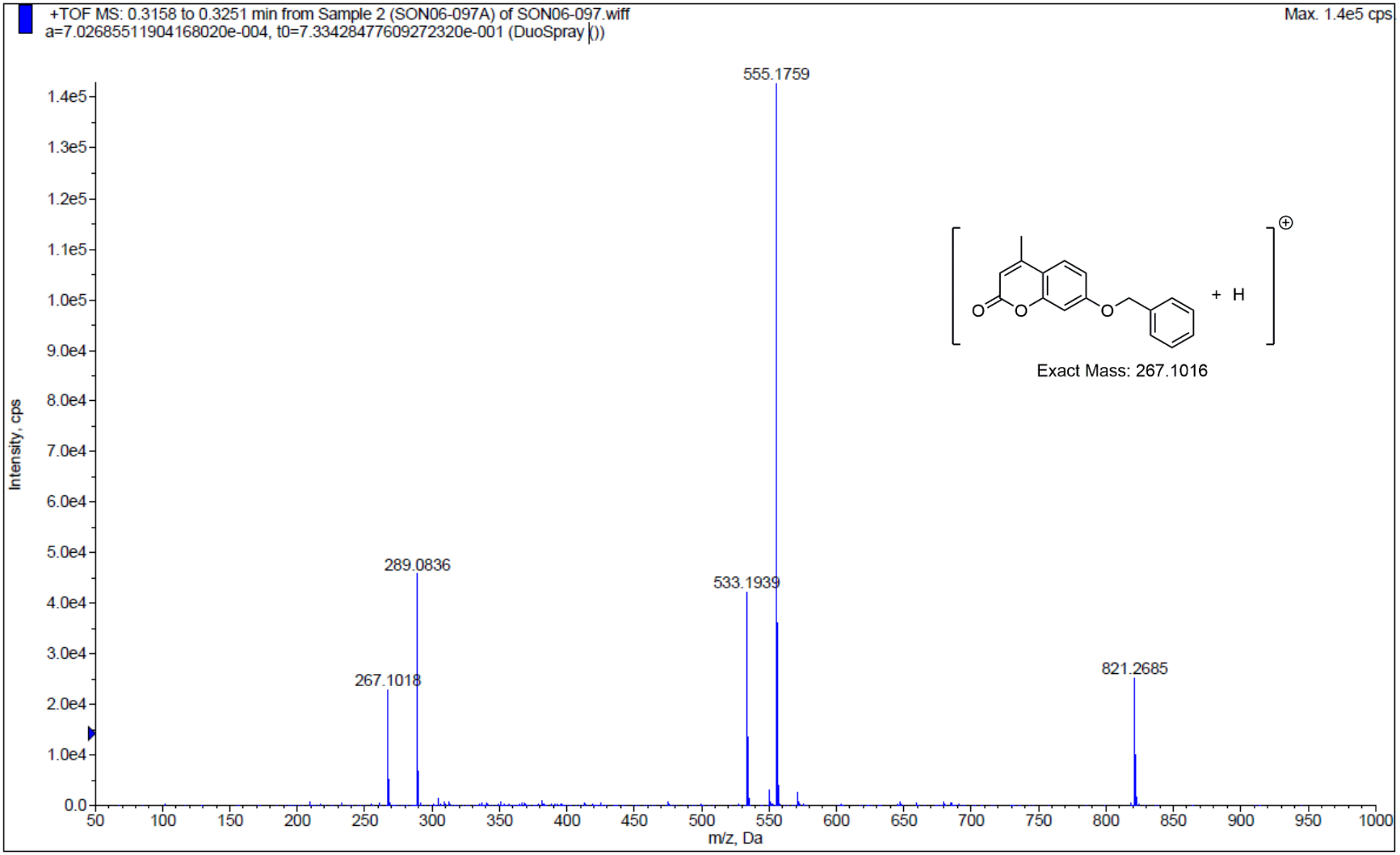

Figure S68: ESI-TOF mass spectrum of coumarin **S2a**.

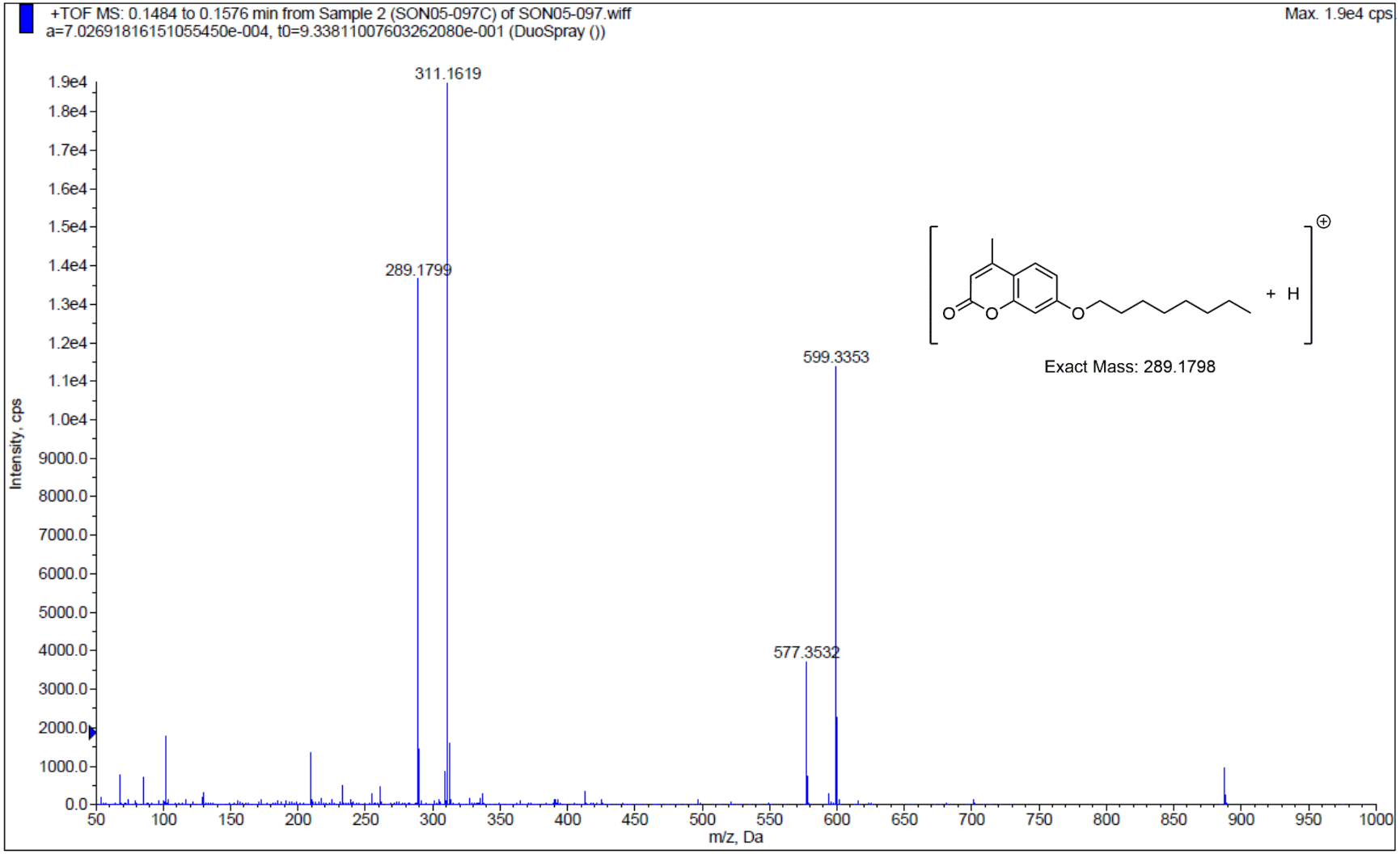

Figure S69: ESI-TOF mass spectrum of coumarin **S2b**.

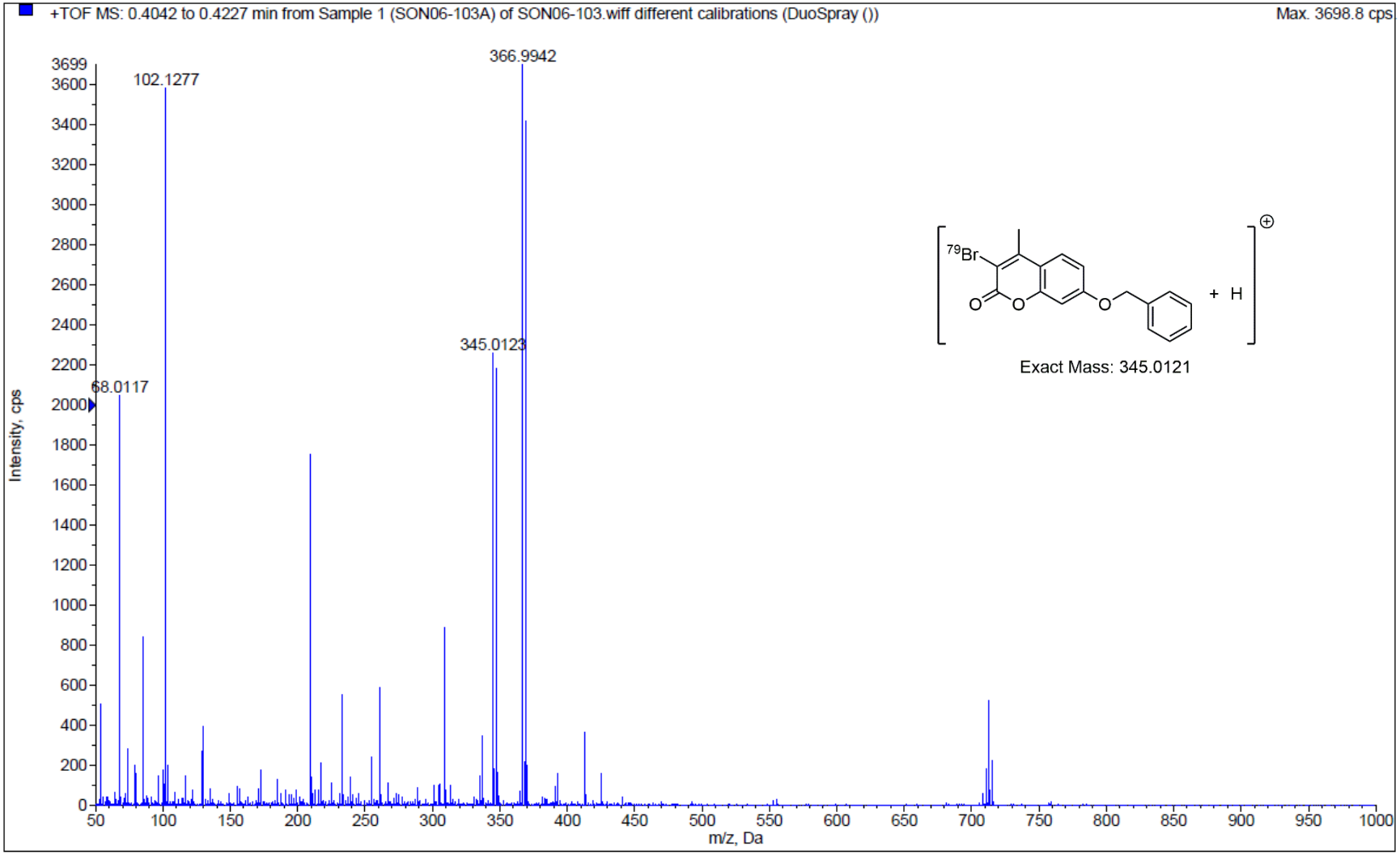

Figure S70: ESI-TOF mass spectrum of coumarin **S3a**.

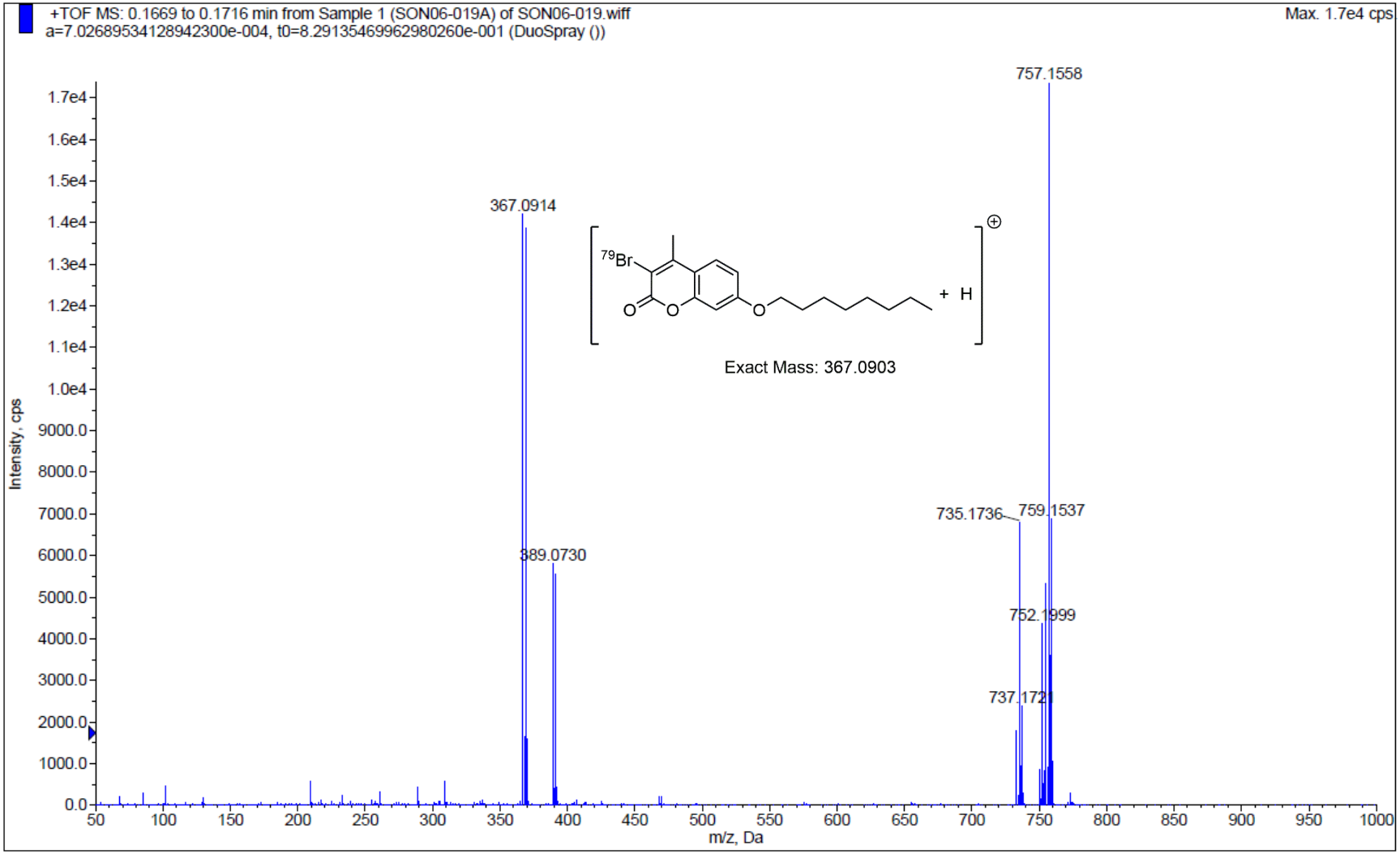

Figure S71: ESI-TOF mass spectrum of coumarin **S3b**.

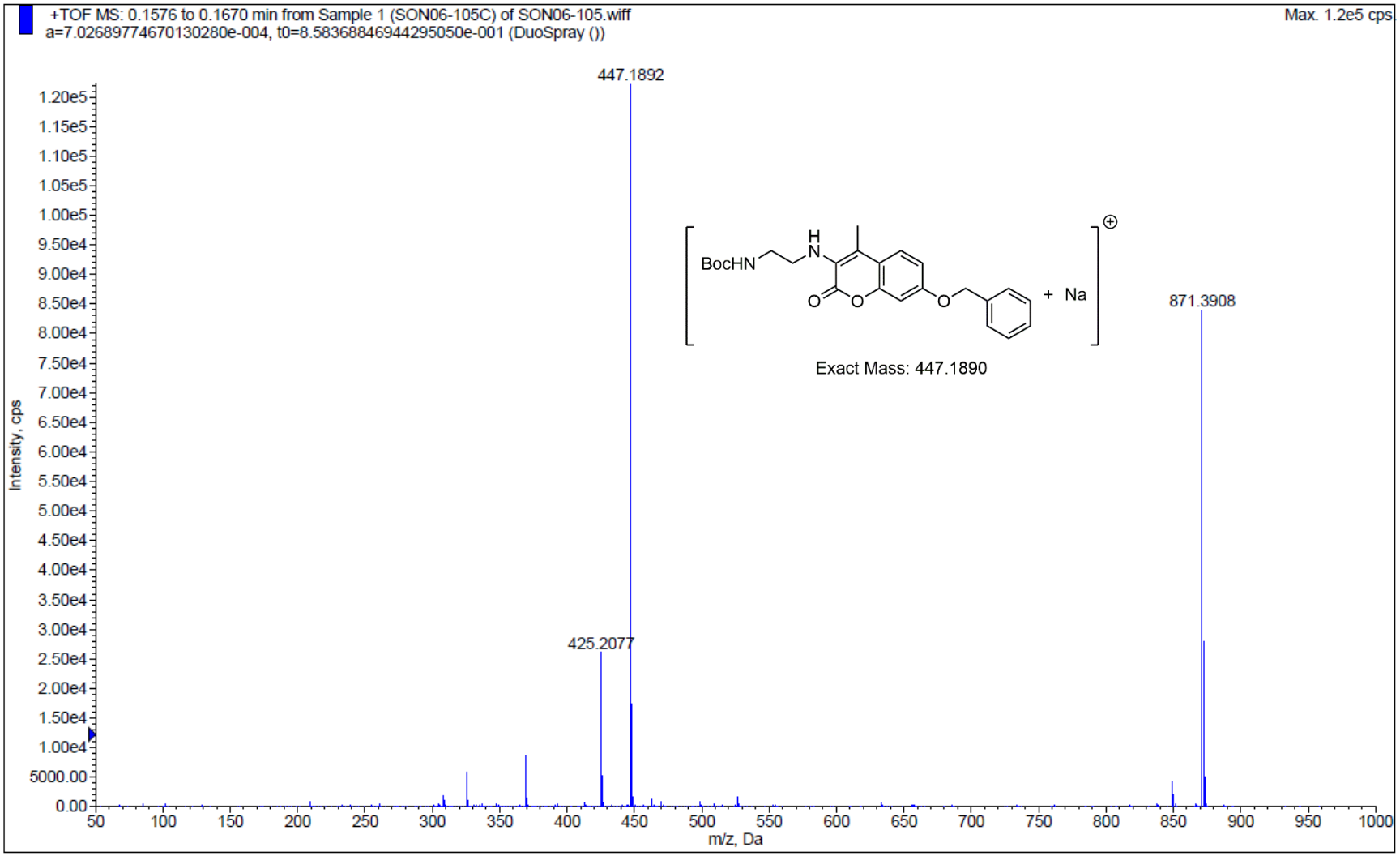

Figure S72: ESI-TOF mass spectrum of coumarin **S5a**.

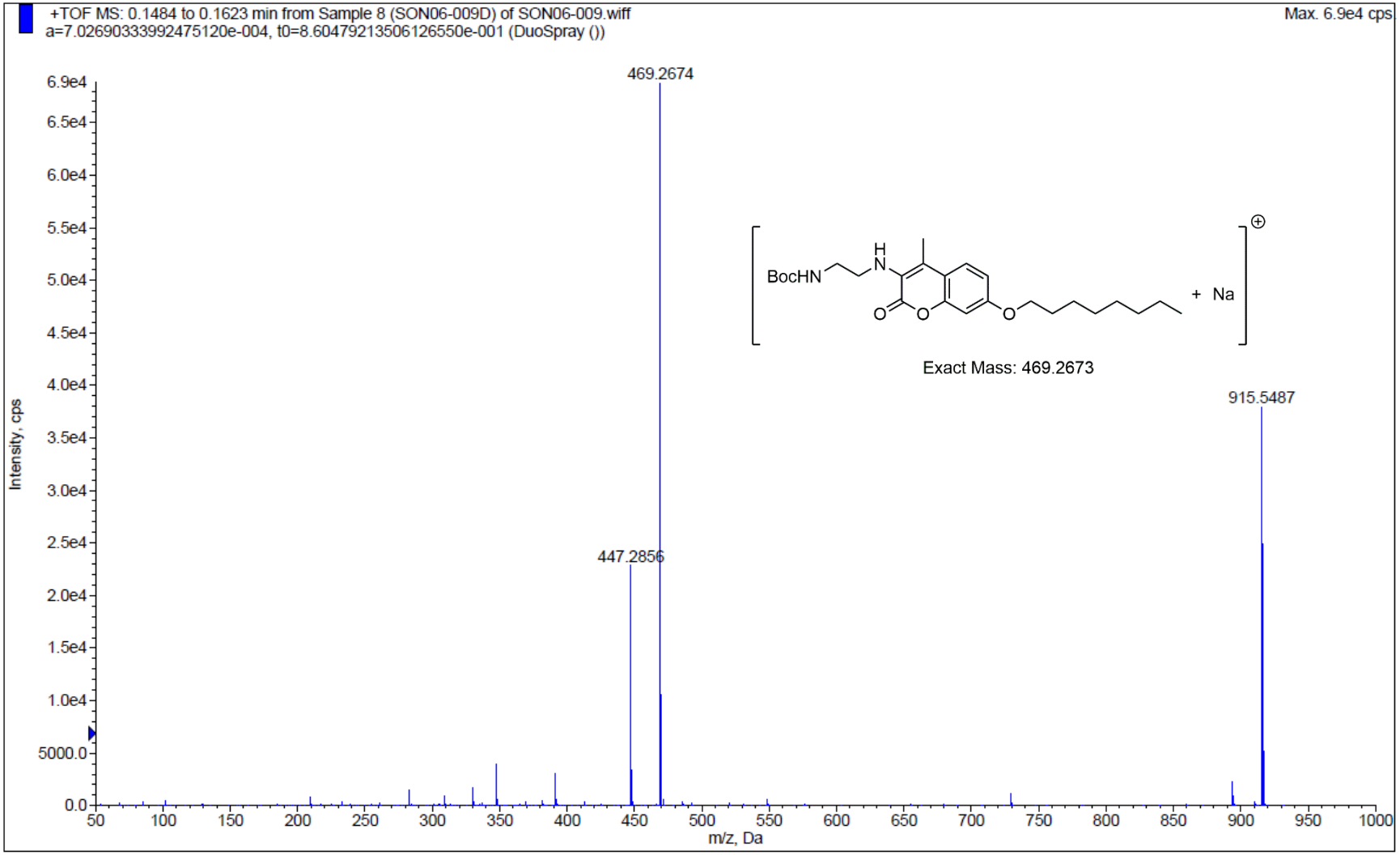

Figure S73: ESI-TOF mass spectrum of coumarin **S5b**.

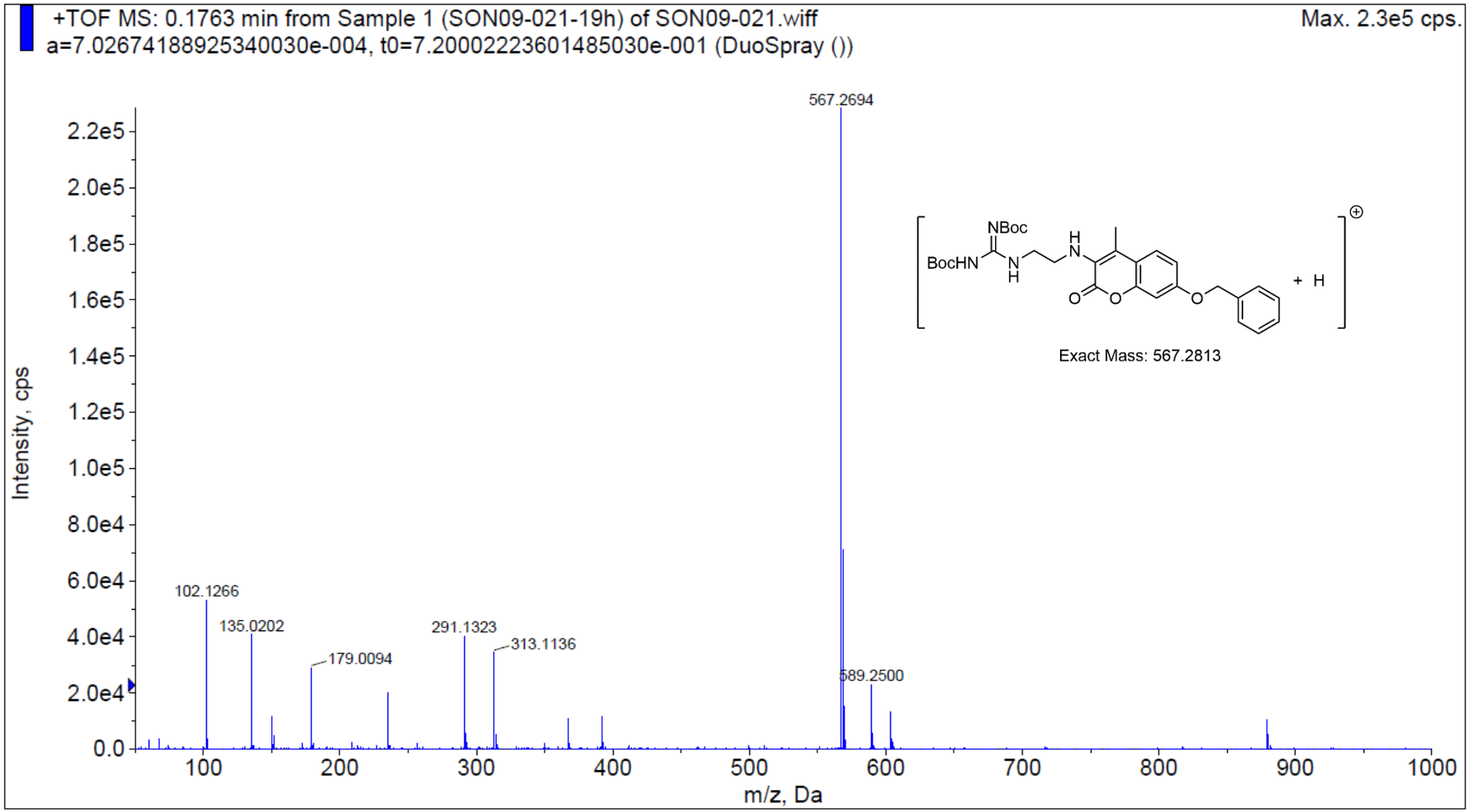

Figure S74: ESI-TOF mass spectrum of coumarin **S8a**.

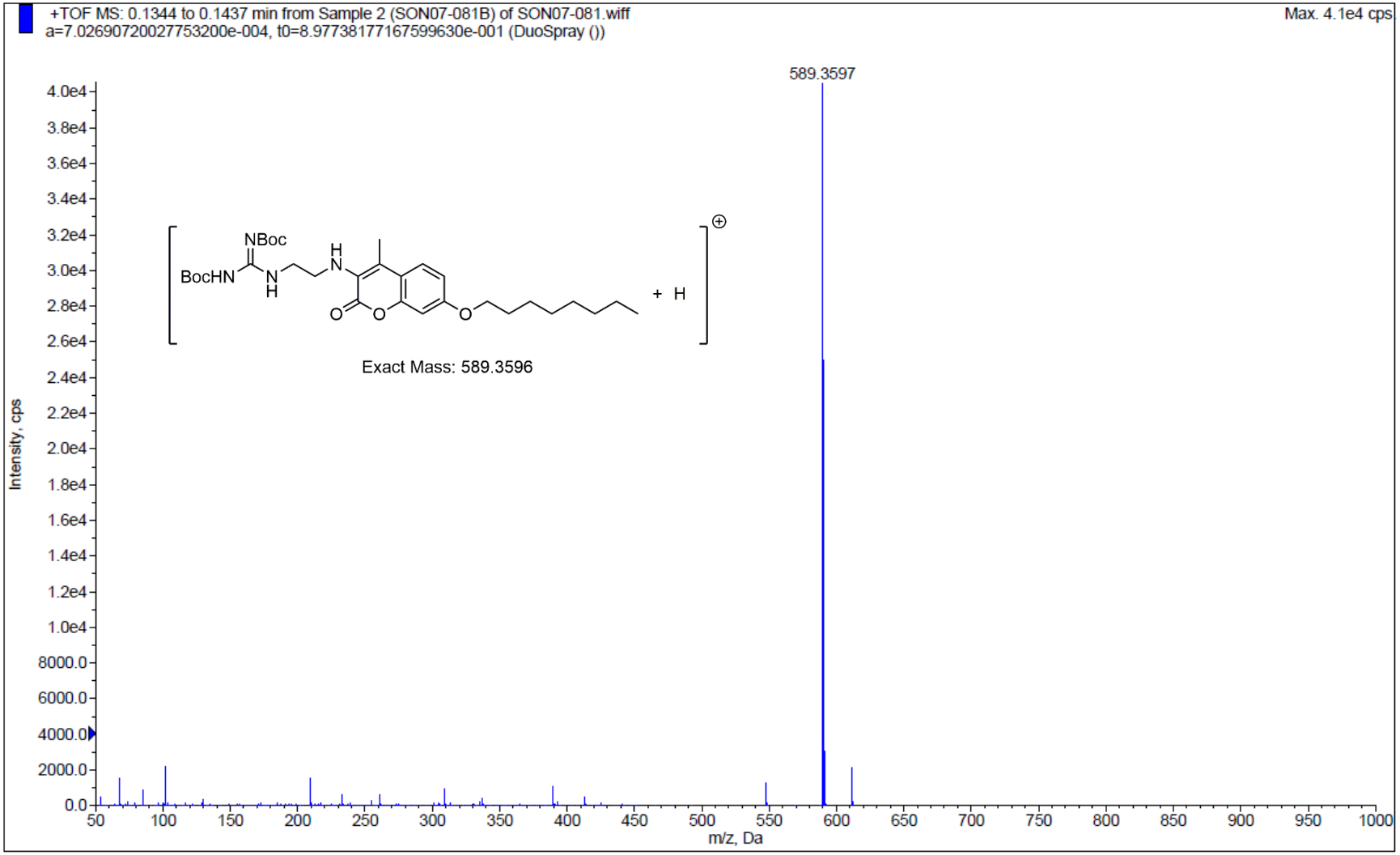

Figure S75: ESI-TOF mass spectrum of coumarin **S8b**.

RP-HPLC Chromatograms

Chromatograms were acquired and processed using Shimadzu LabSolutions 5.54 SP5.

Chromatogram

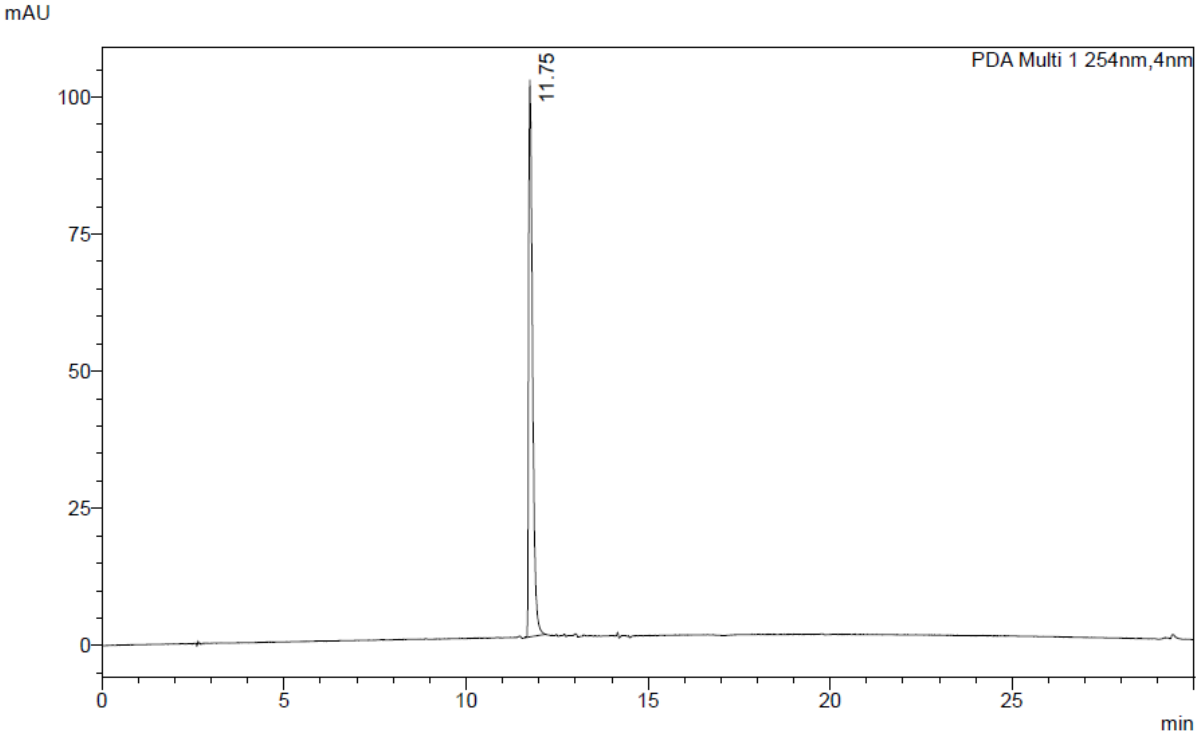

Peak Table

PDA Ch1 254nm

Peak#	Ret. Time	Area	Area%
1	11.75	755804	100.00
Total		755804	100.00

Figure S76: RP-HPLC chromatogram of coumarin **1**.

Chromatogram

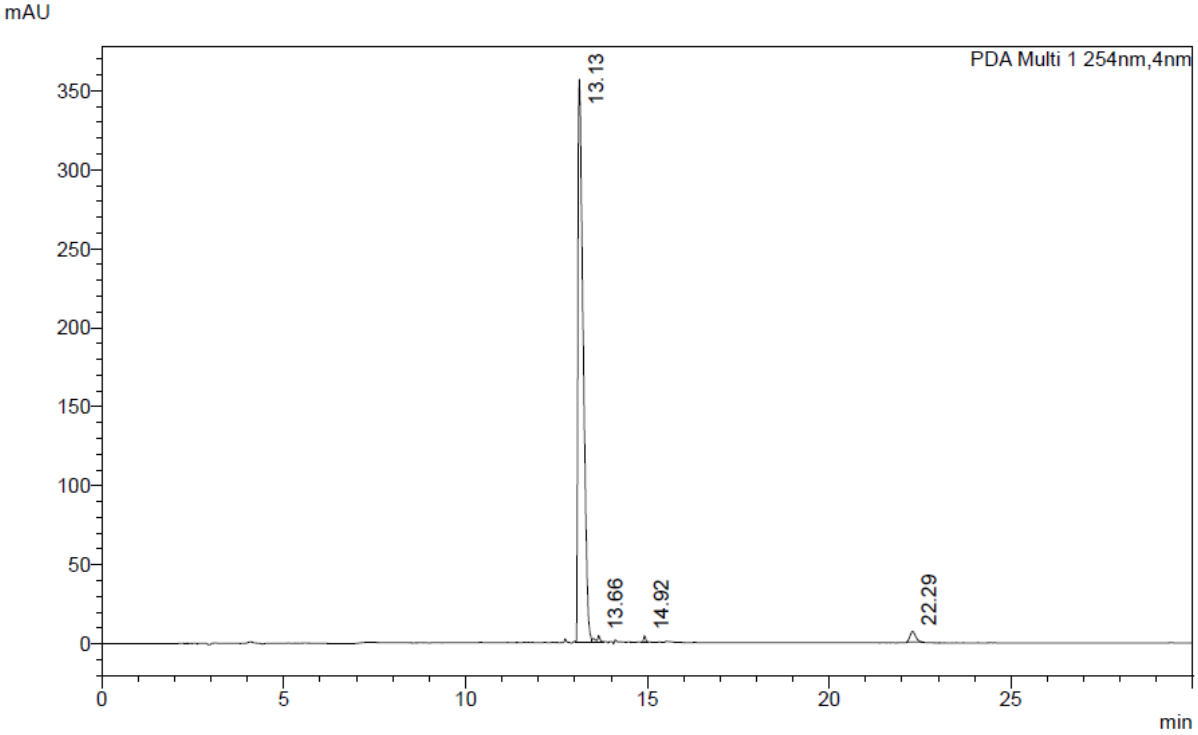

Peak Table

PDA Ch1 254nm

Peak#	Ret. Time	Area	Area%
1	13.13	3553430	96.92
2	13.66	26815	0.73
3	14.92	15029	0.41
4	22.29	71140	1.94
Total		3666414	100.00

Figure S77: RP-HPLC chromatogram of coumarin **2**.

Chromatogram

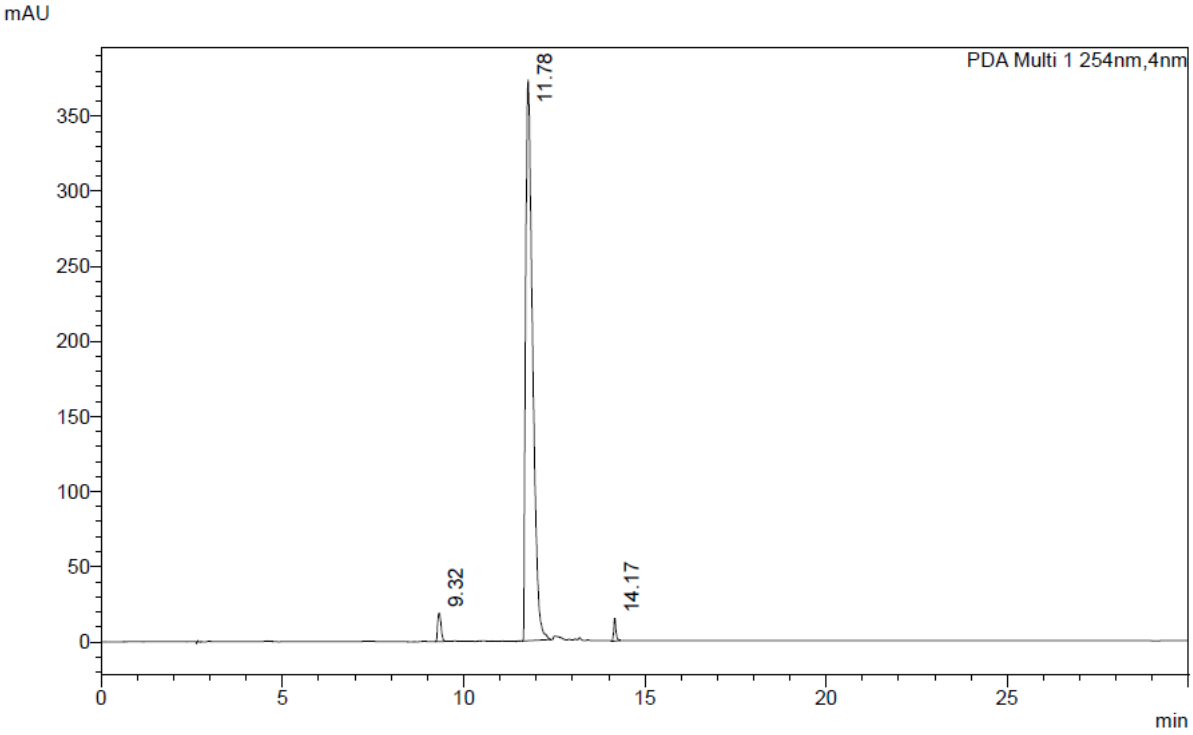

Peak Table

PDA Ch1 254nm

Peak#	Ret. Time	Area	Area%
1	9.32	120773	2.33
2	11.78	4992100	96.44
3	14.17	63688	1.23
Total		5176561	100.00

Figure S78: RP-HPLC chromatogram of coumarin **3**.

Chromatogram

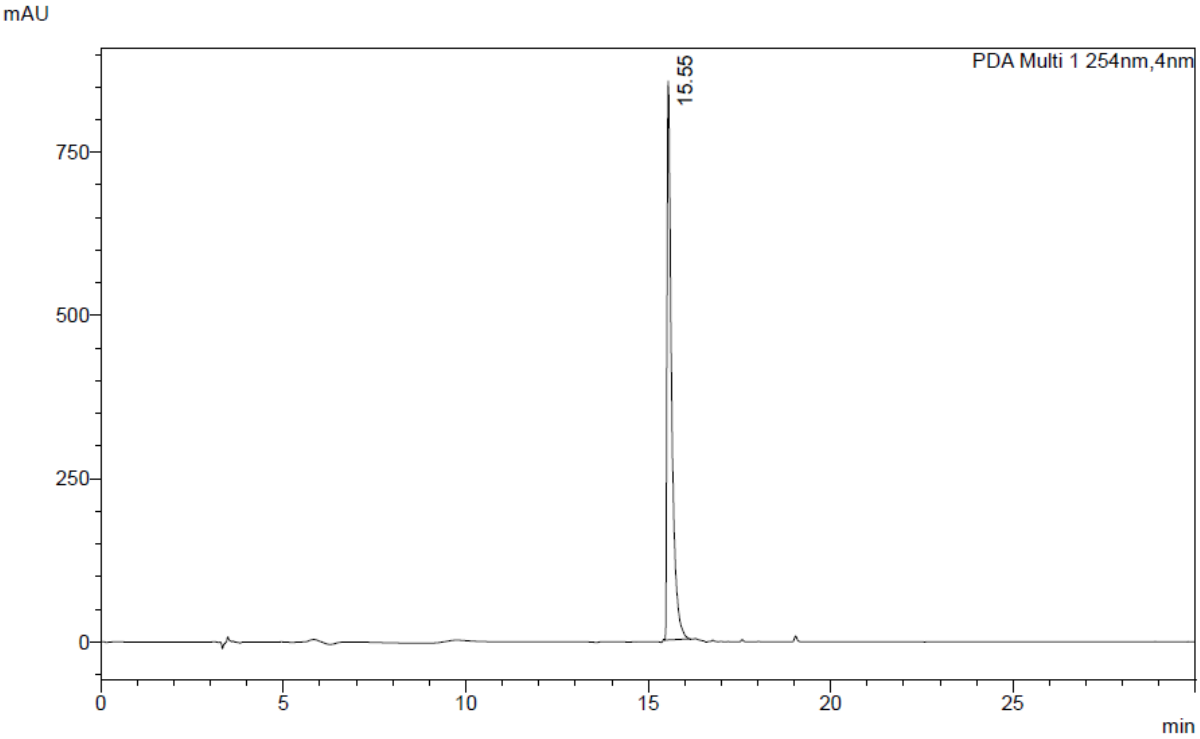

Peak Table

PDA Ch1 254nm

Peak#	Ret. Time	Area	Area%
1	15.55	7467570	100.00
Total		7467570	100.00

Figure S79: RP-HPLC chromatogram of coumarin **4**.

Chromatogram

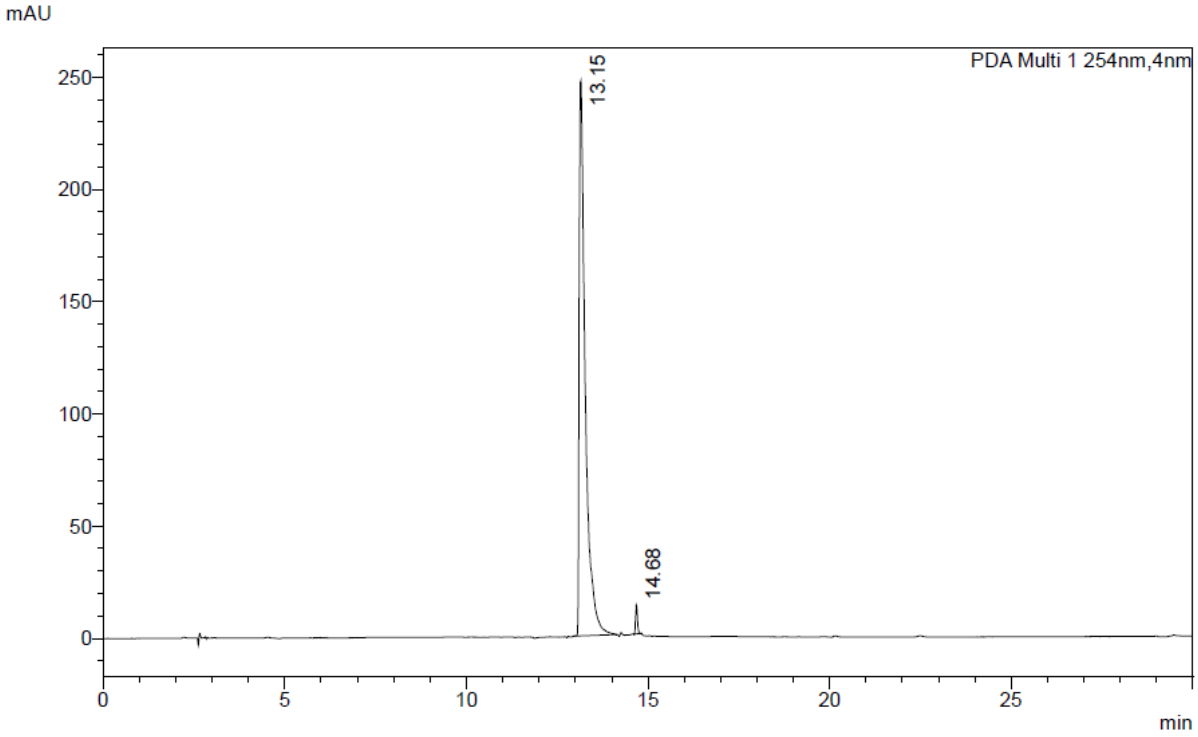

Peak Table

PDA Ch1 254nm

Peak#	Ret. Time	Area	Area%
1	13.15	2886089	98.52
2	14.68	43241	1.48
Total		2929330	100.00

Figure S80: RP-HPLC chromatogram of coumarin **5**.

Chromatogram

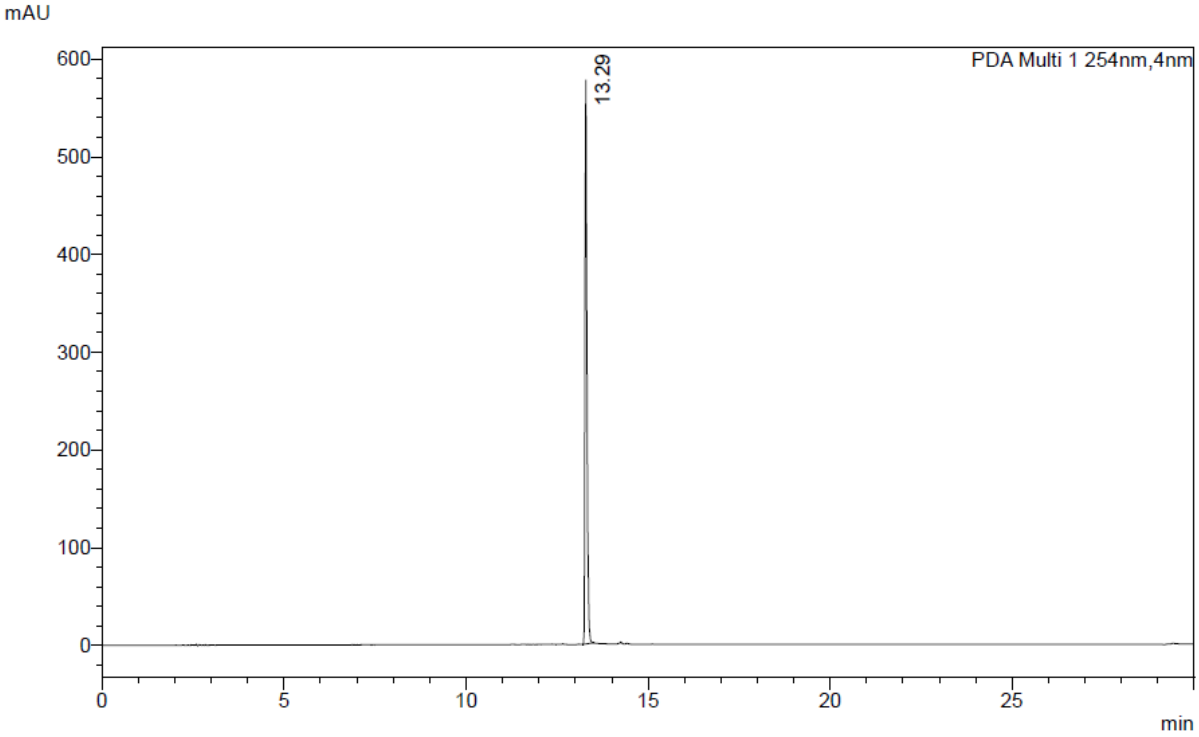

Peak Table

PDA Ch1 254nm

Peak#	Ret. Time	Area	Area%
1	13.29	2163926	100.00
Total		2163926	100.00

Figure S81: RP-HPLC chromatogram of coumarin **S2a**.

Chromatogram

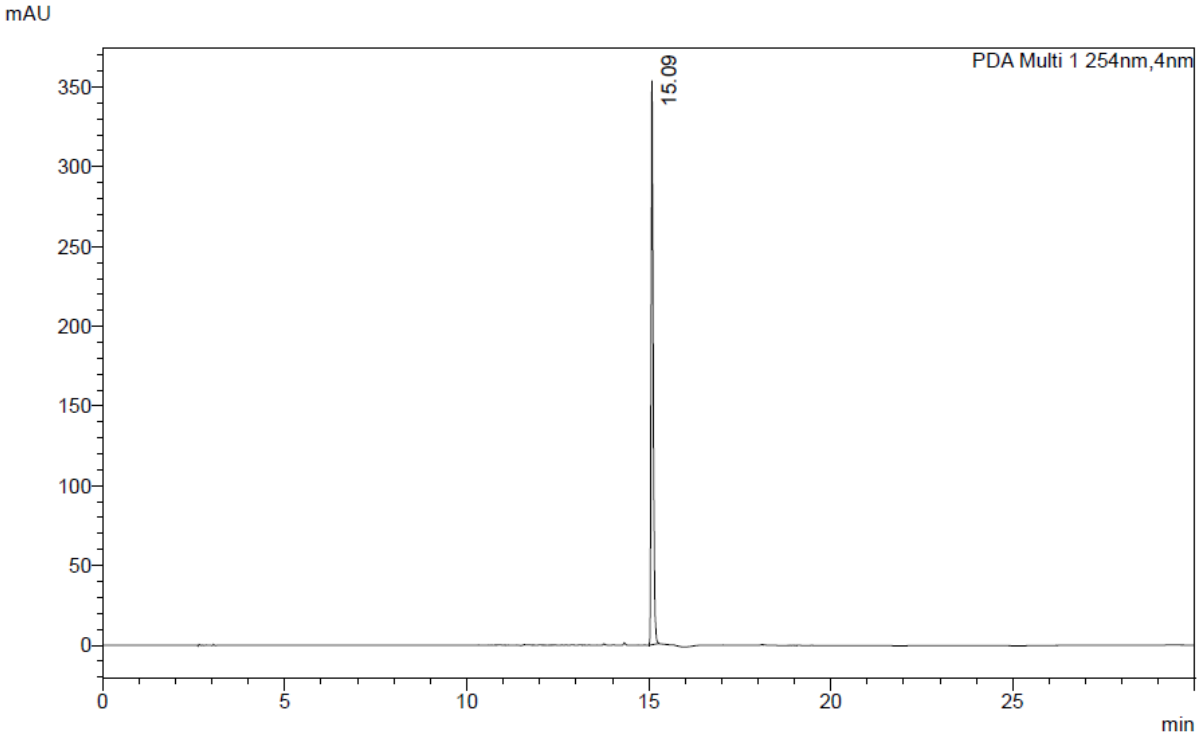

Peak Table

PDA Ch1 254nm

Peak#	Ret. Time	Area	Area%
1	15.09	1407214	100.00
Total		1407214	100.00

Figure S82: RP-HPLC chromatogram of coumarin **S2b**.

Chromatogram

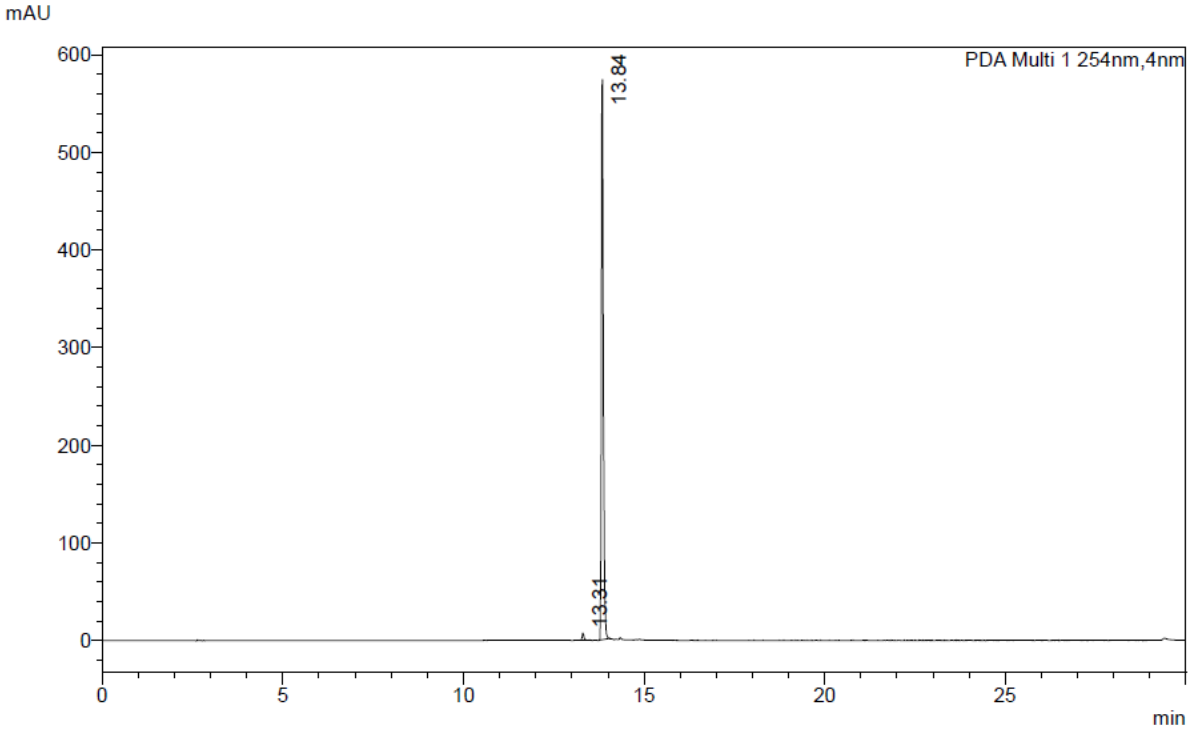

Peak Table

PDA Ch1 254nm

Peak#	Ret. Time	Area	Area%
1	13.31	25828	1.16
2	13.84	2206503	98.84
Total		2232331	100.00

Figure S83: RP-HPLC chromatogram of coumarin **S3a**.

Chromatogram

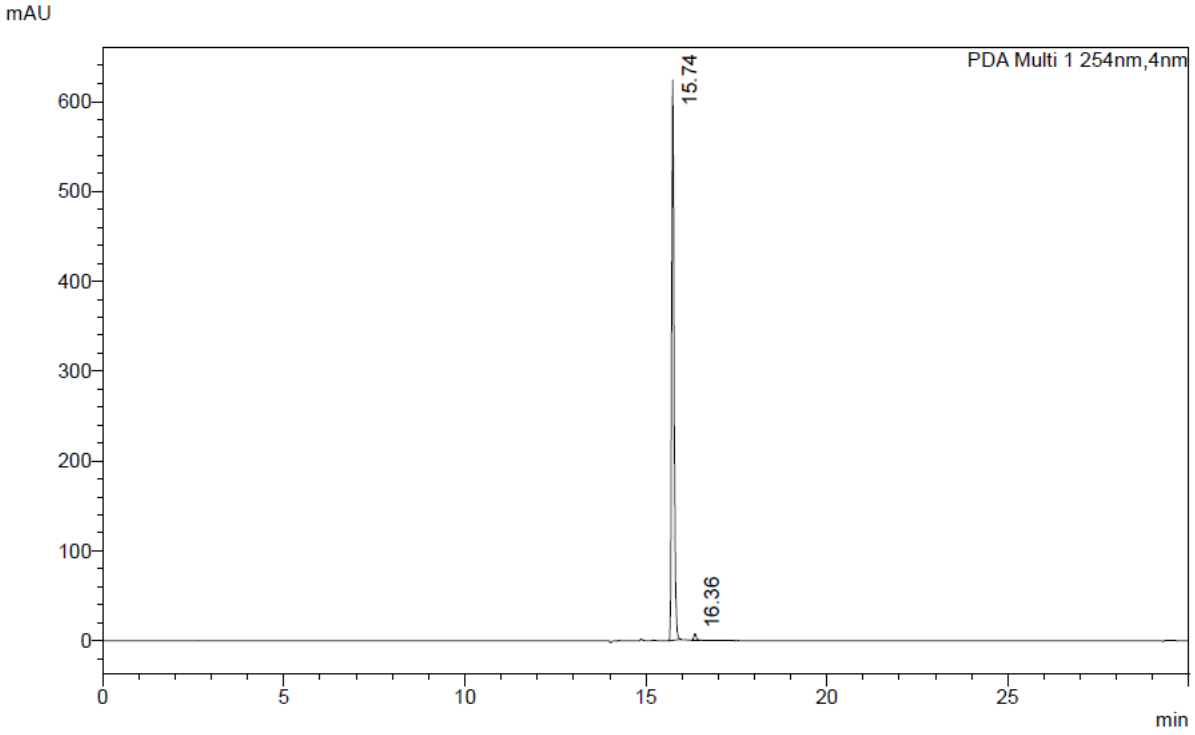

Peak Table

PDA Ch1 254nm

Peak#	Ret. Time	Area	Area%
1	15.74	2858484	98.87
2	16.36	32743	1.13
Total		2891228	100.00

Figure S84: RP-HPLC chromatogram of coumarin **S3b**.

Chromatogram

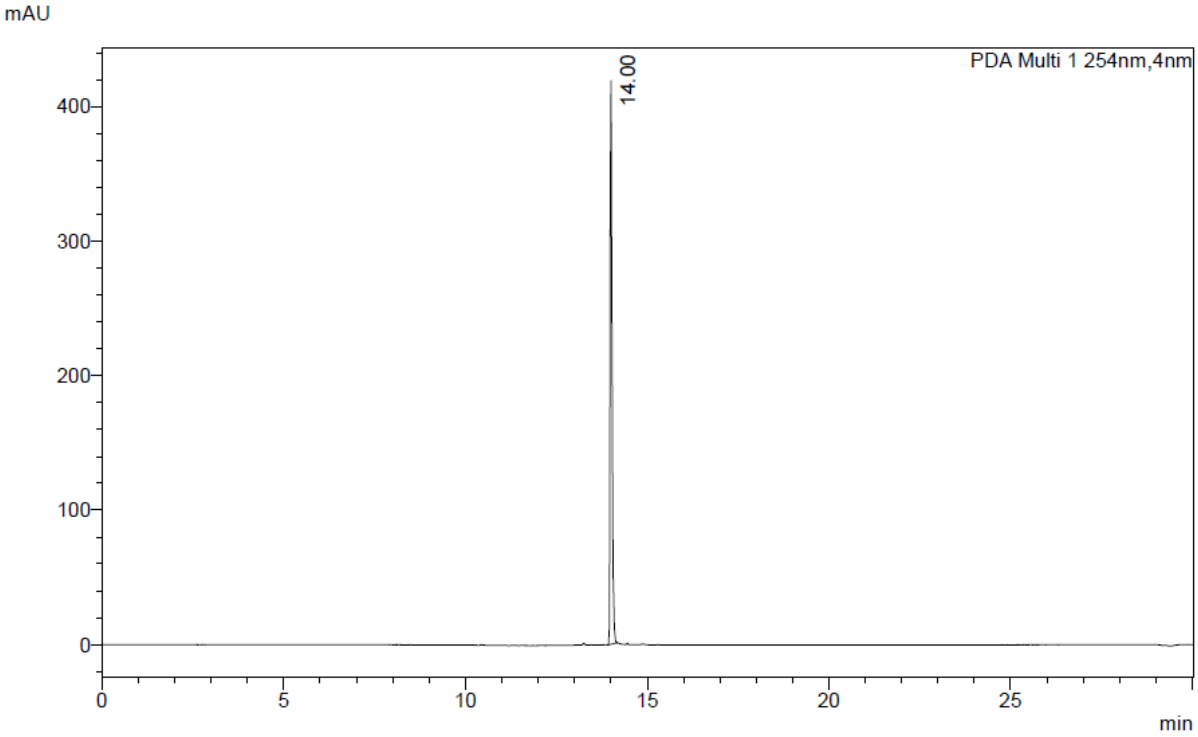

Peak Table

PDA Ch1 254nm

Peak#	Ret. Time	Area	Area%
1	14.00	1578007	100.00
Total		1578007	100.00

Figure S85: RP-HPLC chromatogram of coumarin **S5a**.

Chromatogram

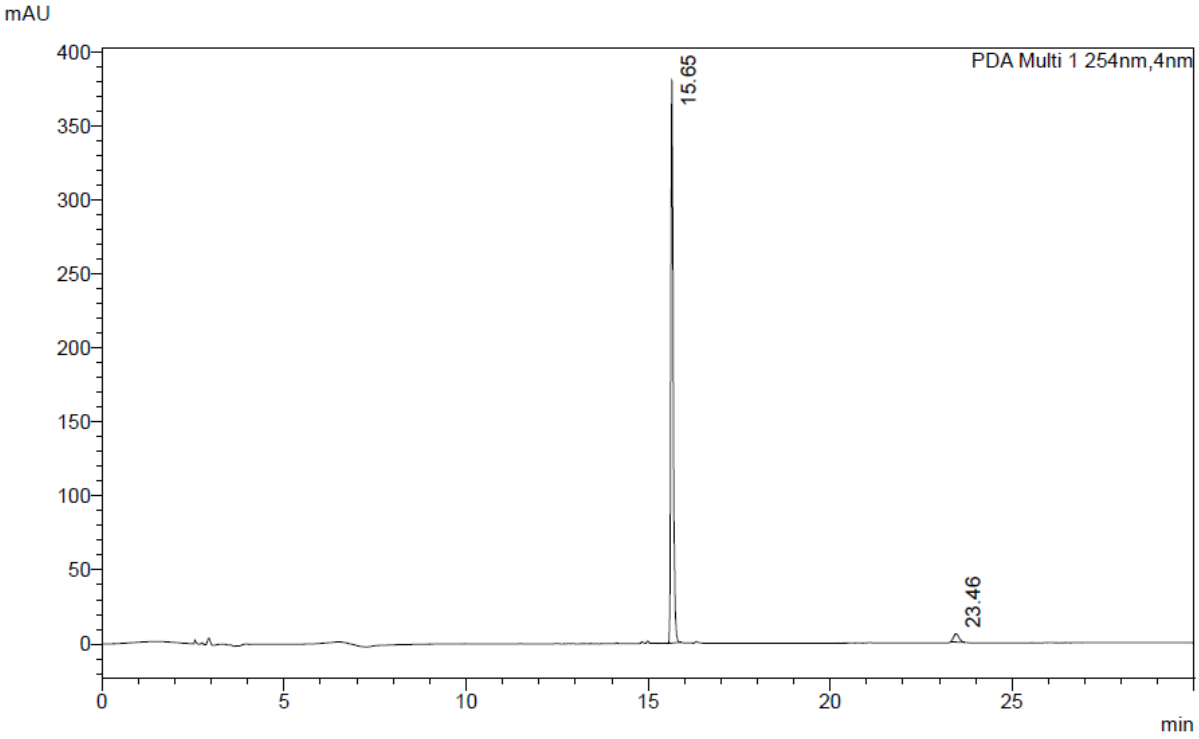

Peak Table

PDA Ch1 254nm

Peak#	Ret. Time	Area	Area%
1	15.65	1737827	96.78
2	23.46	57797	3.22
Total		1795624	100.00

Figure S86: RP-HPLC chromatogram of coumarin **S5b**.

Chromatogram

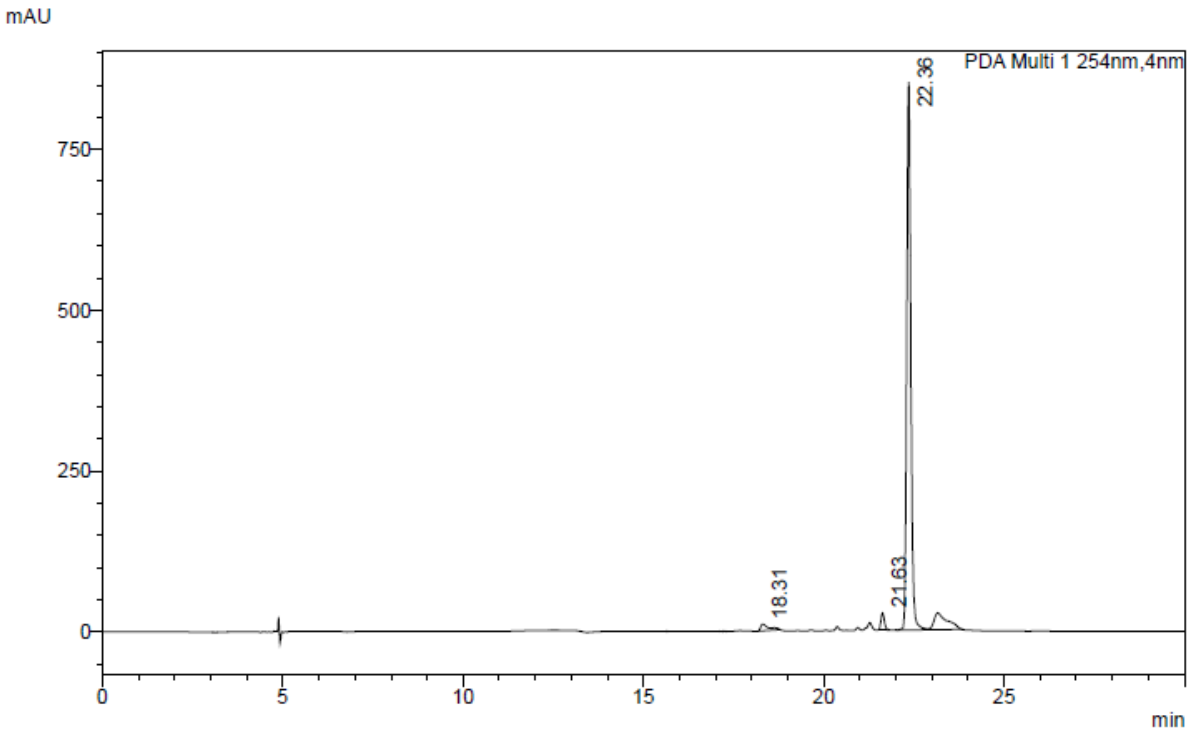

Peak Table

PDA Ch1 254nm

Peak#	Ret. Time	Area	Area%
1	18.31	170045	2.20
2	21.63	170527	2.21
3	22.36	7385875	95.59
Total		7726447	100.00

Figure S87: RP-HPLC chromatogram of coumarin **S8a**.

Chromatogram

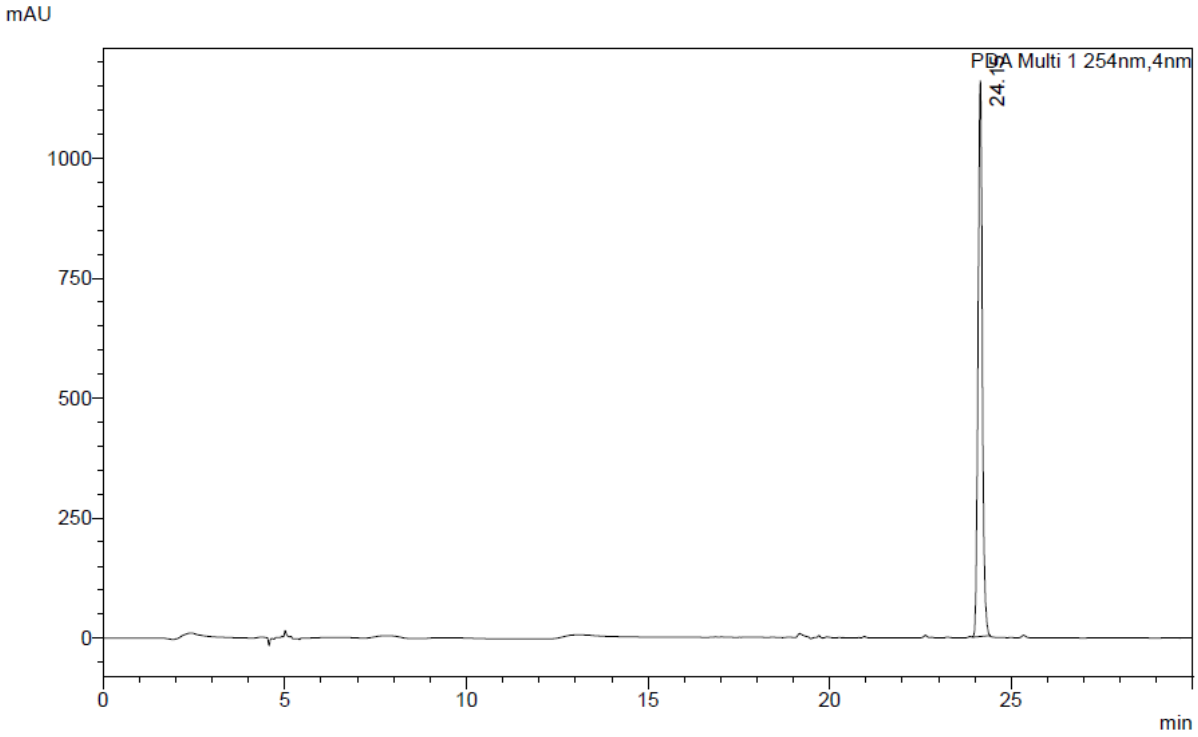

Peak Table

PDA Ch1 254nm

Peak#	Ret. Time	Area	Area%
1	24.15	9617584	100.00
Total		9617584	100.00

Figure S88: RP-HPLC chromatogram of coumarin **S8b**.

Stability Data

The stability of the octyloxy guanidine coumarin **4** was investigated using ^{1}H NMR spectroscopy in DMSO-d_6 and D_2O at room temperature over 5 days at a concentration of 1 μM. No significant changes in chemical shifts or integrations for the resonances shown in Figure S89 and Figure S90 were observed in the ^{1}H NMR spectra over 5 days at room temperature.

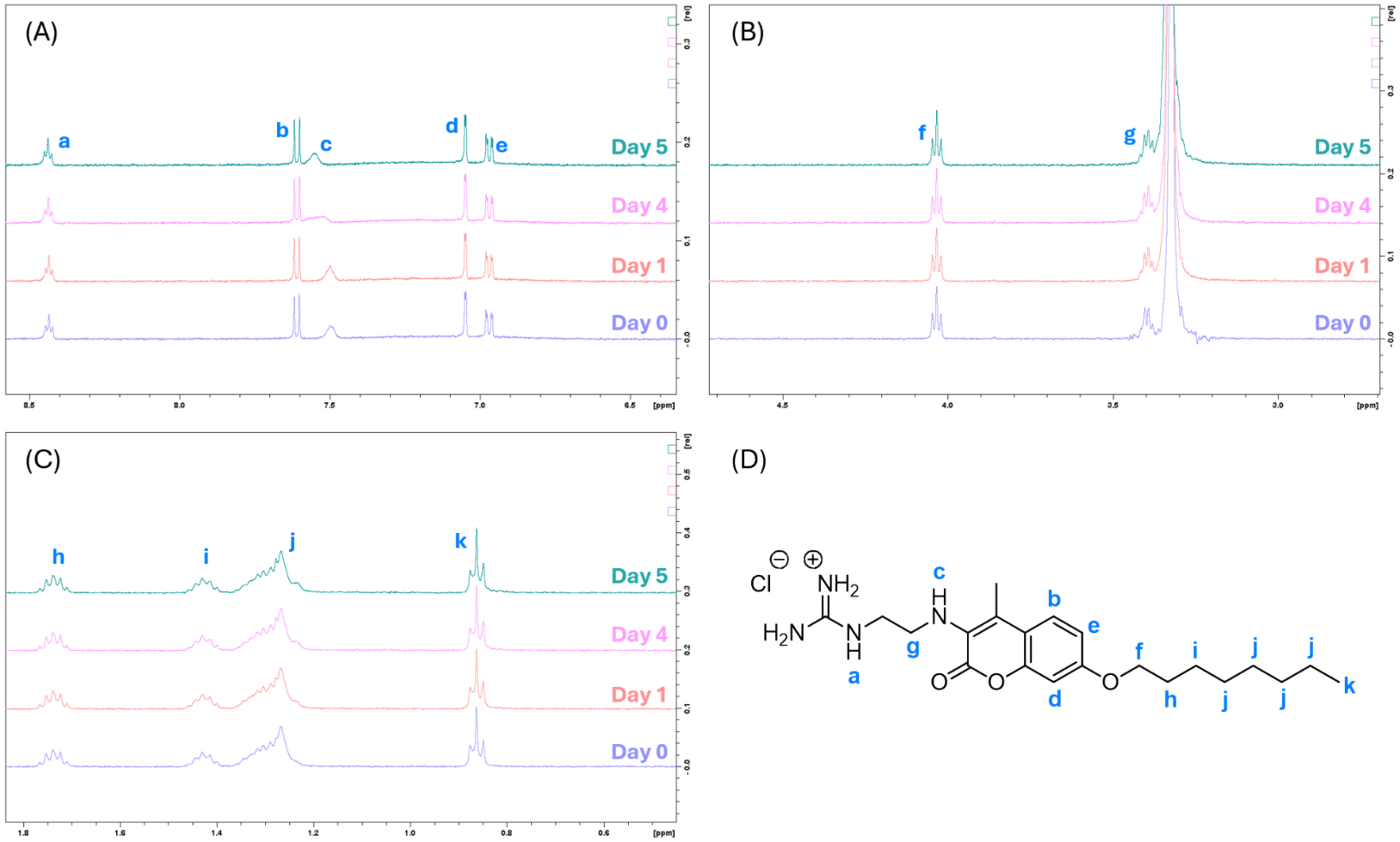

Figure S89: ^{1}H NMR (500 MHz) spectra of coumarin **4** over 5 days at room temperature in DMSO-d_6. (A) Stacked ^{1}H NMR (500 MHz) spectra from 8.5–6.5 ppm. (B) Stacked ^{1}H NMR (500 MHz) spectra from 4.5–3.0 ppm. (C) Stacked ^{1}H NMR (500 MHz) spectra from 1.8–0.6 ppm. (D) Chemical structure of coumarin **4** with labelled resonance correlations.

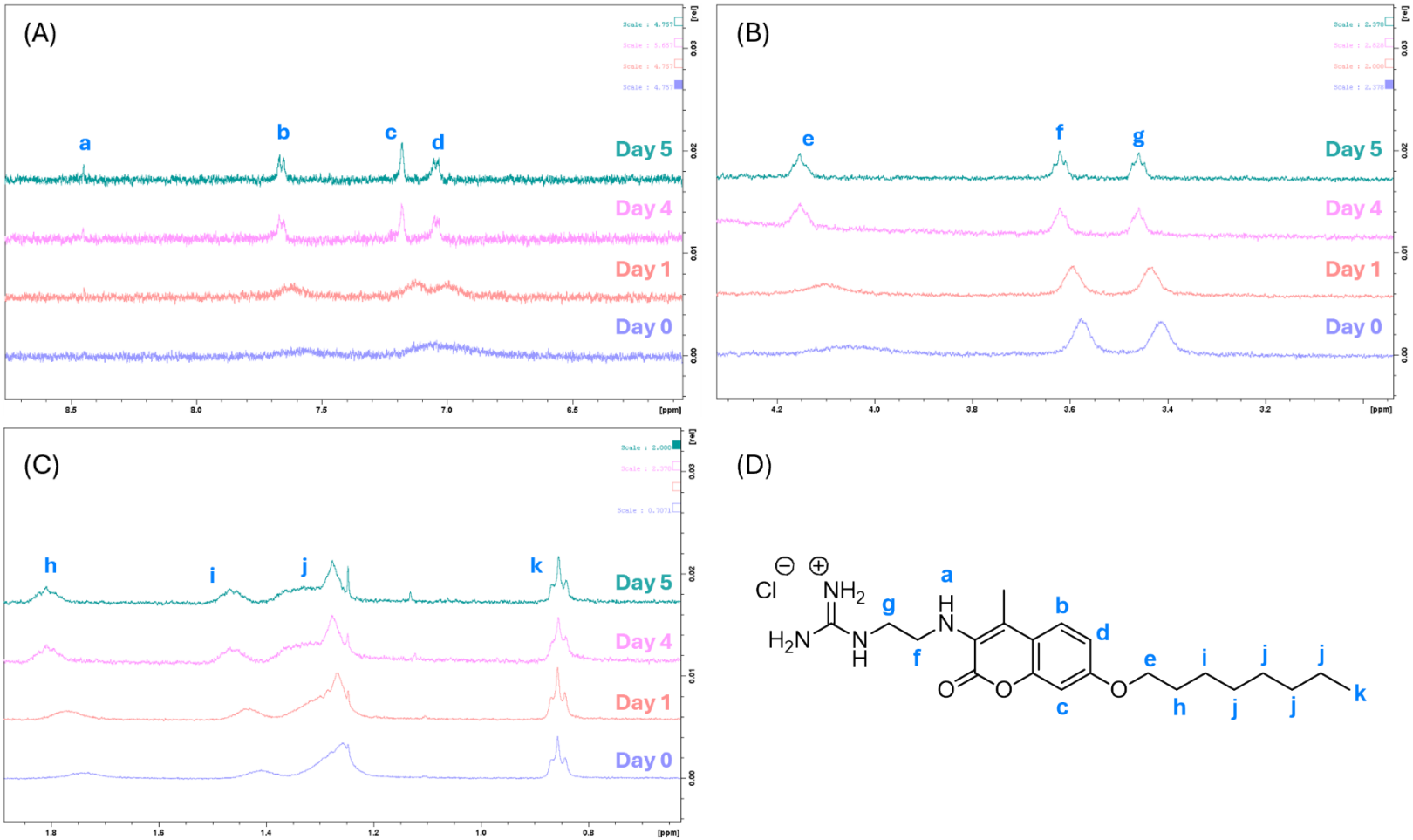

Figure S90: ^{1}H NMR (500 MHz) spectra of coumarin **4** over 5 days at room temperature in 1:99, DMSO-d_6:D_2O. (A) Stacked ^{1}H NMR spectra from 8.5–6.5 ppm. (B) Stacked ^{1}H NMR (500 MHz) spectra from 4.2–3.2 ppm. (C) Stacked ^{1}H NMR (500 MHz) spectra from 1.8–0.8 ppm. (D) Chemical structure of coumarin **4** with labelled resonance correlations.

Supporting References

1. C. C. Zhou and Y. L. Wang, *Current Opinion in Colloid & Interface Science*, 2020, **45**, 28–43.
2. F. Devínsky, A. Kopecka-Leitmanová, F. Šeršeň and P. Balgavý, *Journal of Pharmacy and Pharmacology*, 1990, **42**, 790–794.
3. K. Kuroda, G. A. Caputo and W. F. DeGrado, *Chemistry*, 2009, **15**, 1123–1133.
4. M. E. Levison and J. H. Levison, *Infectious Disease Clinics*, 2009, **23**, 791–815.
5. ChemAxon, *Journal*, 2021.
6. M. N. Melo, R. Ferre, L. Feliu, E. Bardaji, M. Planas and M. A. Castanho, *PLoS One*, 2011, **6**, e28549.
7. A. L. Lehninger, D. L. Nelson and M. M. Cox, *Lehninger Principles of Biochemistry*, Macmillan, 2005.
8. L. Zimmermann, J. Kempf, F. Briee, J. Swain, M. P. Mingeot-Leclercq and J. L. Decout, *European Journal of Medicinal Chemistry*, 2018, **157**, 1512–1525.
9. E. V. Korchagina and O. E. Philippova, *Langmuir*, 2012, **28**, 7880–7888.
10. C.-o. Organisation for Economic and Development, *Test No. 107: Partition Coefficient (n-octanol/water): Shake Flask Method*, OECD Publishing, 1995.
11. A. Andrés, M. Rosés, C. Ràfols, E. Bosch, S. Espinosa, V. Segarra and J. M. Huerta, *European Journal of Pharmaceutical Sciences*, 2015, **76**, 181-191.
12. C. D. Schönsee and T. D. Bucheli, *Journal of Chemical & Engineering Data*, 2020, **65**, 1946–1953.
13. M. A. Blaskovich, J. Zuegg, A. G. Elliott and M. A. Cooper, *ACS Infectious Diseases*, 2015, **1**, 285-287.
14. A. Frei, J. Zuegg, A. G. Elliott, M. Baker, S. Braese, C. Brown, F. Chen, C. G. Dowson, G. Dujardin, N. Jung, A. P. King, A. M. Mansour, M. Massi, J. Moat, H. A. Mohamed, A. K. Renfrew, P. J. Rutledge, P. J. Sadler, M. H. Todd, C. E. Willans, J. J. Wilson, M. A. Cooper and M. A. T. Blaskovich, *Chemical Science*, 2020, **11**, 2627–2639.
15. R. Muthyala, N. Rastogi, W. S. Shin, M. L. Peterson and Y. Y. Sham, *Bioorganic & Medicinal Chemistry Letters*, 2014, **24**, 2535–2538.
16. I. A. Degitz, B. H. Gazioglu, M. B. Aksu, S. Malta, A. D. Sezer and T. Eren, *European Polymer Journal*, 2020, **141**, 110084–110095.
17. A. Gallardo-Godoy, C. Muldoon, B. Becker, A. G. Elliott, L. H. Lash, J. X. Huang, M. S. Butler, R. Pelingon, A. M. Kavanagh and S. Ramu, *Journal of Medicinal Chemistry*, 2016, **59**, 1068–1077.
18. K. S. Witherell, J. Price, A. D. Bandaranayake, J. Olson and D. R. Call, *Scientific Reports*, 2021, **11**, 2151.
19. Y. N. Albayaty, N. Thomas, M. Jambhrunkar, M. Al-Hawwas, A. Kral, C. R. Thorn and C. A. Prestidge, *International Journal of Pharmaceutics*, 2019, **566**, 329–341.
20. G. R. Fulmer, A. J. M. Miller, N. H. Sherden, H. E. Gottlieb, A. Nudelman, B. M. Stoltz, J. E. Bercaw and K. I. Goldberg, *Organometallics*, 2010, **29**, 2176–2179.
21. S. Fortun and A. R. Schmitzer, *ACS Omega*, 2018, **3**, 1889–1896.
22. C. Ritter, N. Nett, C. G. Acevedo-Rocha, R. Lonsdale, K. Kraling, F. Dempwolff, S. Hoebenreich, P. L. Graumann, M. T. Reetz and E. Meggers, *Angewandte Chemie International Edition*, 2015, **54**, 13440–13443.
23. T. Khomenko, A. Zakharenko, T. Odarchenko, H. J. Arabshahi, V. Sannikova, O. Zakharova, D. Korchagina, J. Reynisson, K. Volcho, N. Salakhutdinov and O. Lavrik, *Bioorganic & Medicinal Chemistry*, 2016, **24**, 5573–5581.
24. C. M. Farley, D. F. Dibwe, J. Y. Ueda, E. A. Hall, S. Awale and J. Magolan, *Bioorganic & Medicinal Chemistry Letters*, 2016, **26**, 1471–1474.
25. A. Herrera, W. Castrillón, E. Otero, E. Ruiz, M. Carda, R. Agut, T. Naranjo, G. Moreno, M. E. Maldonado and W. Cardona, *Medicinal Chemistry Research*, 2018, **27**, 1893–1905.
26. J. L. Su, Y. Zhang, M. R. Chen, W. M. Li, X. W. Qin, Y. P. Xie, L. X. Qin, S. H. Huang and M. Zhang, *Synlett*, 2019, **30**, 630–634.

27. L. Vanammoole, R. Kommera, S. H. Kurma, J. R. Vaidya and C. R. Bhimapaka, *ChemistrySelect*, 2020, **5**, 8875–8880.
28. K. Amirbekyan, N. Duchemin, E. Benedetti, R. Joseph, A. Colon, S. A. Markarian, L. Bethge, S. Vonhoff, S. Klussmann and J. Cossy, *ACS Catalysis*, 2016, **6**, 3096–3105.
29. M. A. Soussi, D. Audisio, S. Messaoudi, O. Provot, J. D. Brion and M. Alami, *European Journal of Organic Chemistry*, 2011, **2011**, 5077–5088.
30. A. V. Lipeeva, D. O. Zakharov, Y. V. Gatilov, M. A. Pokrovskii, A. G. Pokrovskii and E. E. Shults, *Chemistry Select*, 2019, **4**, 10197–10201.
31. S. M. Hickey, T. D. Ashton and F. M. Pfeffer, *Asian Journal of Organic Chemistry*, 2015, **4**, 320–326.